Supplementary Information

Abiotic reduction of ketones with silanes catalyzed by carbonic anhydrase through an enzymatic zinc hydride

Pengfei Ji[1], Jeeyoung Park[1], Yang Gu[1], Douglas S. Clark[1,2], and John F. Hartwig[1,*]

[1]Department of Chemistry, University of California, Berkeley, CA, 94720, USA

[2]Department of Chemical & Biomolecular Engineering, University of California, Berkeley, CA, 94720, USA

*email: jhartwig@berkeley.edu

1. Protein Expression and Purification

1.1 Methods and Materials

Unless otherwise noted, all chemicals, salts and solvents were obtained from commercial suppliers (Sigma-Aldrich, Acros, etc.) and used without further purification. All expression media and buffers were prepared with ddH_2O (MilliQ A10 Advantage purification system, Millipore). Expression media was sterilized either by autoclave (45 min, 121°C) or a sterile syringe filter (0.22 um). To maintain sterile conditions, sterile materials and E. coli cells were manipulated near a lit Bunsen burner.

1.2 Preparation of Plasmides

Plasmids encoding hCAVII (Uniprot ID P43166) and hCAXIII (UniProt ID Q8N1Q1) were purchased from Addgene. The plasmid encoding hCAII (UniProt ID P00918) was prepared by mutating 3*His-hCAII. The procedure for preparing the 3*His-hCAII plasmide was previously reported by our group.[1] To prepare the plasmid of wild-type hCAII, we perform three point mutations (R3H, R10H and F15H) step-by-step.

1.3 Protein Expression

Protein Expression (Unlabeled Carbonic Anhydrase): Carbonic anhydrase was over-expressed in chemically competent BL21 DE3 *E. coli.* cells (UC Berkeley Macro Lab) with Terrific Broth (TB) Media. Freshly transformed cells were plated on ampicillin/LB (100mg/L) media and grown overnight at 37 °C in the oven. Single colonies were used to inoculate 3 mL LB/amp cultures, which were shaken at 37 °C at 250 rpm for 6 h. Each 3 mL culture was used to inoculate 1 L of TB media. Expressions were typically conducted in 4 × 1 L batches in baffled flasks, and the flasks were shaken at 37 °C / 250 rpm for 6 h, after which time the temperature was reduced to 28 °C. The culture was supplemented with $ZnSO_4$ (100 mg/L) and IPTG (100 mg/L) and allowed to proceed for additional 12 h. After this time, cells were recovered by centrifugation (5000 rpm, 15 minutes, 4°C). Cell pellets were frozen at -80 °C, thawed, resuspended in Ni-NTA lysis buffer (50 mM NaPi, 300 mM NaCl, 10 mM imidazole, pH 8.0), and flash frozen until purification.

1.4 Protein Purification

Protein Purification. Cell suspensions were thawed in a room-temperature water bath, decanted into 50 mL glass beakers, and lysed on ice by sonication (3 × 30 s on, 2 × 2 min off, 65% power). Cell debris was removed by centrifugation (10,000 rpm, 30 min, 4 °C), and Ni-NTA (5 mL, 50% suspension per 850 mL cell culture) was added. The lysates were briefly incubated with Ni-NTA (30 min, rt, 20 rpm) and poured into glass frits (coarse, 50 mL). The resin was washed with Ni-NTA lysis buffer (3 × 35 mL), and the desired protein was eluted with 18 mL Ni-NTA elution buffer (50 mM NaPi, 250 mM NaCl, 250 mM Imidazole, pH = 8.0). The eluted protein was dialyzed twice against Tris buffer (50 mM, pH = 8.0, 12 h, 4 °C). Gel electrophoreses was then preformed to monitor protein purity (Supplementary Figure 1). Protein concentration was measured with a NanoDrop UV-vis spectrophotometer at 280 nm.

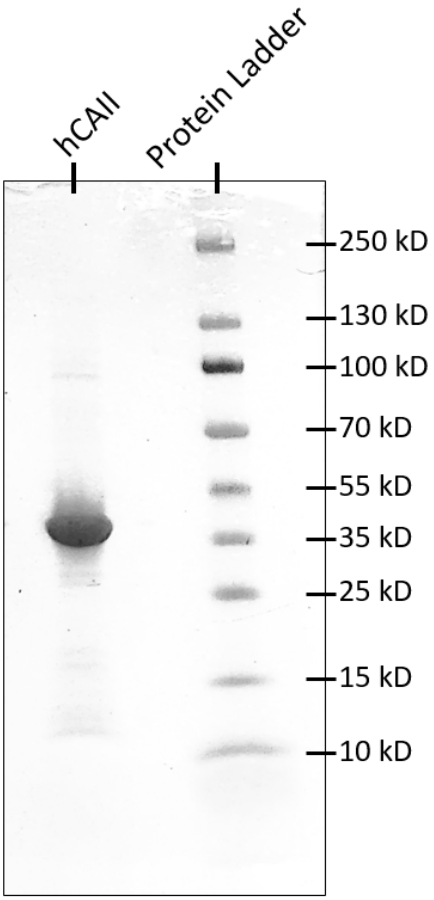

Supplementary Figure 1. Representative SDS-Page gel of hCAII ran at 300 V.

2. DNA and Protein Sequence

2.1 hCAII

DNA Sequence of hCAII

TTATTTGAAGGAAGCTTTGATTTGCCTGTTCTTCAGTGGCTGAGCTGGGCGCCAGTTGTCCACCATCAGTTCTTCGG
GTTCACCCTCCCCATTGAAGTTAAGTTTACGGAATTTCAACACCTGCTCGCTGCTGACGCTGATGGGTTCCTTGAGC
ACAATCCAGGTCACACATTCCAGAAGAGGAGGGGTGGTCAGTGAGCCTGGGTAGGTCCAGTAATCCAGGGATTCAGG
AAGGAGGCCACGAGGATCGAAGTTAGTGAAGTCAGCACTCTTGCCCTTTGTTTTAATGGAATCCAGCACATCAACAA
CTTTCTGAAGGCCCGGTTTAGCGCTGCCAACCTTCAAAAAAATACCTAGAACGGCCAGTCCATCAGGTTGCTGCACA
GCTTTCCCAAAATCCCCATATTTGGTGTTCCAATGAACCAAGTGAAGTTCTGCAGCATATTTCTTTTTATCCACAGT
ATGCTCTGAACCTTGTCCATCAAGTGAACCCCAGTGAAAGTGAAACTGAATCAATCTGTAAGTGCCATCCAGGGGTC
CTCCCTTGAGCACTGCTTTGTCCTGAGAGTCATCAAACTCCACGTTGAAAGCATGACCATTGTTGAGGATCCTCAGG
GAAGTTGCTTGATCATAGGAAACAGACAGGGGCTTCAGGGAAGGGTCATACTTGGCTGTGTGAGTGTCGATGTCAAC
AGGGGACTGGCGCTCTCCCTTGGCAATGGGGAAGTCCTTATGCCAATGCTCAGGTCCGTTGTGTTTGCCGTACCCCC
AGTGATGGGACATTGCATTGGATTGGAAGTACAGGTTTTCATGGTGATGGTGATGGTGAGAAGATTTCAT

Protein Sequence of hCAII

MKSSHHHHHHENLYFQSNAMSHHWGYGKHNGPEHWHKDFPIAKGERQSPVDIDTHTAKYDPSLKPLSVSYDQATSLR
ILNNGHAFNVEFDDSQDKAVLKGGPLDGTYRLIQFHFHWGSLDGQGSEHTVDKKKYAAELHLVHWNTKYGDFGKAVQ
QPDGLAVLGIFLKVGSAKPGLQKVVDVLDSIKTKGKSADFTNFDPRGLLPESLDYWTYPGSLTTPPLLECVTWIVLK
EPISVSSEQVLKFRKLNFNGEGEPEELMVDNWRPAQPLKNRQIKASFK*

2.2 hCAVII

DNA Sequence of hCAVII

```
TCAGAAGGAGGCCTTTACCACGCGGCCCTTCAGTGGCTGTGGTGGCCGGAAGTTGTTCACCATGTGGATCCTCTCAT
CGTCCTCCGAGGTAAAAAGCAGGCTCCGGAACTTCCCCATCTGCCTTTCAGAGATGCAGATGGGCTCCCGGAGCACA
ATCCAGGTGACACTCTCACTGAGTGGGGGAGTCGTCAGAGAGCCCGGGTAGGTCCAGTAGTGCCGGCTGGCAGGCAG
GAGGCACTTGGGGTTGAAGCAGCTGAACTGGGCTTTGGTGCCCTTGAACCGGACCATGTAGAGCGCATCTGTCAGAC
GATTCATGCTGGGGTGCTCGTCTCCTGTCTCCAAAAAAACACCAACCACAGCCAGGCCATCAGGTGCTGAGGCCGCC
TCCCCAAAAGTGCTGTACTTCTTGGCATTCCAGTGAACCAGATGCAGCTCGCTGGGGAAGGACTTGCCGTCCACCGT
GTGCTCAGAACCCACATCGTGCTTCTTGCCCCAGTGGAAGTGAAACTGCTTGAGGCGGTAGGGCCCTTCCAGGGGGC
CCCCAGTCACCACGGTTCGGTCATCGCTGTCATTGAAGTCTACCTGGACAGAGTGGCCATTGTTGGTGATGCTGAGG
GACATGCAGGCCTCATAGGAAAGCTCCAGTGGTTGCAGGCTGGGAGAGTACACAGCCTGGCTGGAGATGATATTGAT
GGGTGATTGGCGATCTCCCTGGGCAATGGGATACAGCTTGTGCCAATGCGAGGGGCCGTCGTCCTGGCCGTAGCCCC
AGCCGTGCATGGATTGGAAGTACAGGTTCTCGGTACCCAGATCTACACCAGAAGAATGATGATGATGATGGTGCAT
```

Protein Sequence of hCAVII

```
MHHHHHHSSGVDLGTENLYFQSMHGWGYGQDDGPSHWHKLYPIAQGDRQSPINIISSQAVYSPSLQPLELSYEACMS
LSITNNGHSVQVDFNDSDDRTVVTGGPLEGPYRLKQFHFHWGKKHDVGSEHTVDGKSFPSELHLVHWNAKKYSTFGE
AASAPDGLAVVGVFLETGDEHPSMNRLTDALYMVRFKGTKAQFSCFNPKCLLPASRHYWTYPGSLTTPPLSESVTWI
VLREPICISERQMGKFRSLLFTSEDDERIHMVNNFRPPQPLKGRVVKASF*
```

2.3 hCAXIII

DNA Sequence of hCAXIII

```
TCAGAAAGAGGCTCTCACTTTGCGGCCCTTTAGAGGCTGTGGTGGGCGGTGATTGCTCACCAGAAAAGCTGCTGCTT
CACCCTCCGCTGTGCACAGGAGACTGCGAAATTTGGCCAGCTGTTGAGAGCTGATGTTTATAGGTTGCTTTAAAACA
ATCCATGTGACACTCTCAAGAAGAGGTGGAACTGTAAGAGAACCAGGATATGTCCAGTAGTCCCAGGATGGTGGAAG
CAGAGACAATAGGTCAAAATTTGTGAATCGAGTTTGTTTACCCTTTTCTTTAATGGAATCCAAAGTGTCAGTAATCT
TTTGCAGTTGGGAATTAGGTTCACCAATCTGTAAAAACACTCCCAAGACAGCCAGTCCATCTGGTTCATGAGCTGCC
TCAACAAAGCTGGGGTATTTGTCTGAATTCCAGTGAACAACATGGAGCTCTGCAGCATAGCTCACTCCATCTACTAT
GTGCTCGGAGCCGTGGTCATCAGCGGACCCCCAGTGAAGGTGAACCTGCCGTAACCTGTAGCTTCCAGTGAGAGGAC
CACCACGCAGAACTGATTTGTTCTCTGTGTCATCAAAGTCAACATTGAAGGAATGGCCGCTGTTGCTGATGATTTTA
GCTGAGCTTGGGTCATACTTGATACTAAGTGGTCGGAGGGAAGAGTCATATTTCACTTCTTTGGTTTTAATCTCAAT
TGGAGATTGCTGATCACCATCAGCAATAGGGAAAAATTCCTTCCAGTGAATAGGACCGTTGTGCTCGCGGTATCCCC
AGCTGAGCCTCGACATGGATTGGAAGTACAGGTTCTCGGTACCCAGATCTACACCAGAAGAATGATGATGATGATGG
TGCAT
```

Protein Sequence of hCAVII

```
MHHHHHHSSGVDLGTENLYFQSMSRLSWGYREHNGPIHWKEFFPIADGDQQSPIEIKTKEVKYDSSLRPLSIKYDPS
SAKIISNSGHSFNVDFDDTENKSVLRGGPLTGSYRLRQVHLHWGSADDHGSEHIVDGVSYAAELHVVHWNSDKYPSF
VEAAHEPDGLAVLGVFLQIGEPNSQLQKITDTLDSIKEKGKQTRFTNFDLLSLLPPSWDYWTYPGSLTVPPLLESVT
WIVLKQPINISSQQLAKFRSLLCTAEGEAAAFLVSNHRPPQPLKGRKVRASF*
```

2.4 DNA and Protein Sequences of 10 different mutants of hCAII

Supplementary Table 1. Sequence comparison for 10 different mutants of hCAII and the catalytic activity of the expressed enzyme for reducing acetophenone in whole cell. The catalyst loading for the hCAII mutants is 0.05 mol%.

Mutants	121 Val	143 Val	198 Leu	209 Trp	Yield (%)	ee (%)
1	V	F	F	W	0	-
2	L	L	V	W	0	-
3	I	L	F	K	0	-
4	I	F	F	K	0	-
5	I	V	V	W	1.5	70
6	V	V	K	L	0	-
7	V	I	I	W	6.0	91
8	L	I	V	W	0	-
9	L	V	F	R	0	-
10	I	L	K	W	0	-
wt-hCAII (0.05 mol%)	V	V	L	W	23	92
wt-hCAII (0.2 mol%)	V	V	L	W	89	94

DNA sequence of mutant 1 VFFW:

TTATTTGAAGGAAGCTTTGATTTGCCTGTTCTTCAGTGGCTGAGCTGGGCGCCAGTTGTCCACC
ATCAGTTCTTCGGGTTCACCCTCCCCATTGAAGTTAAGTTTACGGAATTTCAACACCTGCTCGC
TGCTGACGCTGATGGGTTCCTTGAGCACAATCCAGGTCACACATTCCAGAAGAGGAGGGGTGGT
AAATGAGCCTGGGTAGGTCCAGTAATCCAGGGATTCAGGAAGGAGGCCACGAGGATCGAAGTTA
GTGAAGTCAGCACTCTTGCCCTTTGTTTTAATGGAATCCAGCACATCAACAACTTTCTGAAGGC
CCGGTTTAGCGCTGCCAACCTTCAAAAAAATACCTAGAAAGGCCAGTCCATCAGGTTGCTGCAC
AGCTTTCCCAAAATCCCCATATTTGGTGTTCCAATGAACCAAGTGAAGTTCTGCAGCATATTTC
TTTTTATCCACAGTATGCTCTGAACCTTGTCCATCAAGTGAACCCCAGTGAAAGTGAAACTGAA
TCAATCTGTAAGTGCCATCCAGGGGTCCTCCCTTGAGCACTGCTTTGTCCTGAGAGTCATCAAA
CTCCACGTTGAAAGCATGACCATTGTTGAGGATCCTCAGGGAAGTTGCTTGATCATAGGAAACA
GACAGGGGCTTCAGGGAAGGGTCATACTTGGCTGTGTGAGTGTCGATGTCAACAGGGGACTGGC
GCTCTCCCTTGGCAATGGGGAAGTCCTTATGCCAATGCTCAGGTCCGTTGTGTTTGCCGTACCC
CCAGTGATGGGACATTGCATTGGATTGGAAGTACAGGTTTTCATGGTGATGGTGATGGTGAGAA
GATTTCAT

Protein sequence of mutant 1 VFFW:

MKSSHHHHHHENLYFQSNAMSHHWGYGKHNGPEHWHKDFPIAKGERQSPVDIDTHTAKYDPSLK
PLSVSYDQATSLRILNNGHAFNVEFDDSQDKAVLKGGPLDGTYRLIQFHFHWGSLDGQGSEHTV
DKKKYAAELHLVHWNTKYGDFGKAVQQPDGLAFLGIFLKVGSAKPGLQKVVDVLDSIKTKGKSA

DFTNFDPRGLLPESLDYWTYPGSFTTPPLLECVTWIVLKEPISVSSEQVLKFRKLNFNGEGEPE
ELMVDNWRPAQPLKNRQIKASFK*

DNA sequence of mutant 2 LLVW:

TTATTTGAAGGAAGCTTTGATTTGCCTGTTCTTCAGTGGCTGAGCTGGGCGCCAGTTGTCCACC
ATCAGTTCTTCGGGTTCACCCTCCCCATTGAAGTTAAGTTTACGGAATTTCAACACCTGCTCGC
TGCTGACGCTGATGGGTTCCTTGAGCACAATCCAGGTCACACATTCCAGAAGAGGAGGGGTGGT
AACTGAGCCTGGGTAGGTCCAGTAATCCAGGGATTCAGGAAGGAGGCCACGAGGATCGAAGTTA
GTGAAGTCAGCACTCTTGCCCTTTGTTTTAATGGAATCCAGCACATCAACAACTTTCTGAAGGC
CCGGTTTAGCGCTGCCAACCTTCAAAAAAATACCTAGAAGGGCCAGTCCATCAGGTTGCTGCAC
AGCTTTCCCAAAATCCCCATATTTGGTGTTCCAATGAAGCAAGTGAAGTTCTGCAGCATATTTC
TTTTTATCCACAGTATGCTCTGAACCTTGTCCATCAAGTGAACCCCAGTGAAAGTGAAACTGAA
TCAATCTGTAAGTGCCATCCAGGGGTCCTCCCTTGAGCACTGCTTTGTCCTGAGAGTCATCAAA
CTCCACGTTGAAAGCATGACCATTGTTGAGGATCCTCAGGGAAGTTGCTTGATCATAGGAAACA
GACAGGGGCTTCAGGGAAGGGTCATACTTGGCTGTGTGAGTGTCGATGTCAACAGGGGACTGGC
GCTCTCCCTTGGCAATGGGGAAGTCCTTATGCCAATGCTCAGGTCCGTTGTGTTTGCCGTACCC
CCAGTGATGGGACATTGCATTGGATTGGAAGTACAGGTTTTCATGGTGATGGTGATGGTGAGAA
GATTTCAT

Protein sequence of mutant 2 LLVW:

MKSSHHHHHHENLYFQSNAMSHHWGYGKHNGPEHWHKDFPIAKGERQSPVDIDTHTAKYDPSLK
PLSVSYDQATSLRILNNGHAFNVEFDDSQDKAVLKGGPLDGTYRLIQFHFHWGSLDGQGSEHTV
DKKKYAAELHLLHWNTKYGDFGKAVQQPDGLALLGIFLKVGSAKPGLQKVVDVLDSIKTKGKSA
DFTNFDPRGLLPESLDYWTYPGSVTTPPLLECVTWIVLKEPISVSSEQVLKFRKLNFNGEGEPE
ELMVDNWRPAQPLKNRQIKASFK*

DNA sequence of mutant 3 ILFK:

TTATTTGAAGGAAGCTTTGATTTGCCTGTTCTTCAGTGGCTGAGCTGGGCGCCAGTTGTCCACC
ATCAGTTCTTCGGGTTCACCCTCCCCATTGAAGTTAAGTTTACGGAATTTCAACACCTGCTCGC
TGCTGACGCTGATGGGTTCCTTGAGCACAATTTTGGTCACACATTCCAGAAGAGGAGGGGTGGT
AAATGAGCCTGGGTAGGTCCAGTAATCCAGGGATTCAGGAAGGAGGCCACGAGGATCGAAGTTA
GTGAAGTCAGCACTCTTGCCCTTTGTTTTAATGGAATCCAGCACATCAACAACTTTCTGAAGGC
CCGGTTTAGCGCTACCAACCTTCAAAAAAATACCTAGAAGGGCCAGTCCATCAGGTTGCTGCAC
AGCTTTCCCAAAATCCCCATATTTGGTGTTCCAATGAATCAAGTGAAGTTCTGCAGCATATTTC
TTTTTATCCACAGTATGCTCTGAACCTTGTCCATCAAGTGAACCCCAGTGAAAGTGAAACTGAA
TCAATCTGTAAGTGCCATCCAGGGGTCCTCCCTTGAGCACTGCTTTGTCCTGAGAGTCATCAAA
CTCCACGTTGAAAGCATGACCATTGTTGAGGATCCTCAGGGAAGTTGCTTGATCATAGGAAACA
GACAGGGGCTTCAGGGAAGGGTCATACTTGGCTGTGTGAGTGTCGATGTCAACAGGGGACTGGC
GCTCTCCCTTGGCAATGGGGAAGTCCTTATGCCAATGCTCAGGTCCGTTGTGTTTGCCGTACCC
CCAGTGATGGGACATTGCATTGGATTGGAAGTACAGGTTTTCATGGTGATGGTGATGGTGAGAA
GATTTCAT

Protein sequence of mutant 3 ILFK:

MKSSHHHHHHENLYFQSNAMSHHWGYGKHNGPEHWHKDFPIAKGERQSPVDIDTHTAKYDPSLK
PLSVSYDQATSLRILNNGHAFNVEFDDSQDKAVLKGGPLDGTYRLIQFHFHWGSLDGQGSEHTV
DKKKYAAELHLIHWNTKYGDFGKAVQQPDGLALLGIFLKVGSAKPGLQKVVDVLDSIKTKGKSA

DFTNFDPRGLLPESLDYWTYPGSFTTPPLLECVTKIVLKEPISVSSEQVLKFRKLNFNGEGEPE
ELMVDNWRPAQPLKNRQIKASFK*

DNA sequence of mutant 4 IFFK:

TTATTTGAAGGAAGCTTTGATTTGCCTGTTCTTCAGTGGCTGAGCTGGGCGCCAGTTGTCCACC
ATCAGTTCTTCGGGTTCACCCTCCCCATTGAAGTTAAGTTTACGGAATTTCAACACCTGCTCGC
TGCTGACGCTGATGGGTTCCTTGAGCACAATTTTGGTCACACATTCCAGAAGAGGAGGGGTGGT
AAATGAGCCTGGGTAGGTCCAGTAATCCAGGGATTCAGGAAGGAGGCCACGAGGATCGAAGTTA
GTGAAGTCAGCACTCTTGCCCTTTGTTTTAATGGAATCCAGCACATCAACAACTTTCTGAAGGC
CCGGTTTAGCGCTGCCAACCTTCAAAAAAATACCTAGAAAGGCCAGTCCATCAGGTTGCTGCAC
AGCTTTCCCAAAATCCCCATATTTGGTGTTCCAATGAATCAAGTGAAGTTCTGCAGCATATTTC
TTTTTATCCACAGTATGCTCTGAACCTTGTCCATCAAGTGAACCCCAGTGAAAGTGAAACTGAA
TCAATCTGTAAGTGCCATCCAGGGGTCCTCCCTTGAGCACTGCTTTGTCCTGAGAGTCATCAAA
CTCCACGTTGAAAGCATGACCATTGTTGAGGATCCTCAGGGAAGTTGCTTGATCATAGGAAACA
GACAGGGGCTTCAGGGAAGGGTCATACTTGGCTGTGTGAGTGTCGATGTCAACAGGGGACTGGC
GCTCTCCCTTGGCAATGGGGAAGTCCTTATGCCAATGCTCAGGTCCGTTGTGTTTGCCGTACCC
CCAGTGATGGGACATTGCATTGGATTGGAAGTACAGGTTTTCATGGTGATGGTGATGGTGAGAA
GATTTCAT

Protein sequence of mutant 4 IFFK:

MKSSHHHHHHENLYFQSNAMSHHWGYGKHNGPEHWHKDFPIAKGERQSPVDIDTHTAKYDPSLK
PLSVSYDQATSLRILNNGHAFNVEFDDSQDKAVLKGGPLDGTYRLIQFHFHWGSLDGQGSEHTV
DKKKYAAELHLIHWNTKYGDFGKAVQQPDGLAFLGIFLKVGSAKPGLQKVVDVLDSIKTKGKSA
DFTNFDPRGLLPESLDYWTYPGSFTTPPLLECVTKIVLKEPISVSSEQVLKFRKLNFNGEGEPE
ELMVDNWRPAQPLKNRQIKASFK*

DNA sequence of mutant 5 IVVW:

TTATTTGAAGGAAGCTTTGATTTGCCTGTTCTTCAGTGGCTGAGCTGGGCGCCAGTTGTCCACC
ATCAGTTCTTCGGGTTCACCCTCCCCATTGAAGTTAAGTTTACGGAATTTCAACACCTGCTCGC
TGCTGACGCTGATGGGTTCCTTGAGCACAATCCAGGTCACACATTCCAGAAGAGGAGGGGTGGT
AACTGAGCCTGGGTAGGTCCAGTAATCCAGGGATTCAGGAAGGAGGCCACGAGGATCGAAGTTA
GTGAAGTCAGCACTCTTGCCCTTTGTTTTAATGGAATCCAGCACATCAACAACTTTCTGAAGGC
CCGGTTTAGCGCTGCCAACCTTCAAAAAAATACCTAGAACGGCCAGTCCATCAGGTTGCTGCAC
AGCTTTCCCAAAATCCCCATATTTGGTGTTCCAATGAATCAAGTGAAGTTCTGCAGCATATTTC
TTTTTATCCACAGTATGCTCTGAACCTTGTCCATCAAGTGAACCCCAGTGAAAGTGAAACTGAA
TCAATCTGTAAGTGCCATCCAGGGGTCCTCCCTTGAGCACTGCTTTGTCCTGAGAGTCATCAAA
CTCCACGTTGAAAGCATGACCATTGTTGAGGATCCTCAGGGAAGTTGCTTGATCATAGGAAACA
GACAGGGGCTTCAGGGAAGGGTCATACTTGGCTGTGTGAGTGTCGATGTCAACAGGGGACTGGC
GCTCTCCCTTGGCAATGGGGAAGTCCTTATGCCAATGCTCAGGTCCGTTGTGTTTGCCGTACCC
CCAGTGATGGGACATTGCATTGGATTGGAAGTACAGGTTTTCATGGTGATGGTGATGGTGAGAA
GATTTCAT

Protein sequence of mutant 5 IVVW:

MKSSHHHHHHENLYFQSNAMSHHWGYGKHNGPEHWHKDFPIAKGERQSPVDIDTHTAKYDPSLK
PLSVSYDQATSLRILNNGHAFNVEFDDSQDKAVLKGGPLDGTYRLIQFHFHWGSLDGQGSEHTV
DKKKYAAELHLIHWNTKYGDFGKAVQQPDGLAVLGIFLKVGSAKPGLQKVVDVLDSIKTKGKSA

DFTNFDPRGLLPESLDYWTYPGSVTTPPLLECVTWIVLKEPISVSSEQVLKFRKLNFNGEGEPE
ELMVDNWRPAQPLKNRQIKASFK*

DNA sequence of mutant 6 VVKL:

TTATTTGAAGGAAGCTTTGATTTGCCTGTTCTTCAGTGGCTGAGCTGGGCGCCAGTTGTCCACC
ATCAGTTCTTCGGGTTCACCCTCCCCATTGAAGTTAAGTTTACGGAATTTCAACACCTGCTCGC
TGCTGACGCTGATGGGTTCCTTGAGCACAATAAGGGTCACACATTCCAGAAGAGGAGGGGTGGT
TTTTGAGCCTGGGTAGGTCCAGTAATCCAGGGATTCAGGAAGGAGGCCACGAGGATCGAAGTTA
GTGAAGTCAGCACTCTTGCCCTTTGTTTTAATGGAATCCAGCACATCAACAACTTTCTGAAGGC
CCGGTTTAGCGCTGCCAACCTTCAAAAAAATACCTAGAACGGCCAGTCCATCAGGTTGCTGCAC
AGCTTTCCCAAAATCCCCATATTTGGTGTTCCAATGAACCAAGTGAAGTTCTGCAGCATATTTC
TTTTTATCCACAGTATGCTCTGAACCTTGTCCATCAAGTGAACCCCAGTGAAAGTGAAACTGAA
TCAATCTGTAAGTGCCATCCAGGGGTCCTCCCTTGAGCACTGCTTTGTCCTGAGAGTCATCAAA
CTCCACGTTGAAAGCATGACCATTGTTGAGGATCCTCAGGGAAGTTGCTTGATCATAGGAAACA
GACAGGGGCTTCAGGGAAGGGTCATACTTGGCTGTGTGAGTGTCGATGTCAACAGGGGACTGGC
GCTCTCCCTTGGCAATGGGGAAGTCCTTATGCCAATGCTCAGGTCCGTTGTGTTTGCCGTACCC
CCAGTGATGGGACATTGCATTGGATTGGAAGTACAGGTTTTCATGGTGATGGTGATGGTGAGAA
GATTTCAT

Protein sequence of mutant 6 VVKL:

MKSSHHHHHHENLYFQSNAMSHHWGYGKHNGPEHWHKDFPIAKGERQSPVDIDTHTAKYDPSLK
PLSVSYDQATSLRILNNGHAFNVEFDDSQDKAVLKGGPLDGTYRLIQFHFHWGSLDGQGSEHTV
DKKKYAAELHLVHWNTKYGDFGKAVQQPDGLAVLGIFLKVGSAKPGLQKVVDVLDSIKTKGKSA
DFTNFDPRGLLPESLDYWTYPGSKTTPPLLECVTLIVLKEPISVSSEQVLKFRKLNFNGEGEPE
ELMVDNWRPAQPLKNRQIKASFK*

DNA sequence of mutant 7 VIIW:

TTATTTGAAGGAAGCTTTGATTTGCCTGTTCTTCAGTGGCTGAGCTGGGCGCCAGTTGTCCACC
ATCAGTTCTTCGGGTTCACCCTCCCCATTGAAGTTAAGTTTACGGAATTTCAACACCTGCTCGC
TGCTGACGCTGATGGGTTCCTTGAGCACAATCCAGGTCACACATTCCAGAAGAGGAGGGGTGGT
AATTGAGCCTGGGTAGGTCCAGTAATCCAGGGATTCAGGAAGGAGGCCACGAGGATCGAAGTTA
GTGAAGTCAGCACTCTTGCCCTTTGTTTTAATGGAATCCAGCACATCAACAACTTTCTGAAGGC
CCGGTTTAGCGCTGCCAACCTTCAAAAAAATACCTAGAATGGCCAGTCCATCAGGTTGCTGCAC
AGCTTTCCCAAAATCCCCATATTTGGTGTTCCAATGAACCAAGTGAAGTTCTGCAGCATATTTC
TTTTTATCCACAGTATGCTCTGAACCTTGTCCATCAAGTGAACCCCAGTGAAAGTGAAACTGAA
TCAATCTGTAAGTGCCATCCAGGGGTCCTCCCTTGAGCACTGCTTTGTCCTGAGAGTCATCAAA
CTCCACGTTGAAAGCATGACCATTGTTGAGGATCCTCAGGGAAGTTGCTTGATCATAGGAAACA
GACAGGGGCTTCAGGGAAGGGTCATACTTGGCTGTGTGAGTGTCGATGTCAACAGGGGACTGGC
GCTCTCCCTTGGCAATGGGGAAGTCCTTATGCCAATGCTCAGGTCCGTTGTGTTTGCCGTACCC
CCAGTGATGGGACATTGCATTGGATTGGAAGTACAGGTTTTCATGGTGATGGTGATGGTGAGAA
GATTTCAT

Protein sequence of mutant 7 VIIW:

MKSSHHHHHHENLYFQSNAMSHHWGYGKHNGPEHWHKDFPIAKGERQSPVDIDTHTAKYDPSLK
PLSVSYDQATSLRILNNGHAFNVEFDDSQDKAVLKGGPLDGTYRLIQFHFHWGSLDGQGSEHTV
DKKKYAAELHLVHWNTKYGDFGKAVQQPDGLAILGIFLKVGSAKPGLQKVVDVLDSIKTKGKSA

DFTNFDPRGLLPESLDYWTYPGSITTPPLLECVTWIVLKEPISVSSEQVLKFRKLNFNGEGEPE
ELMVDNWRPAQPLKNRQIKASFK*

DNA sequence of mutant 8 LIVW:

TTATTTGAAGGAAGCTTTGATTTGCCTGTTCTTCAGTGGCTGAGCTGGGCGCCAGTTGTCCACC
ATCAGTTCTTCGGGTTCACCCTCCCCATTGAAGTTAAGTTTACGGAATTTCAACACCTGCTCGC
TGCTGACGCTGATGGGTTCCTTGAGCACAATCCAGGTCACACATTCCAGAAGAGGAGGGGTGGT
AACTGAGCCTGGGTAGGTCCAGTAATCCAGGGATTCAGGAAGGAGGCCACGAGGATCGAAGTTA
GTGAAGTCAGCACTCTTGCCCTTTGTTTTAATGGAATCCAGCACATCAACAACTTTCTGAAGGC
CCGGTTTAGCGCTGCCAACCTTCAAAAAAATACCTAGAATGGCCAGTCCATCAGGTTGCTGCAC
AGCTTTCCCAAAATCCCCATATTTGGTGTTCCAATGAAGCAAGTGAAGTTCTGCAGCATATTTC
TTTTTATCCACAGTATGCTCTGAACCTTGTCCATCAAGTGAACCCCAGTGAAAGTGAAACTGAA
TCAATCTGTAAGTGCCATCCAGGGGTCCTCCCTTGAGCACTGCTTTGTCCTGAGAGTCATCAAA
CTCCACGTTGAAAGCATGACCATTGTTGAGGATCCTCAGGGAAGTTGCTTGATCATAGGAAACA
GACAGGGGCTTCAGGGAAGGGTCATACTTGGCTGTGTGAGTGTCGATGTCAACAGGGGACTGGC
GCTCTCCCTTGGCAATGGGGAAGTCCTTATGCCAATGCTCAGGTCCGTTGTGTTTGCCGTACCC
CCAGTGATGGGACATTGCATTGGATTGGAAGTACAGGTTTTCATGGTGATGGTGATGGTGAGAA
GATTTCAT

Protein sequence of mutant 8 LIVW:

MKSSHHHHHHENLYFQSNAMSHHWGYGKHNGPEHWHKDFPIAKGERQSPVDIDTHTAKYDPSLK
PLSVSYDQATSLRILNNGHAFNVEFDDSQDKAVLKGGPLDGTYRLIQFHFHWGSLDGQGSEHTV
DKKKYAAELHLLHWNTKYGDFGKAVQQPDGLAILGIFLKVGSAKPGLQKVVDVLDSIKTKGKSA
DFTNFDPRGLLPESLDYWTYPGSVTTPPLLECVTWIVLKEPISVSSEQVLKFRKLNFNGEGEPE
ELMVDNWRPAQPLKNRQIKASFK*

DNA sequence of mutant 9 LVFR:

TTATTTGAAGGAAGCTTTGATTTGCCTGTTCTTCAGTGGCTGAGCTGGGCGCCAGTTGTCCACC
ATCAGTTCTTCGGGTTCACCCTCCCCATTGAAGTTAAGTTTACGGAATTTCAACACCTGCTCGC
TGCTGACGCTGATGGGTTCCTTGAGCACAATTCGGGTCACACATTCCAGAAGAGGAGGGGTGGT
AAATGAGCCTGGGTAGGTCCAGTAATCCAGGGATTCAGGAAGGAGGCCACGAGGATCGAAGTTA
GTGAAGTCAGCACTCTTGCCCTTTGTTTTAATGGAATCCAGCACATCAACAACTTTCTGAAGGC
CCGGTTTAGCGCTGCCAACCTTCAAAAAAATACCTAGAACGGCCAGTCCATCAGGTTGCTGCAC
AGCTTTCCCAAAATCCCCATATTTGGTGTTCCAATGAAGCAAGTGAAGTTCTGCAGCATATTTC
TTTTTATCCACAGTATGCTCTGAACCTTGTCCATCAAGTGAACCCCAGTGAAAGTGAAACTGAA
TCAATCTGTAAGTGCCATCCAGGGGTCCTCCCTTGAGCACTGCTTTGTCCTGAGAGTCATCAAA
CTCCACGTTGAAAGCATGACCATTGTTGAGGATCCTCAGGGAAGTTGCTTGATCATAGGAAACA
GACAGGGGCTTCAGGGAAGGGTCATACTTGGCTGTGTGAGTGTCGATGTCAACAGGNGACTGGC
GCTCTCCCTTGGCAATGGGGAAGTCCTTATGCCAATGCTCAGGTCCGTTGTGTTTGCCGTACCC
CCAGTGATGGGACATTGCATTGGATTGGAAGTACAGGTTTTCATGGTGATGGTGATGGTGAGAA
GATTTCAT

Protein sequence of mutant 9 LVFR:

MKSSHHHHHHENLYFQSNAMSHHWGYGKHNGPEHWHKDFPIAKGERQSPVDIDTHTAKYDPSLK
PLSVSYDQATSLRILNNGHAFNVEFDDSQDKAVLKGGPLDGTYRLIQFHFHWGSLDGQGSEHTV
DKKKYAAELHLLHWNTKYGDFGKAVQQPDGLAVLGIFLKVGSAKPGLQKVVDVLDSIKTKGKSA

DFTNFDPRGLLPESLDYWTYPGSFTTPPLLECVTRIVLKEPISVSSEQVLKFRKLNFNGEGEPE
ELMVDNWRPAQPLKNRQIKASFK*

DNA sequence of mutant 10 ILKW:

TTATTTGAAGGAAGCTTTGATTTGCCTGTTCTTCAGTGGCTGAGCTGGGCGCCAGTTGTCCACC
ATCAGTTCTTCGGGTTCACCCTCCCCATTGAAGTTAAGTTTACGGAATTTCAACACCTGCTCGC
TGCTGACGCTGATGGGTTCCTTGAGCACAATCCAGGTCACACATTCCAGAAGAGGAGGGGTGGT
TTTTGAGCCTGGGTAGGTCCAGTAATCCAGGGATTCAGGAAGGAGGCCACGAGGATCGAAGTTA
GTGAAGTCAGCACTCTTGCCCTTTGTTTTAATGGAATCCAGCACATCAACAACTTTCTGAAGGC
CCGGTTTAGCGCTGCCAACCTTCAAAAAAATACCTAGAAGGGCCAGTCCATCAGGTTGCTGCAC
AGCTTTCCCAAAATCCCCATATTTGGTGTTCCAATGAATCAAGTGAAGTTCTGCAGCATATTTC
TTTTTATCCACAGTATGCTCTGAACCTTGTCCATCAAGTGAACCCCAGTGAAAGTGAAACTGAA
TCAATCTGTAAGTGCCATCCAGGGGTCCTCCCTTGAGCACTGCTTTGTCCTGAGAGTCATCAAA
CTCCACGTTGAAAGCATGACCATTGTTGAGGATCCTCAGGGAAGTTGCTTGATCATAGGAAACA
GACAGGGGCTTCAGGGAAGGGTCATACTTGGCTGTGTGAGTGTCGATGTCAACAGGGGACTGGC
GCTCTCCCTTGGCAATGGGGAAGTCCTTATGCCAATGCTCAGGTCCGTTGTGTTTGCCGTACCC
CCAGTGATGGGACATTGCATTGGATTGGAAGTACAGGTTTTCATGGTGATGGTGATGGTGAGAA
GATTTCAT

Protein sequence of mutant 10 ILKW:

MKSSHHHHHHENLYFQSNAMSHHWGYGKHNGPEHWHKDFPIAKGERQSPVDIDTHTAKYDPSLK
PLSVSYDQATSLRILNNGHAFNVEFDDSQDKAVLKGGPLDGTYRLIQFHFHWGSLDGQGSEHTV
DKKKYAAELHLIHWNTKYGDFGKAVQQPDGLALLGIFLKVGSAKPGLQKVVDVLDSIKTKGKSA
DFTNFDPRGLLPESLDYWTYPGSKTTPPLLECVTWIVLKEPISVSSEQVLKFRKLNFNGEGEPE
ELMVDNWRPAQPLKNRQIKASFK*

3. Catalytic Reactions

3.1 General Method

All enzyme-catalyzed reactions were performed at room temperature (23 °C) on an orbital shaker at the rate of 300 rpm. Unless otherwise noted, catalytic reactions were performed in 20 mL scintillation vials. The vials were loosely capped during catalytic reactions to avoid pressure accumulation due to the evolution of hydrogen. Protein catalysts were diluted to reaction concentrations in Tris buffer (50 mM, pH = 8.0) before adding to the reaction vials. To purify the reaction product, silica gel chromatography was conducted with AMD Silica Gel 60, 230-400 mesh. ^{1}H NMR spectra and ^{19}F NMR spectra were recorded on the Bruker AVB-400 instrument with ^{1}H operating frequencies of 400 MHz and ^{19}F operating frequency of 376 MHz. Chemical shifts (δ) are reported in ppm, relative to the residual solvent signal ($CDCl_3$: 7.26 ppm for ^{1}H NMR).

3.2 Procedure for typical catalytic experiments

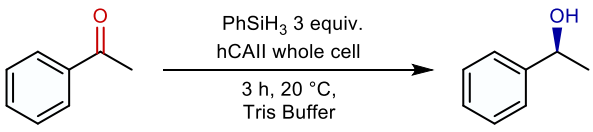

Catalysis with purified enzyme:

The 0.1 mM solution of hCAII in Tris Buffer (50 mM, pH 8.0) was stored at -80 °C, and warmed to room temperature before catalytic reactions. To a 20 mL scintillation vial was added 1 ml of the catalyst stock solution (0.1 umol of hCAII), followed by phenylsilane (18 μL, 150 μmol), ketone (50 μmol) and 2 mL of Tris buffer (50 mM, pH = 8.0). The vial was capped and incubated on an orbital shaker (20 °C, 300 rpm) for 3 h. Upon completion, the reaction mixture was extracted with 5 mL EtOAc and evaporated under vacuum. The chiral alcohol products were dissolved in $CDCl_3$, mesitylene was added as the internal standard, and the reaction yields were measured by ^1H NMR spectroscopy. The products were purified by silica column chromatography eluting with EtOAc/hexane (2%-20%), and e.e.'s were determined by supercritical fluid chromatography (SFC) or high performance liquid chromatography (HPLC).

Catalysis with lyophilized cell powder:

The amount of hCAII in lyophilized cell powder was determined by first purifying the enzyme with Ni-NTA resin, followed by measurement of protein concentration with NanoDrop UV-Vis spectrophotometer (see section 1.3 for details). The amount of hCAII was quantified to be 19 mg per 100 mg of lyophilized cell powder.

To a 20 mL scintillation vial containing 3 mL of Tris buffer (50 mM, pH = 8.0) was added 15 mg of the lyophilized cell powder (containing 0.1 umol of hCAII), followed by phenylsilane (18 μL, 150 μmol) and ketone (50 μmol). The vial was capped, vortexed briefly, and incubated on an orbital shaker (20 °C, 300 rpm) for 3 h. Upon completion, the reaction mixture was extracted with EtOAc, and the chiral alcohol product was measured by ^1H NMR spectroscopy for yields and SFC or HPLC for e.e. values.

3.3 Procedure for gram-scale reaction

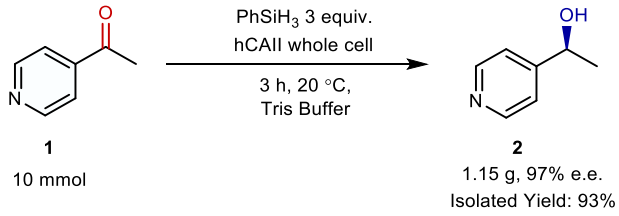

1
10 mmol

2
1.15 g, 97% e.e.
Isolated Yield: 93%

To a 1 L Erlenmeyer flask containing 500 mL of Tris buffer (50 mM, pH = 8.0) was added 1.2 g of the lyophilized cell powder (containing 8 umol of hCAII), followed by phenylsilane (3.6 mL, 30 mmol) and ketone (1.1 mL, 10 mmol). The reaction mixture was vigorously stirred on an stir plate (20 °C, 600 rpm) for 3 h. Upon completion, the reaction mixture was monitored by ^1H NMR spectroscopy to measure the conversion of ketone. The mixture was extracted with EtOAc three times (1.5 L), washed with water three times (1.5 L), and then dried with Na_2SO_4. Upon evaporation to dryness, the chiral alcohol product was obtained in 93% isolated yield (1.15 g) as a white solid without further purification. The configuration and enantiomeric excess of the product was analyzed by SFC to be mainly the S-enantiomer in 97% e.e.

4 Preparation of Racemic Standards

4.1 Procedure for typical synthesis of racemic alcohol

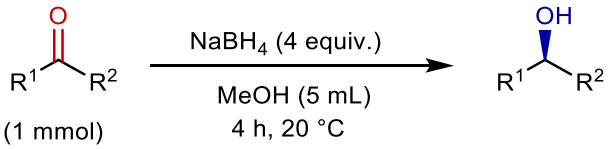

The ketone (1 mmol) was dissolved in 4 mL of methanol, cooled to 0 °C in ice, and $NaBH_4$ (4 mmol, 152 mg) was added with stirring. The mixture was stirred at room temperature for 3 h, then 20 mL of water was added to the reaction mixture to quench the excess $NaBH_4$. The mixture was extracted with 30 mL of EtOAc and dried with Na_2SO_4. The alcohol product was obtained by evaporation of EtOAc and was purified by silica column chromatography eluting with hexane/EtOAc. All compounds were obtained in high chemical yields and purity, as determined by ^{1}H NMR spectroscopy.

4.2 Synthesis of racemic 3-hydroxy-1-phenylbutan-1-one

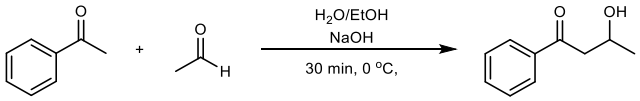

The racemic sample of 3-hydroxy-1-phenylbutan-1-one was synthesized following a modified literature procedure.[2] To a solution of NaOH (0.184 g, 4.6 mmol) in water (1 mL) and EtOH (2 mL), acetophenone (0.49 mL, 4.16 mmol) and acetaldehyde (0.3 mL. 5.3 mmol) were sequentially added. After stirring for 15 min, a saturated aqueous solution of NH_4Cl (5 mL) was added, and the solution was extracted with EtOAc. (3 × 15 mL). The residue was purified by silica gel column chromatography eluting with 30% EtOAc in hexane. 3-hydroxy-1-phenylbutan-1-one was obtained in 60% yield as a colorless oil.

^{1}H NMR (400 MHz, $CDCl_3$) δ 8.01 (dt, J = 8.5, 1.1 Hz, 2H), 7.73 – 7.63 (m, 1H), 7.58 – 7.47 (m, 2H), 4.46 (dqd, J = 9.3, 6.3, 3.1 Hz, 1H), 3.37 (d, J = 3.1 Hz, 1H), 3.23 (ddd, J = 17.7, 2.8, 1.0 Hz, 1H), 3.09 (dd, J = 17.8, 9.0 Hz, 1H), 1.35 (d, J = 6.4 Hz, 3H).

4.3 Synthesis of racemic 2-hydroxy-1-phenylpropan-1-one

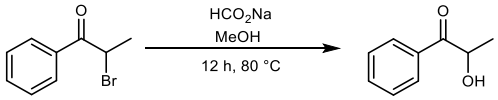

The racemic sample of 2-hydroxy-1-phenylpropan-1-one was synthesized following a modified literature procedure.[3] To a solution of 2-bromopropiophenone (3.5 g, 16.4 mmol) in MeOH (20 mL) was added sodium formate (4.4 g, 64.8 mmol). After the mixture was refluxed for 12 h, the solvent was evaporated. The residue was extracted with EtOAc, and the resulting solution was washed with water and brine. After drying the solution with anhydrous $MgSO_4$, filtration and evaporation, the crude product was purified by silica gel column chromatography eluting with 10% EtOAc in hexane to give 2-hydroxy-1-phenylpropan-1-one in 90% yield as a colorless oil.

^{1}H NMR (400 MHz, $CDCl_3$) δ 7.93 (dt, J = 8.5, 1.8 Hz, 2H), 7.74 – 7.59 (m, 1H), 7.51 (td, J = 7.8, 7.3, 1.6 Hz, 2H), 5.26 – 5.12 (m, 1H), 3.79 (d, J = 6.3 Hz, 1H), 1.46 (d, J = 7.1 Hz, 3H).

5. Detection of H_2 and HD

5.1 Procedure for detection of H_2

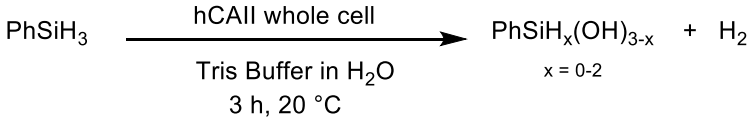

A 4 mL vial was charged with 1 mL of the 0.1 mM solution of the hCAII enzyme in Tris buffer (50 mM in water, pH 8.0), followed by the lyophilized hCAII (3.1 mg, 0.1 μmol), and 1,000 equivalents of $PhSiH_3$ (12 μL, 100 μmol) relative to hCAII. The vial was sealed with a septum and incubated on an orbital shaker (20 °C, 300 rpm) for 30 min. Upon completion, 0.8 mL of benzene-d_6 was added through the septum by syringe. The vial was gently shaken to ensure that the H_2 gas in the head space dissolved. After the aqueous layer was separated from the organic layer, the benzene-d_6 solution was transferred to an evacuated J Young NMR tube via cannula. The identity of H_2 was confirmed by ^{1}H NMR spectroscopy

5.2 Procedure for detection of HD

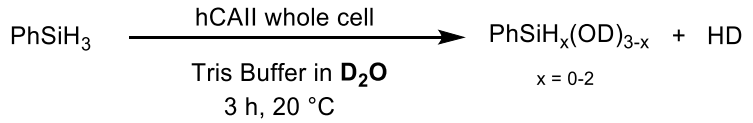

A 4 mL vial was charged with 1 mL of Tris buffer (50 mM, pH 8.0) that was prepared with D_2O, followed by the lyophilized hCAII (3.1 mg, 0.1 μmol), and 1,000 equivalents of $PhSiH_3$ (12 μL, 100 μmol) relative to hCAII. The vial was sealed with a septum and incubated on an orbital shaker (20 °C, 300 rpm) for 30 min. Upon completion, 0.8 mL of benzene-d_6 was added through the septum by syringe. The vial was gently shaken to ensure that the HD gas in the head space dissolved. After the aqueous layer was separated from the organic layer, the benzene-d_6 solution was transferred to an evacuated J Young NMR tube via cannula. The identity of HD was confirmed by ^{1}H NMR spectroscopy.

6. Products and Characterizations

(S)-1-(pyridin-4-yl)ethan-1-ol (**2**)

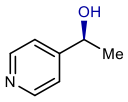

^{1}H NMR (400 MHz, $CDCl_3$) δ 8.83 – 8.33 (m, 2H), 7.29 – 7.26 (m, 2H), 4.88 (q, J = 6.5 Hz, 1H), 1.48 (d, J = 6.6 Hz, 3H).

^{13}C NMR (151 MHz, $CDCl_3$) δ 155.44, 149.61, 120.64, 68.78, 25.21.

Spectral data match those previously reported.[4]

Separation of enantiomers: SFC IC column, 20% iPrOH in $scCO_2$, 2.5 mL/min flow rate.

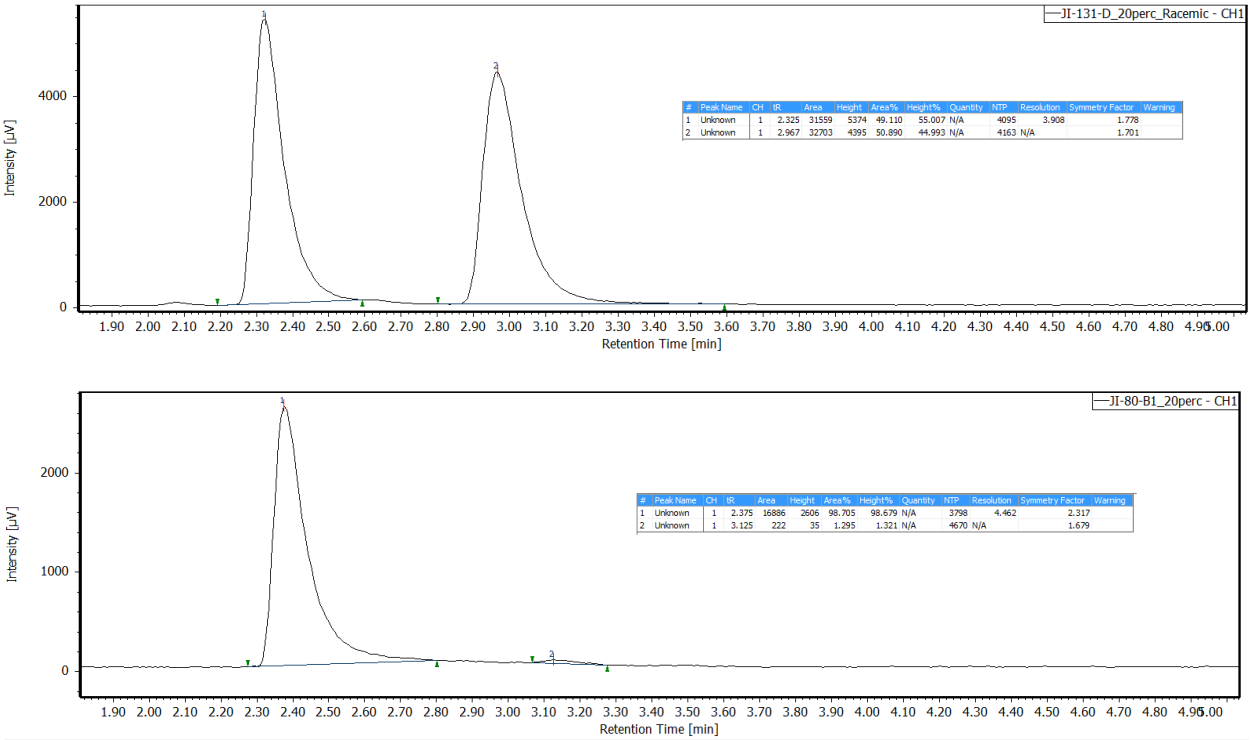

Supplementary Figure 2. SFC traces of the racemic 1-(pyridin-4-yl)ethan-1-ol (top) and the enantioenriched products of the hCAII-catalyzed reduction (bottom).

(S)-1-(pyridin-4-yl)ethan-1-d-1-ol (**4**)

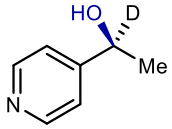

^{1}H NMR (400 MHz, $CDCl_3$) δ 8.69 – 8.37 (m, 1H), 7.66 – 6.96 (m, 1H), 1.52 (s, 1H).

^{2}H NMR (92 MHz, $CDCl_3$) δ 4.87.

^{13}C NMR (151 MHz, $CDCl_3$) δ 155.55, 149.50, 120.68, 68.30, 25.07.

HRMS (EI+) calcd for $[C_7H_8{}^2HNO]^+$: m/z 125.0820, found 125.0819.

Optical Rotation: $[\alpha]20_D$ = -39.8 (c 1.0, CH_2Cl_2)

Separation of enantiomers: HPLC OD-H column, 10% iPrOH in hexane, 1.0 mL/min flow rate.

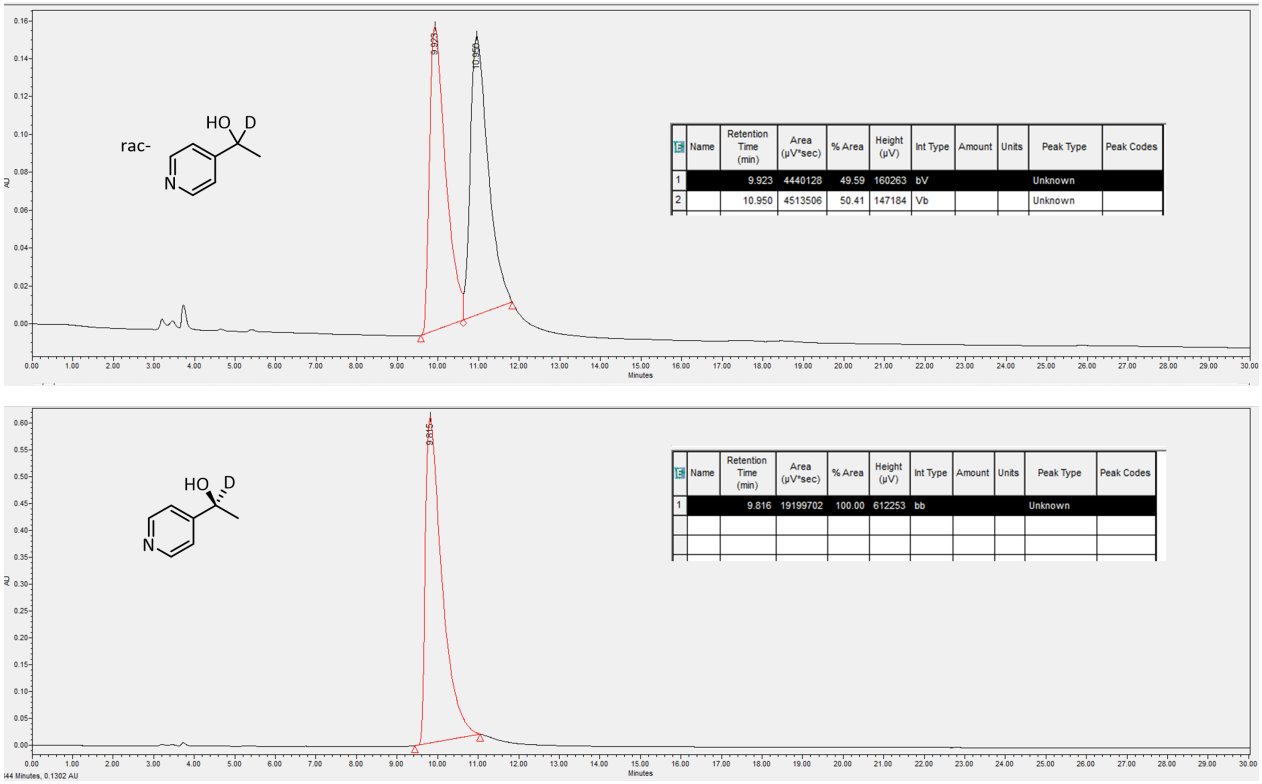

Supplementary Figure 3. HPLC traces of the racemic 1-(pyridin-4-yl)ethan-1-*d*-1-ol (top) and the enantioenriched products of the hCAII-catalyzed reduction (bottom).

(S)-1-phenylethan-1-d-1-ol (**6**)

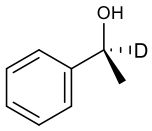

^{1}H NMR (400 MHz, $CDCl_3$) δ 7.46 – 7.39 (m, 3H), 7.39 – 7.29 (m, 2H), 1.54 (t, J = 0.9 Hz, 3H).

^{2}H NMR (77 MHz, $CDCl_3$) δ 4.91

^{13}C NMR (151 MHz, $CDCl_3$) δ 145.77, 128.55, 128.52, 127.52, 127.50, 125.42, 125.40, 70.16, 70.01, 69.87, 25.03.

Spectral data match those previously reported.[5,6]

Separation of enantiomers: HPLC OJ-H column, 5.0% iPrOH in hexanes, 1.0 mL/min flow rate.

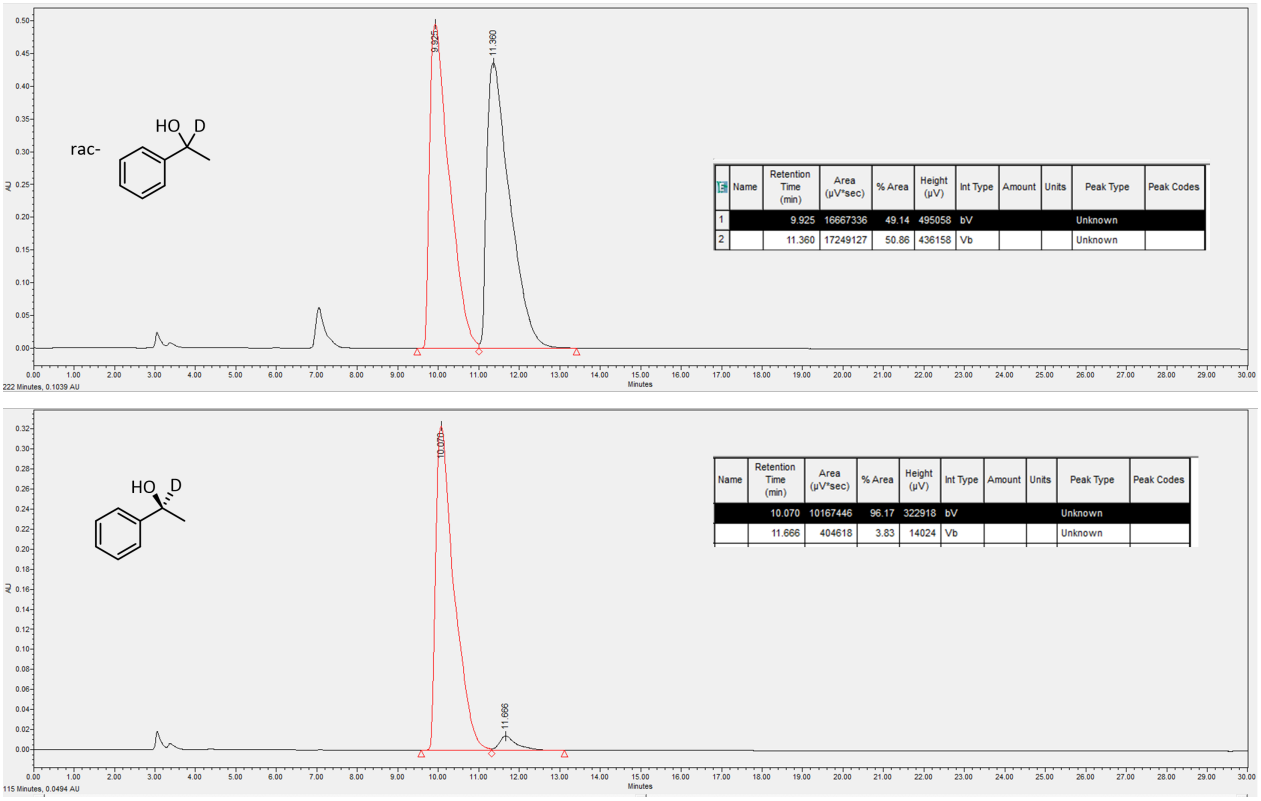

Supplementary Figure 4. HPLC traces of the racemic 1-phenylethan-1-*d*-1-ol (top) and the enantioenriched products of the hCAII-catalyzed reduction (bottom).

(S)-1-phenylethan-1-ol (**7**)

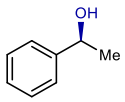

^{1}H NMR (400 MHz, $CDCl_3$) δ 7.40 - 7.31 (m, 4H), 7.30 - 7.23 (m, 1H), 4.93-4.85 (m, 1H), 1.90 (d, J = 3.6 Hz, 1H), 1.49 (d, J = 6.4 Hz, 3H).

^{13}C NMR (151 MHz, $CDCl_3$) δ 145.97, 128.63, 127.60, 125.53, 70.53, 25.28.

Spectral data match those previously reported.[4]

Enantiomer separation: SFC OJ-H column, 5% iPrOH in $scCO_2$, 2.5 mL/min flow rate.

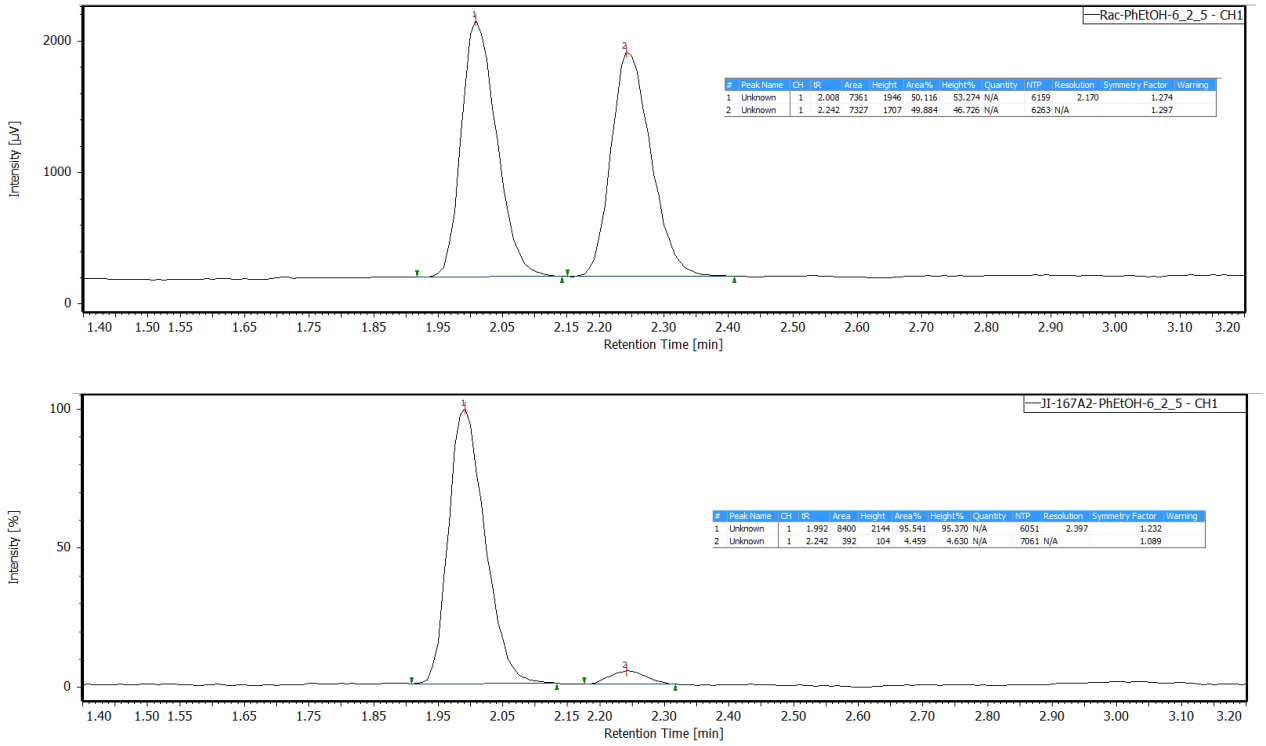

Supplementary Figure 5. SFC traces of the racemic 1-phenylethan-1-ol (top) and the enantioenriched products of the hCAII-catalyzed reduction (bottom).

(S)-1-(4-chlorophenyl)ethan-1-ol (**8**)

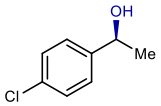

^{1}H NMR (400 MHz, $CDCl_3$) δ 7.90 – 7.81 (m, 2H), 7.43 – 7.33 (m, 2H), 4.83 (q, J = 6.5 Hz, 1H), 1.42 (d, J = 6.5 Hz, 3H).

^{13}C NMR (151 MHz, $CDCl_3$) δ 144.38, 133.20, 128.73, 126.92, 69.87, 25.40.

Spectral data match those previously reported.[4]

Enantiomer separation: SFC OJ-H column, 5% iPrOH in $scCO_2$, 2.5 mL/min flow rate.

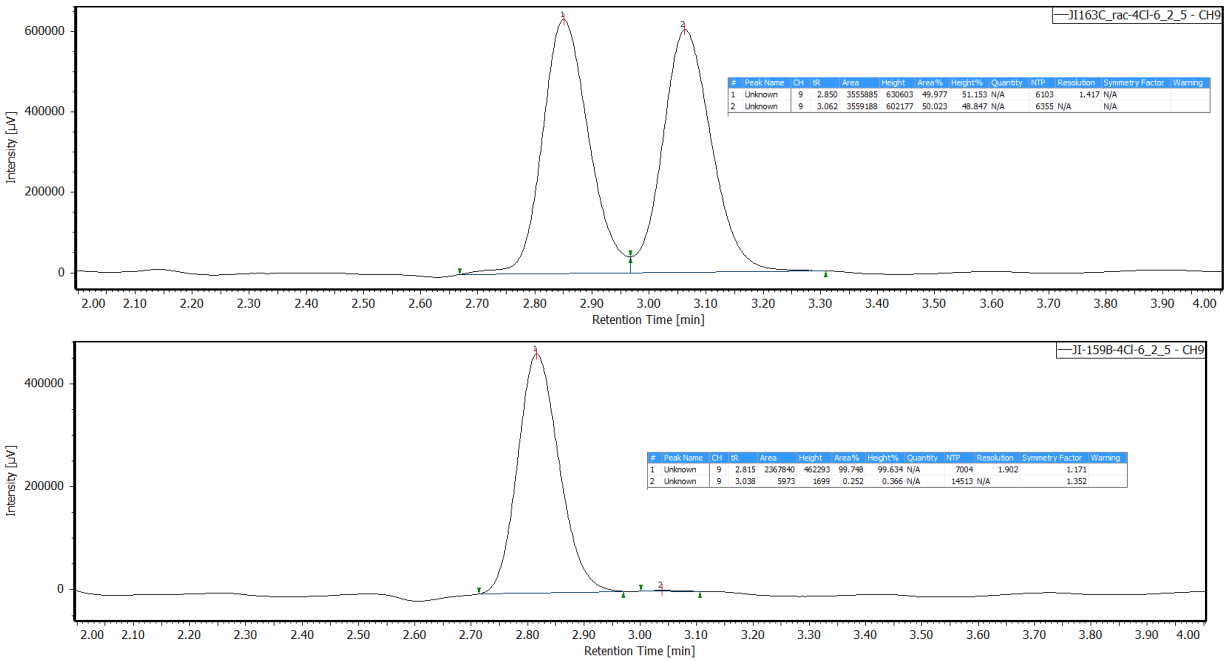

Supplementary Figure 6. SFC traces of the racemic 1-(4-chlorophenyl)ethan-1-ol (top) and the enantioenriched products of the hCAII-catalyzed reduction (bottom).

(S)-1-(4-bromophenyl)ethan-1-ol (**9**)

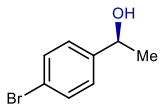

^{1}H NMR (400 MHz, $CDCl_3$) δ 7.46 (d, *J* = 8.0 Hz, 2H), 7.24 (d, *J* = 8.4 Hz, 2H), 4.85 (q, *J* = 6.0 Hz, 1H), 1.96 (s, 1H), 1.46 (d, *J* = 6.4 Hz, 3H).
^{13}C NMR (151 MHz, $CDCl_3$) δ 144.88, 131.66, 127.27, 121.27, 69.88, 25.34.
Spectral data match those previously reported.[4]

Enantiomer separation: SFC OJ-H column, 5% iPrOH in $scCO_2$, 2.5 mL/min flow rate.

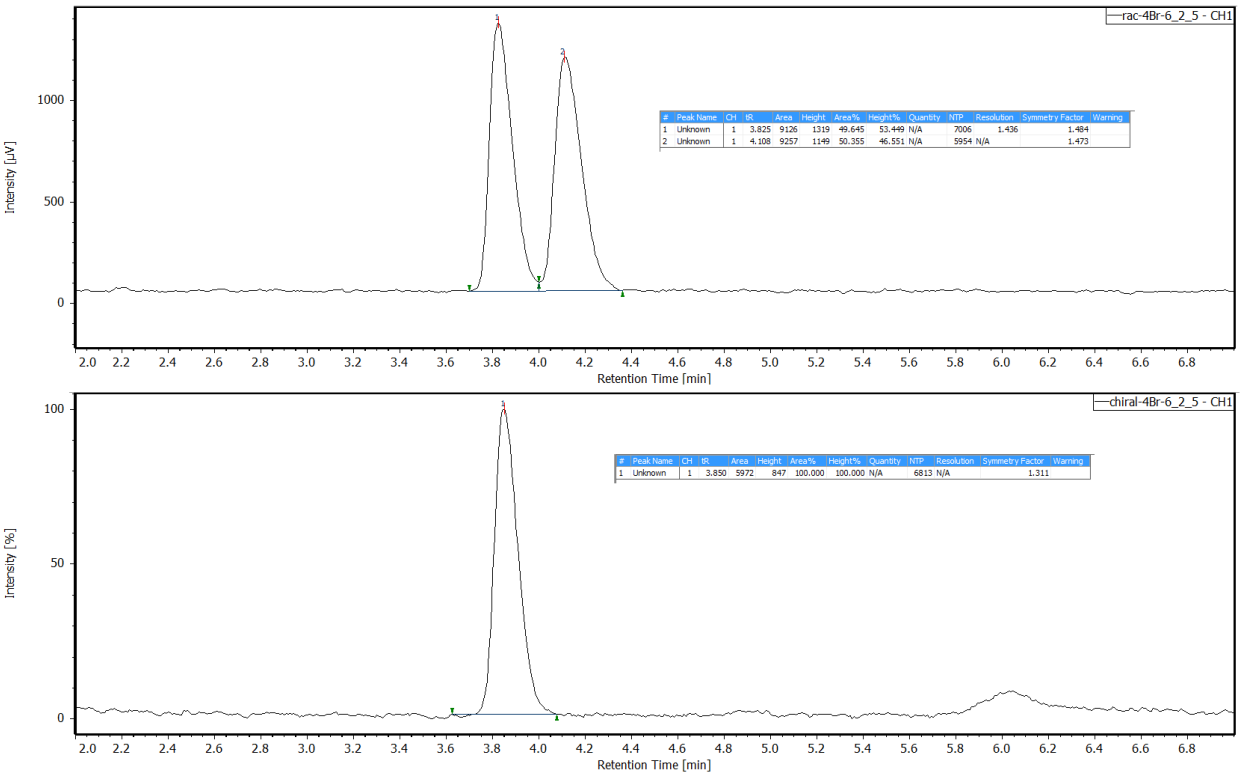

Supplementary Figure 7. SFC traces of the racemic 1-(4-bromophenyl)ethan-1-ol (top) and the enantioenriched products of the hCAII-catalyzed reduction (bottom).

(S)-1-(p-tolyl)ethan-1-ol (**10**)

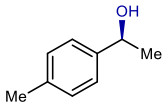

^{1}H NMR (400 MHz, $CDCl_3$) δ 7.26 (d, 2H), 7.16 (d, J = 7.8 Hz, 2H), 4.88 (dd, J = 6.5, 3.3 Hz, 1H), 2.35 (s, 3H), 1.49 (d, J = 6.4 Hz, 3H).

^{13}C NMR (151 MHz, $CDCl_3$) δ 143.04, 137.28, 129.30, 125.51, 70.38, 25.22, 21.23.

Spectral data match those previously reported.[4]

Enantiomer separation: SFC OJ-H column, 5% iPrOH in $scCO_2$, 2.5 mL/min flow rate.

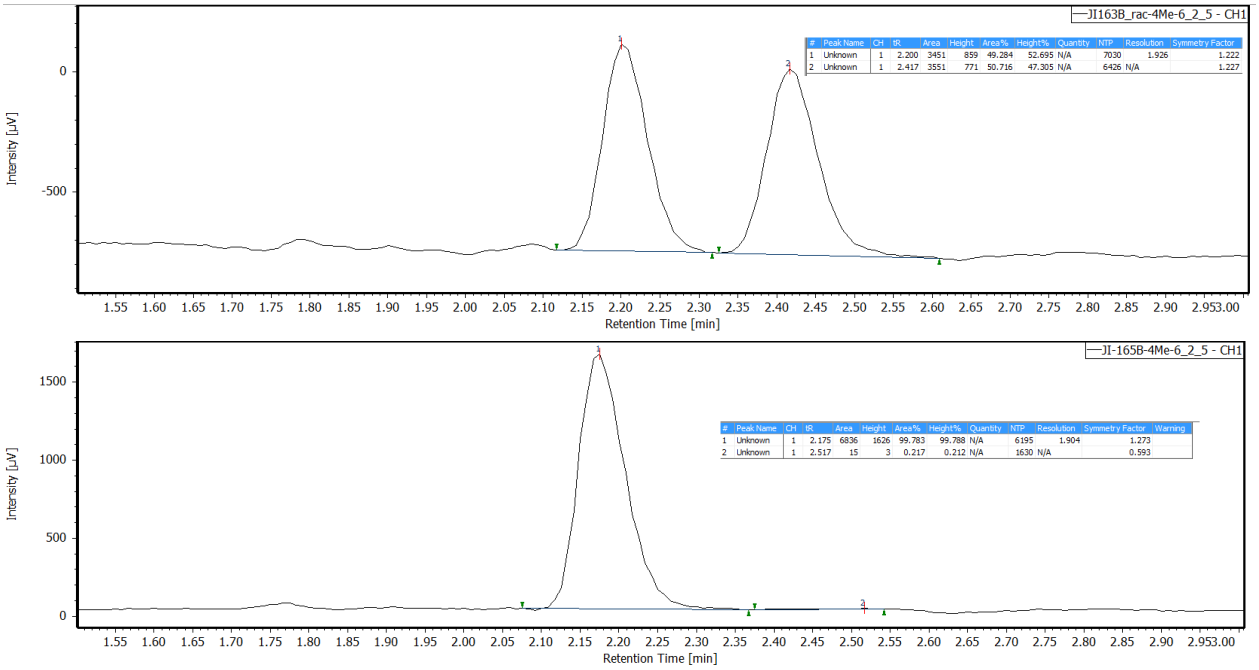

Supplementary Figure 8. SFC traces of the racemic 1-(p-tolyl)ethan-1-ol (top) and the enantioenriched products of the hCAII-catalyzed reduction (bottom).

(S)-1-(4-methoxyphenyl)ethan-1-ol (**11**)

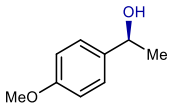

^{1}H NMR (400 MHz, $CDCl_3$) δ 7.31 (d, J = 8.7 Hz, 2H), 6.93 – 6.84 (m, 2H), 4.86 (q, J = 6.4 Hz, 1H), 3.81 (s, 3H), 1.48 (d, J = 6.4 Hz, 3H).
^{13}C NMR (151 MHz, $CDCl_3$) δ 159.08, 138.15, 126.79, 113.96, 70.07, 55.41, 25.13.
Spectral data match those previously reported.[7]

Enantiomer separation: SFC AS-H column, 5% iPrOH in $scCO_2$, 2.5 mL/min flow rate.

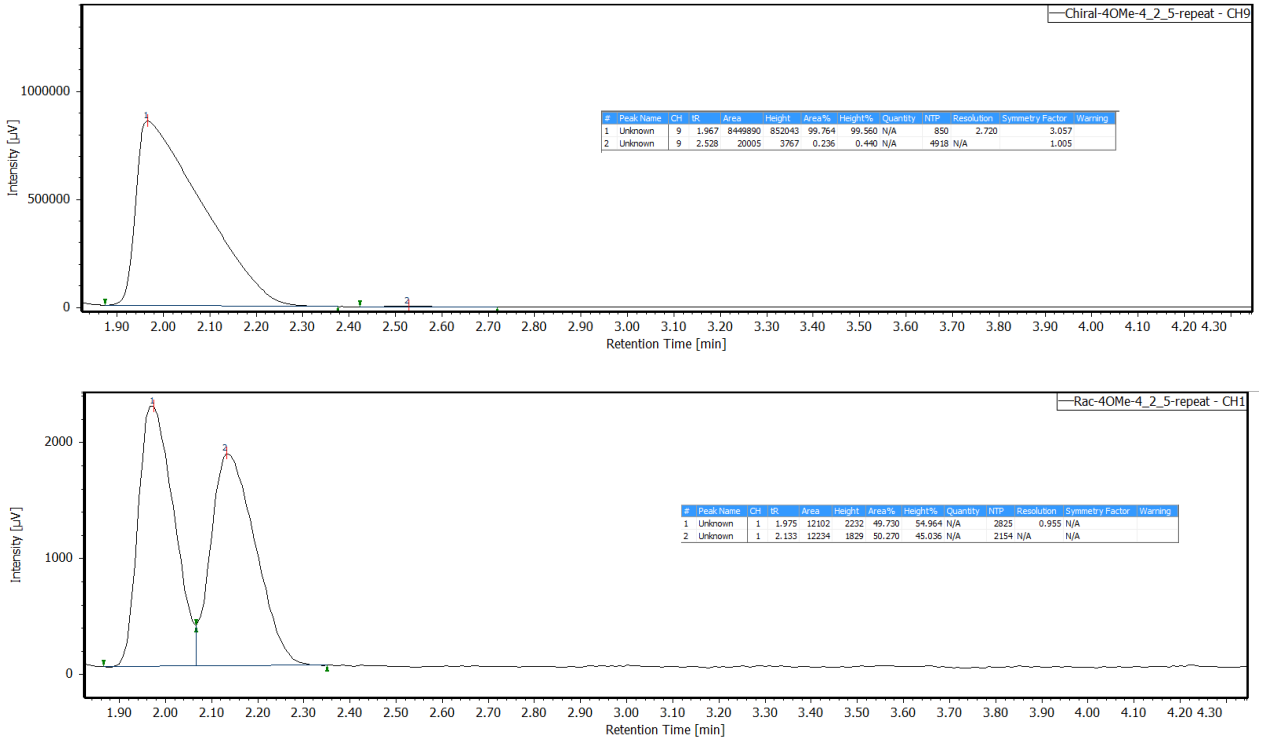

Supplementary Figure 9. SFC traces of the racemic 1-(4-methoxyphenyl)ethan-1-ol (top) and the enantioenriched products of the hCAII-catalyzed reduction (bottom).

(S)-1-(4-(methylthio)phenyl)ethan-1-ol (**12**)

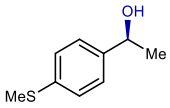

^{1}H NMR (400 MHz, $CDCl_3$) δ 7.30 (d, J = 8.4 Hz, 2H), 7.25 (d, J = 8.5 Hz, 3H), 4.87 (q, J = 6.5 Hz, 1H), 2.48 (s, 3H), 1.48 (d, J = 6.4 Hz, 3H).
^{13}C NMR (151 MHz, $CDCl_3$) δ 142.94, 137.57, 127.00, 126.12, 70.13, 25.22, 16.16.
Spectral data match those previously reported.[4]

Enantiomer separation: SFC OJ-H column, 15% iPrOH in $scCO_2$, 2.5 mL/min flow rate.

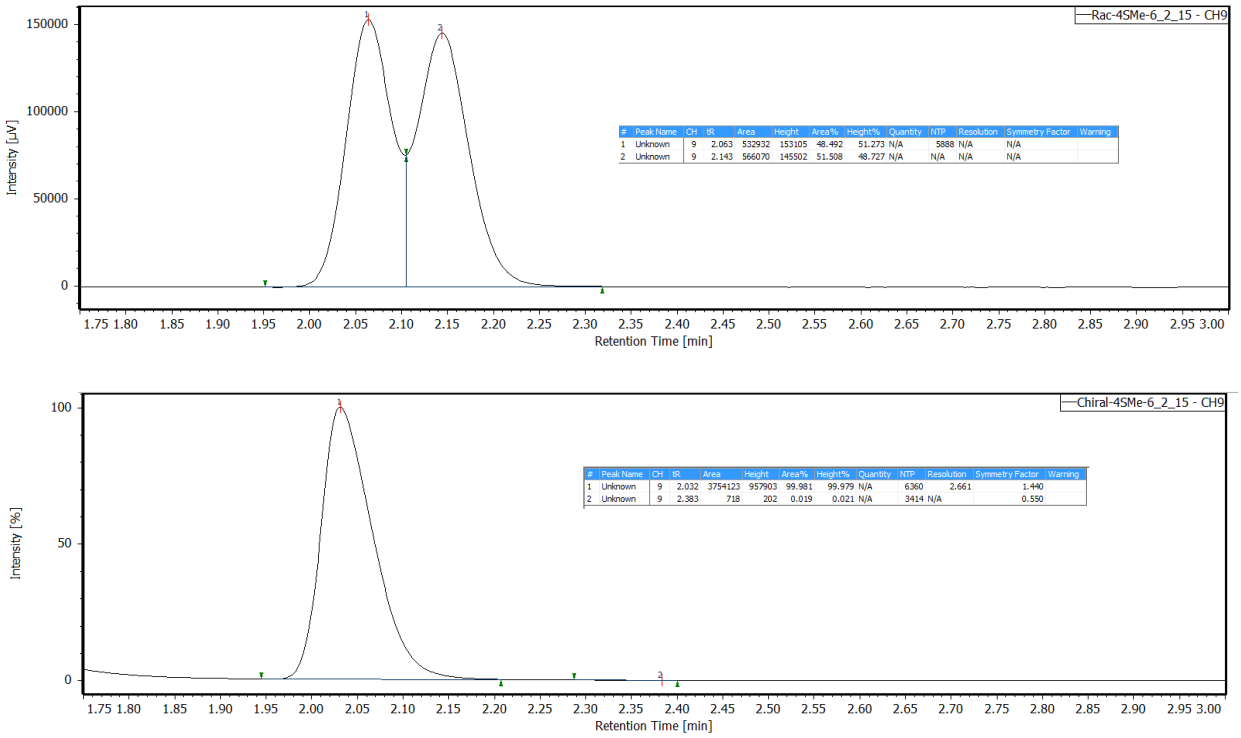

Supplementary Figure 10. SFC traces of the racemic 1-(4-(methylthio)phenyl)ethan-1-ol (top) and the enantioenriched products of the hCAII-catalyzed reduction (bottom).

(S)-1-(2-methoxyphenyl)ethan-1-ol (**13**)

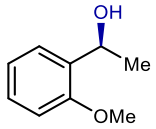

^{1}H NMR (400 MHz, $CDCl_3$) δ 7.34 (dd, *J* = 7.6, 1.7 Hz, 1H), 7.30 – 7.21 (m, 1H), 6.97 (tt, *J* = 7.5, 1.0 Hz, 1H), 6.89 (dd, *J* = 8.2, 1.1 Hz, 1H), 5.10 (q, *J* = 6.5 Hz, 1H), 3.87 (d, *J* = 0.8 Hz, 3H), 1.51 (dd, *J* = 6.5, 0.8 Hz, 3H).

^{13}C NMR (151 MHz, $CDCl_3$) δ 156.69, 133.59, 128.43, 126.23, 120.94, 110.58, 66.65, 55.40, 23.00.

Spectral data match those previously reported.[7]

Enantiomer separation: SFC OJ-H column, 5% iPrOH in $scCO_2$, 2.5 mL/min flow rate.

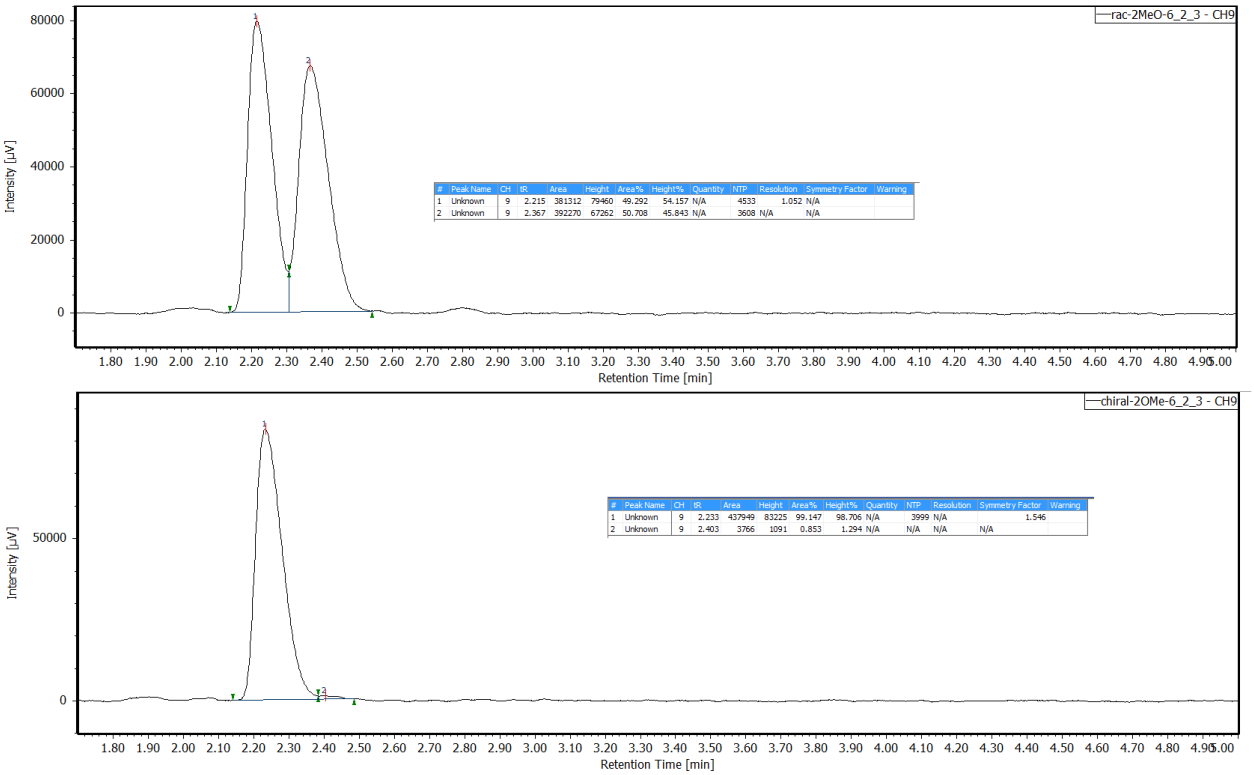

Supplementary Figure 11. SFC traces of the racemic 1-(2-methoxyphenyl)ethan-1-ol (top) and the enantioenriched products of the hCAII-catalyzed reduction (bottom).

(S)-1-(3-bromophenyl)ethan-1-ol (**14**)

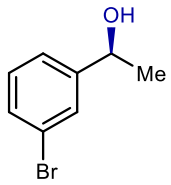

^{1}H NMR (400 MHz, $CDCl_3$) δ 7.58 (t, *J* = 1.8 Hz, 1H), 7.44 (ddd, *J* = 7.9, 2.1, 1.3 Hz, 1H), 7.34 (dt, *J* = 7.7, 1.6 Hz, 1H), 7.26 (t, *J* = 7.7 Hz, 1H), 4.92 (qd, *J* = 6.4, 3.6 Hz, 1H), 1.53 (d, *J* = 6.4 Hz, 3H).

^{13}C NMR (151 MHz, $CDCl_3$) δ 148.24, 130.59, 130.21, 128.69, 124.14, 122.73, 69.86, 25.36.

Spectral data match those previously reported.[4]

Enantiomer separation: SFC OJ-H column, 5% iPrOH in $scCO_2$, 2.5 mL/min flow rate.

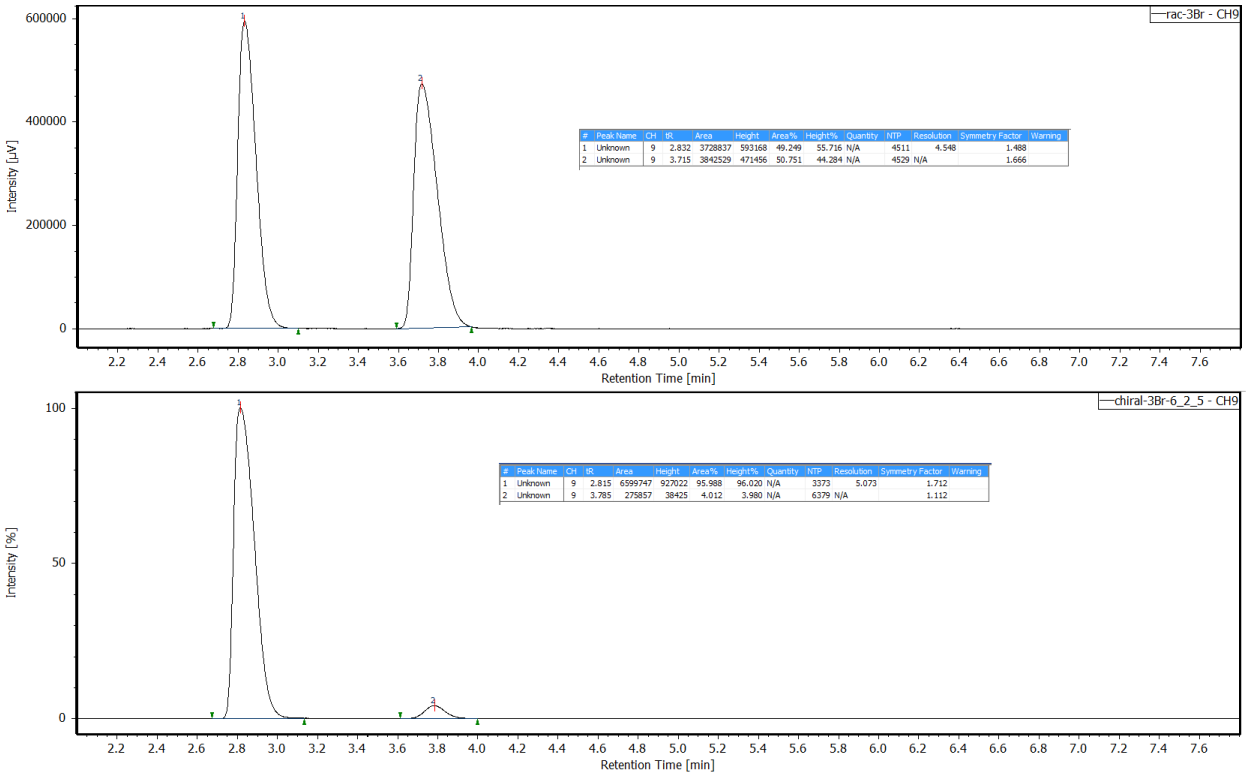

Supplementary Figure 12. SFC traces of the racemic 1-(3-bromophenyl)ethan-1-ol (top) and the enantioenriched products of the hCAII-catalyzed reduction (bottom).

(S)-1-(2-chlorophenyl)ethan-1-ol (**15**)

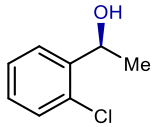

^{1}H NMR (400 MHz, $CDCl_3$) δ 7.60 (dd, *J* = 7.7, 1.7 Hz, 1H), 7.38 – 7.28 (m, 2H), 7.20 (td, *J* = 7.6, 1.8 Hz, 1H), 5.30 (qd, *J* = 6.4, 2.8 Hz, 1H), 1.50 (d, *J* = 6.4 Hz, 3H).
^{13}C NMR (151 MHz, $CDCl_3$) δ 143.20, 131.76, 129.52, 128.52, 127.34, 126.55, 67.08, 23.63.
Spectral data match those previously reported.[4]

Enantiomer separation: SFC OJ-H column, 3% iPrOH in $scCO_2$, 4.0 mL/min flow rate.

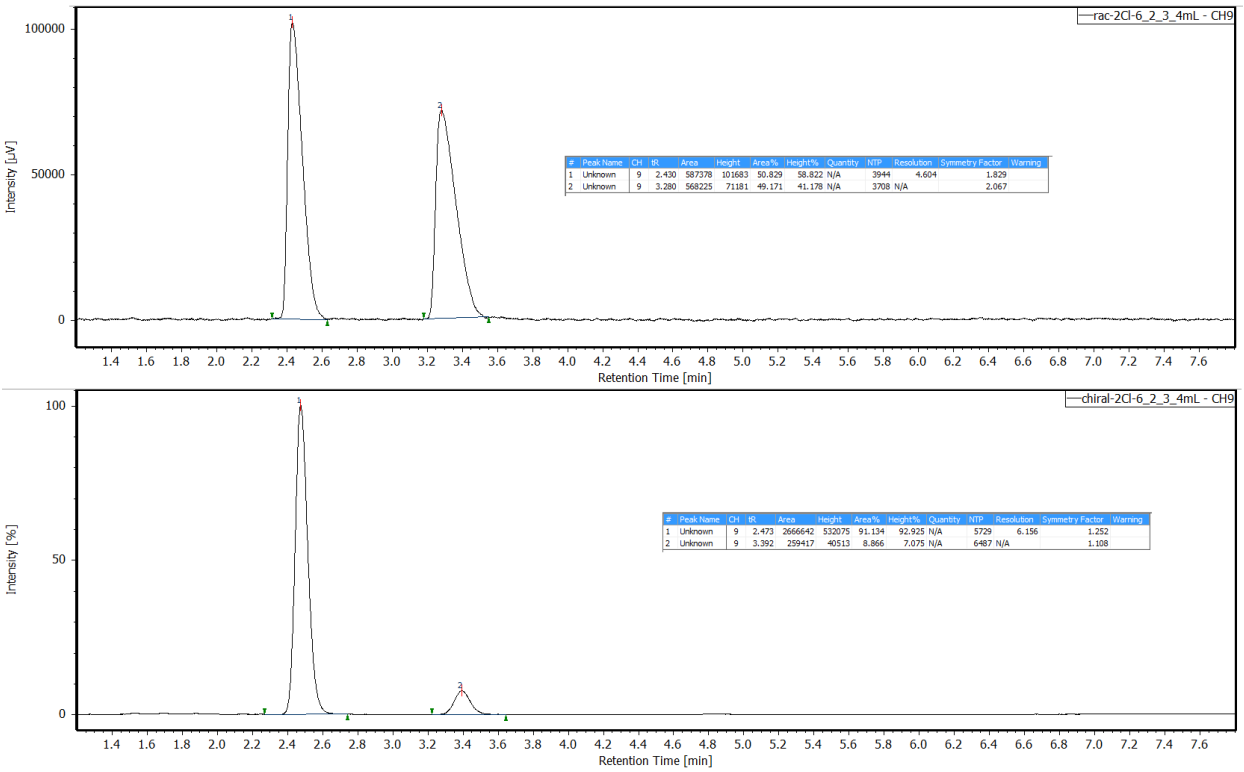

Supplementary Figure 13. SFC traces of the racemic 1-(2-chlorophenyl)ethan-1-ol (top) and the enantioenriched products of the hCAII-catalyzed reduction (bottom).

(S)-1-(2,6-dichloro-3-fluorophenyl)ethan-1-ol (**16**)

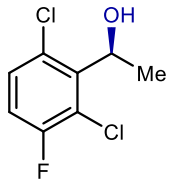

^{1}H NMR (400 MHz, $CDCl_3$) δ 7.38 – 7.27 (m, 1H), 7.12 – 7.03 (m, 1H), 5.62 (q, J = 6.9 Hz, 1H), 1.69 (d, J = 6.8 Hz, 3H).

^{13}C NMR (151 MHz, $CDCl_3$) δ 158.23, 156.58, 140.66, 129.76, 129.71, 115.85, 115.70, 68.51, 21.42.

^{19}F NMR (376 MHz, $CDCl_3$) δ -113.31 (s)

Spectral data match those previously reported.[8]

Enantiomer separation: SFC OJ-H column, 5% iPrOH in $scCO_2$, 2.5 mL/min flow rate.

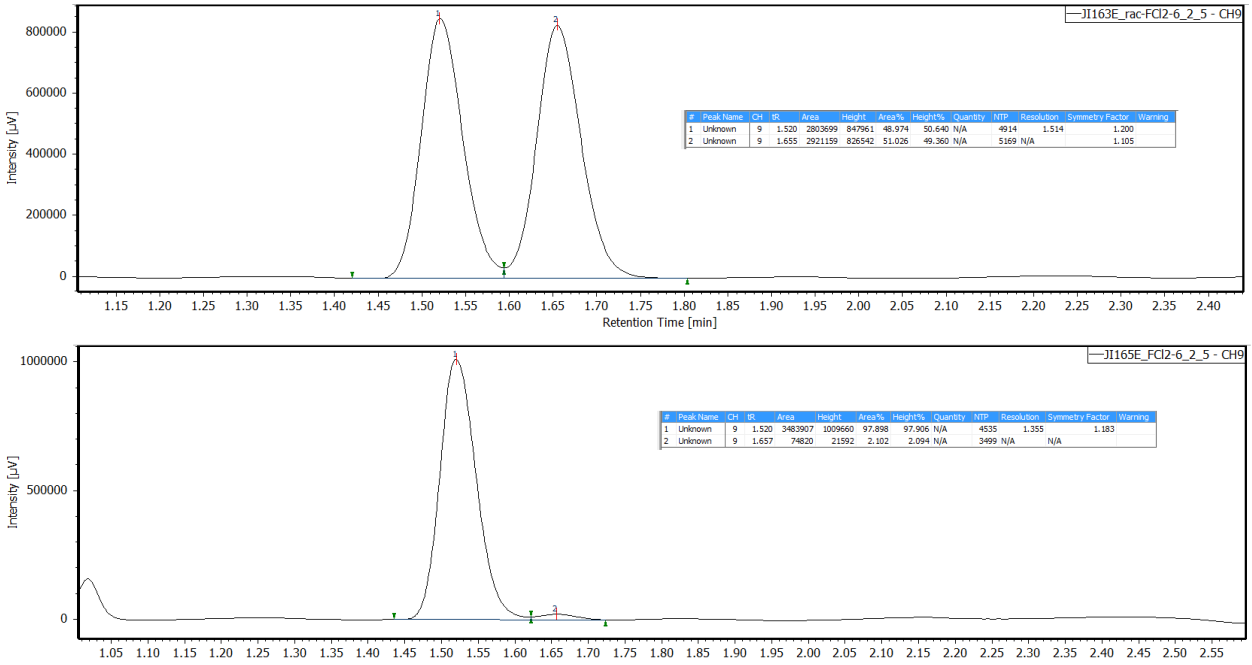

Supplementary Figure 14. SFC traces of the racemic 1-(2,6-dichloro-3-fluorophenyl)ethan-1-ol (top) and the enantioenriched products of the hCAII-catalyzed reduction (bottom).

(S)-1-(3,5-bis(trifluoromethyl)phenyl)ethan-1-ol (**17**)

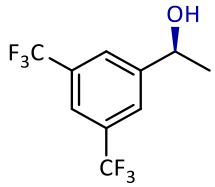

^{1}H NMR (400 MHz, $CDCl_3$) δ 7.89 (s, 2H), 7.83 (s, 1H), 5.22 – 4.99 (m, 1H).

^{13}C NMR (151 MHz, $CDCl_3$) δ 148.33, 131.97, 125.74, 124.36, 121.41, 69.37, 25.68.

^{19}F NMR (376 MHz, $CDCl_3$) δ -62.81 (s)

Spectral data match those previously reported.[7]

Enantiomer separation: HPLC AS-H column, 1% iPrOH in hexane, 1.0 mL/min flow rate.

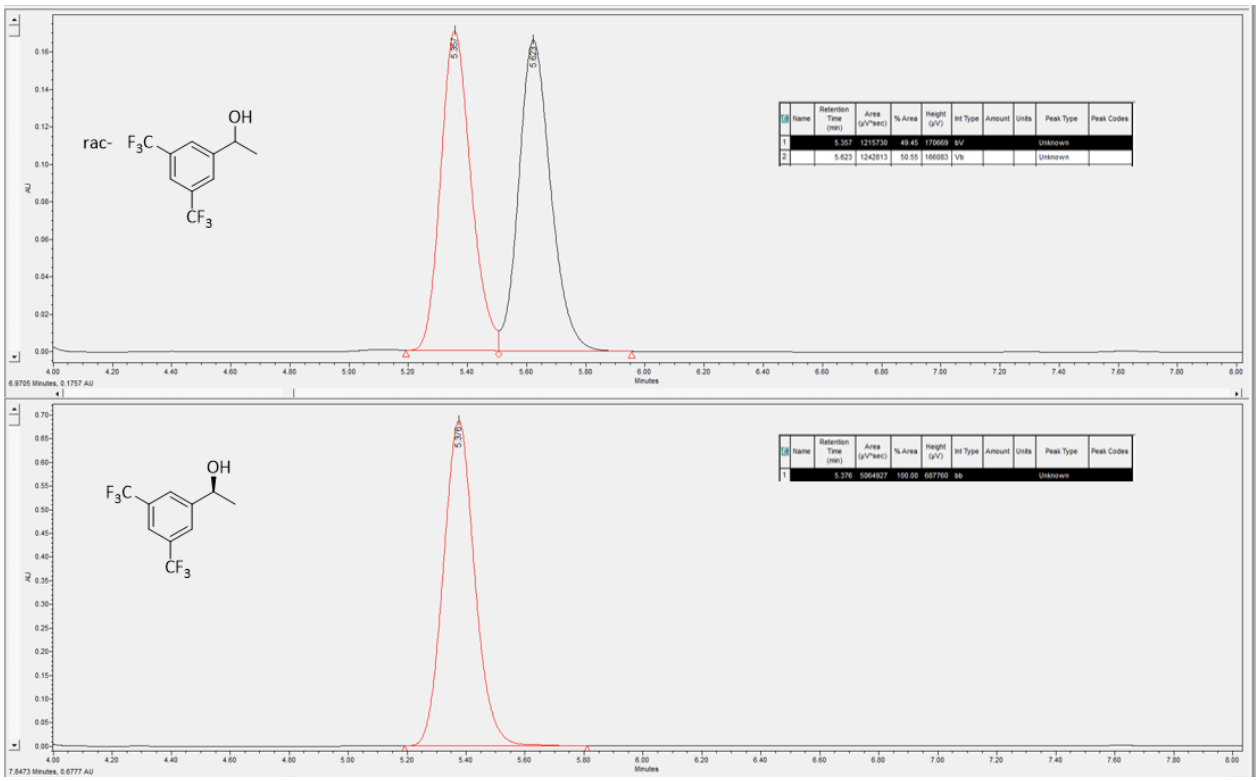

Supplementary Figure 15. HPLC traces of the racemic 1-(3,5-bis(trifluoromethyl)phenyl)ethan-1-ol (top) and the enantioenriched products of the hCAII-catalyzed reduction (bottom).

(S)-1-(naphthalen-2-yl)ethan-1-ol (**18**)

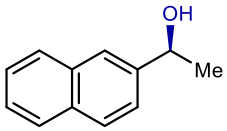

^{1}H NMR (400 MHz, $CDCl_3$) δ 7.88 (m, 4H), 7.56 (m, 1H), 7.54 – 7.50 (m, 2H), 5.13 (qd, J = 6.5, 3.5 Hz, 1H), 1.63 (d, J = 6.5 Hz, 3H).

^{13}C NMR (151 MHz, $CDCl_3$) δ 143.30, 133.46, 133.05, 128.44, 128.06, 127.80, 126.28, 125.92, 123.94, 123.93, 70.66, 25.25.

Spectral data match those previously reported.[4]

Enantiomer separation: SFC OD-H column, 10% iPrOH in $scCO_2$, 2.5 mL/min flow rate.

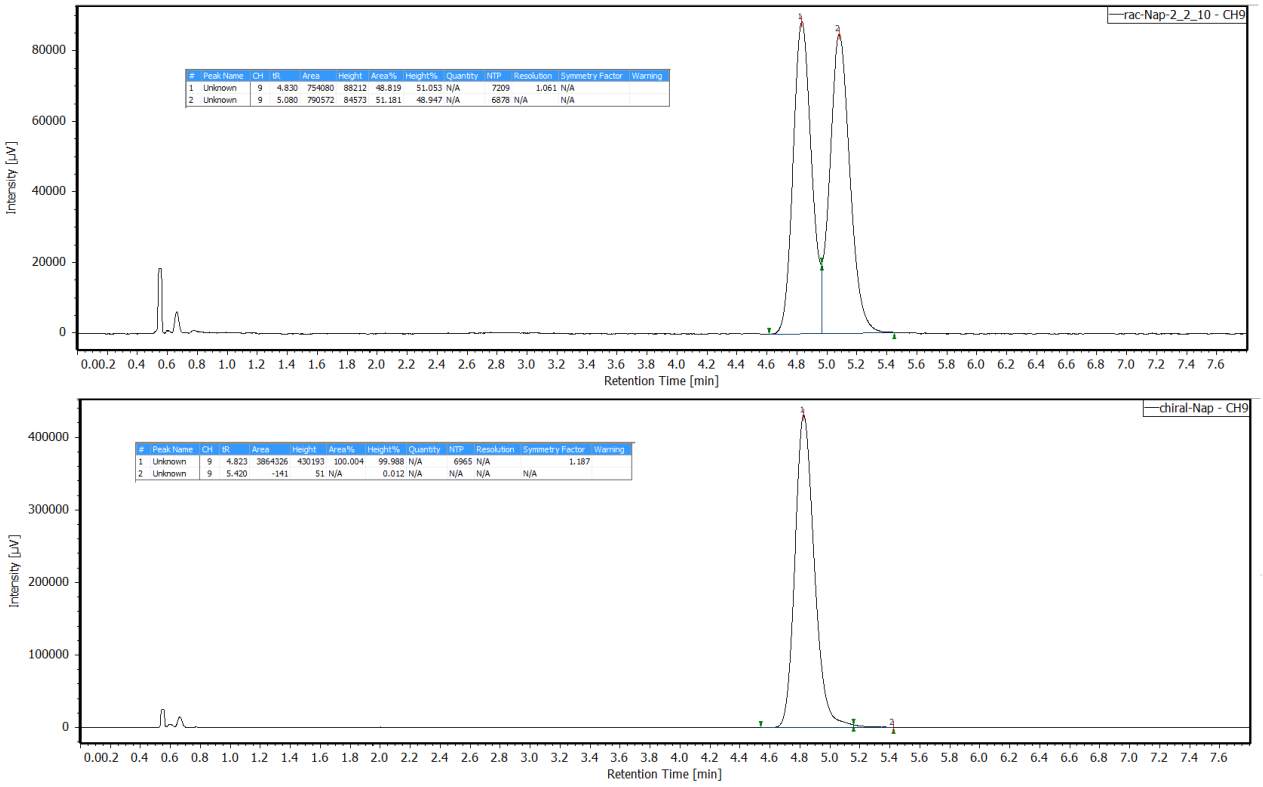

Supplementary Figure 16. SFC traces of the racemic 1-(naphthalen-2-yl)ethan-1-ol (top) and the enantioenriched products of the hCAII-catalyzed reduction (bottom).

(S)-1-phenylpropan-1-ol (**19**)

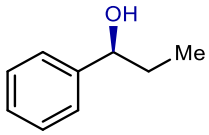

^{1}H NMR (400 MHz, $CDCl_3$) δ 7.42 – 7.32 (m, 4H), 7.32 – 7.27 (m, 1H), 4.60 (dd, J = 7.1, 6.1 Hz, 1H), 1.96 – 1.71 (m, 2H), 0.92 (t, J = 7.4 Hz, 3H).

^{13}C NMR (151 MHz, $CDCl_3$) δ 144.75, 128.51, 127.59, 126.12, 76.11, 31.99, 10.26.

Spectral data match those previously reported.[7]

Enantiomer separation: HPLC AD-H column, 2% iPrOH in hexane, 1.0 mL/min flow rate.

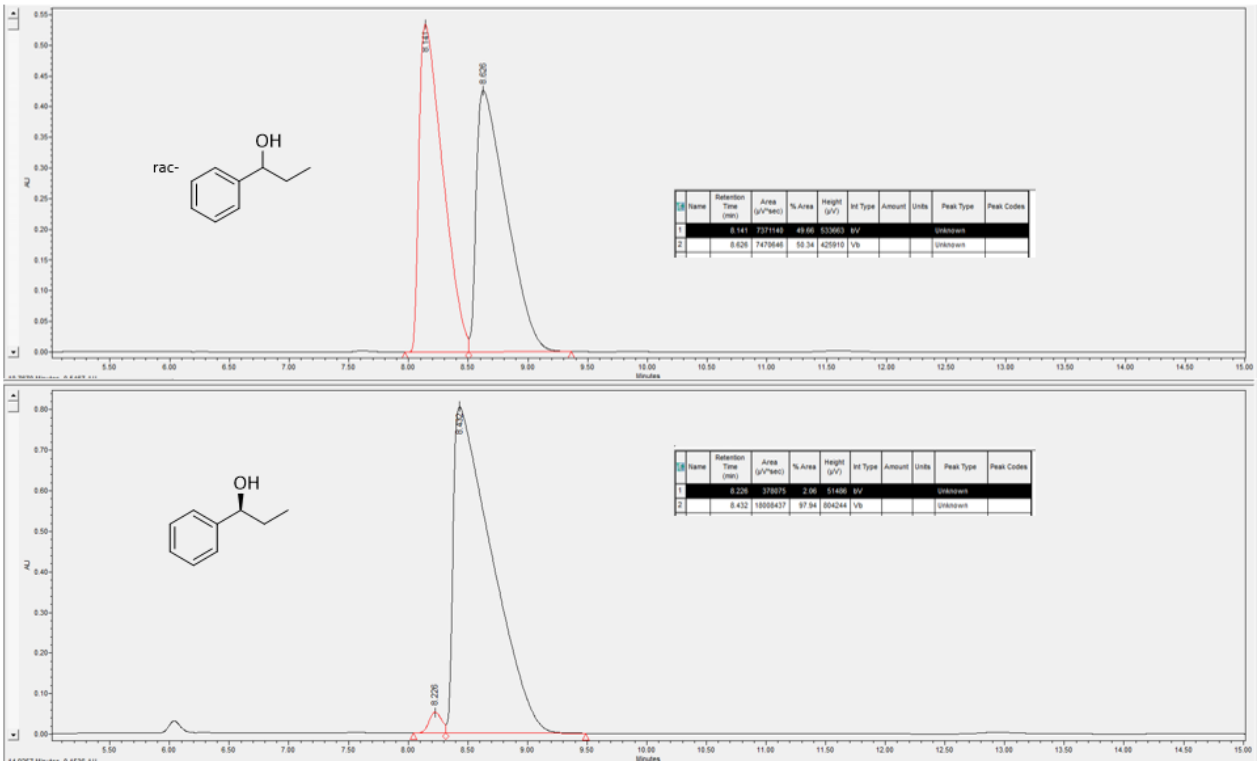

Supplementary Figure 17. HPLC traces of the racemic 1-phenylpropan-1-ol (top) and the enantioenriched products of the hCAII-catalyzed reduction (bottom).

(S)-1-(3-bromophenyl)propan-1-ol (**20**)

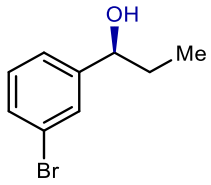

^{1}H NMR (400 MHz, $CDCl_3$) δ 7.54 – 7.50 (m, 1H), 7.44 – 7.38 (m, 1H), 7.34 (dd, *J* = 15.5, 7.6 Hz, 1H), 7.25 – 7.18 (m, 1H), 4.59 (t, *J* = 6.5 Hz, 1H), 1.88 – 1.67 (m, 2H), 0.93 (t, *J* = 7.4 Hz, 3H).
^{13}C NMR (151 MHz, $CDCl_3$) δ 147.05, 130.61, 130.09, 129.20, 124.72, 122.67, 75.38, 32.04, 10.09.
Spectral data match those previously reported.[9]

Enantiomer separation: SFC OJ-H column, 5% iPrOH in $scCO_2$, 2.5 mL/min flow rate.

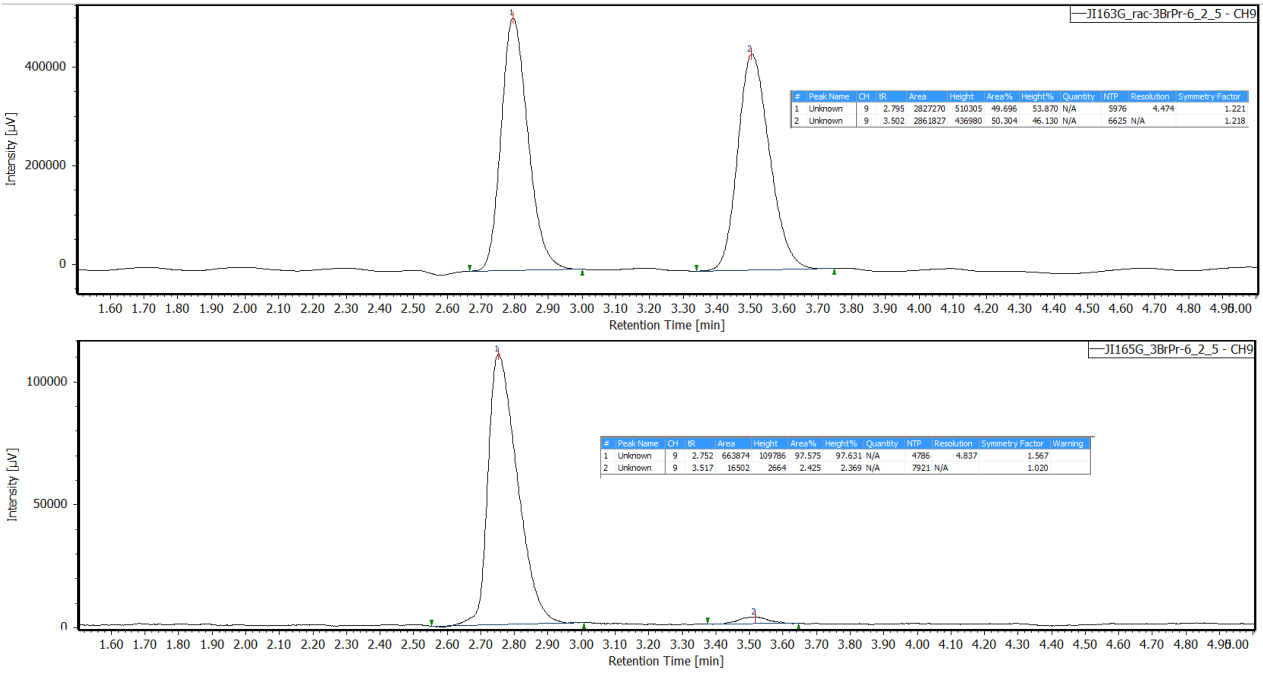

Supplementary Figure 18. SFC traces of the racemic 1-(3-bromophenyl)propan-1-ol (top) and the enantioenriched products of the hCAII-catalyzed reduction (bottom).

(R)-2-fluoro-1-phenylethan-1-ol (**21**)

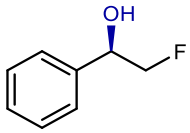

^{1}H NMR (400 MHz, $CDCl_3$) δ 7.42 – 7.31 (m, 5H), 5.10 – 4.87 (m, 1H), 4.63 – 4.32 (m, 2H).

^{13}C NMR (151 MHz, $CDCl_3$) δ 138.36, 138.30, 128.77, 128.54, 126.48, 87.87, 86.71, 73.14, 73.01.

^{19}F NMR (376 MHz, $CDCl_3$) δ -220.73 (m)

Spectral data match those previously reported.[10]

Enantiomer separation: SFC OJ-H column, 5% iPrOH in $scCO_2$, 2.5 mL/min flow rate.

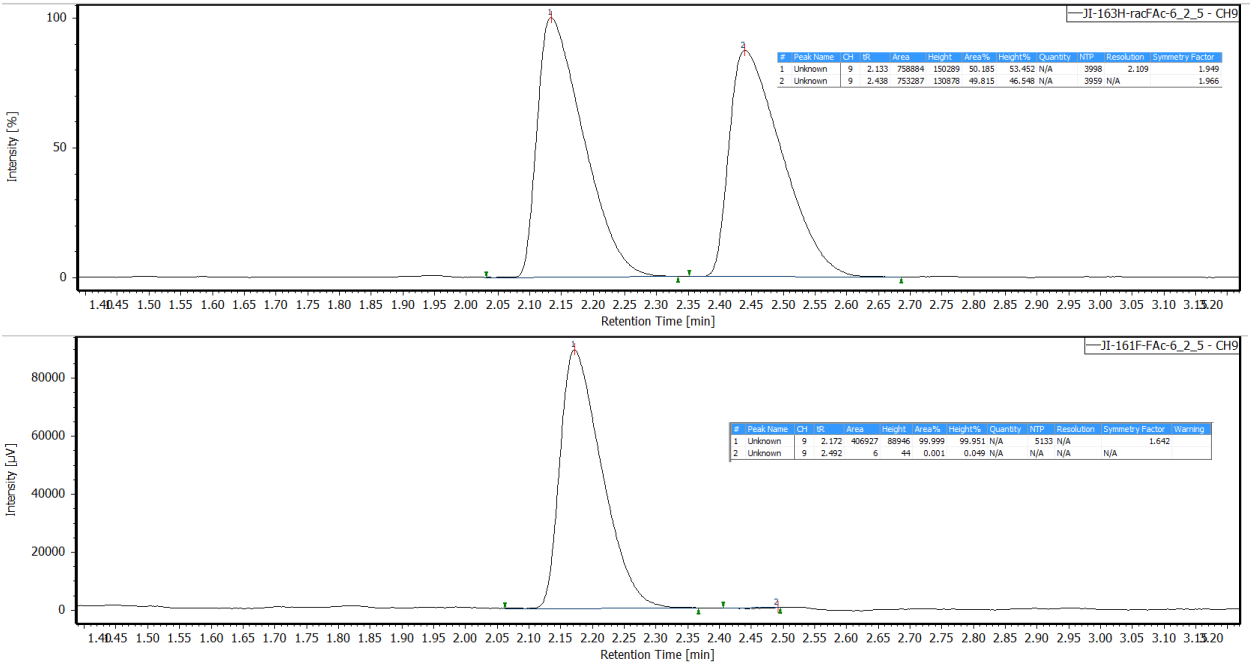

Supplementary Figure 19. SFC traces of the racemic 2-fluoro-1-phenylethan-1-ol (top) and the enantioenriched products of the hCAII-catalyzed reduction (bottom).

(R)-2,2,2-trifluoro-1-phenylethan-1-ol (**22**)

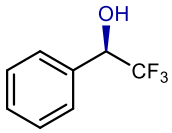

^{1}H NMR (400 MHz, $CDCl_3$) δ 7.58 – 7.45 (m, 2H), 7.44 – 7.38 (m, 3H), 5.03 (q, J = 6.7 Hz, 1H).
^{13}C NMR (151 MHz, $CDCl_3$) δ 134.17, 129.64, 128.73, 127.56, 125.33, 73.03.
^{19}F NMR (376 MHz, $CDCl_3$) δ -78.36 (d, J = 56.6 Hz)
Spectral data match those previously reported.[11]

Enantiomer separation: SFC OJ-H column, 5% iPrOH in $scCO_2$, 2.5 mL/min flow rate.

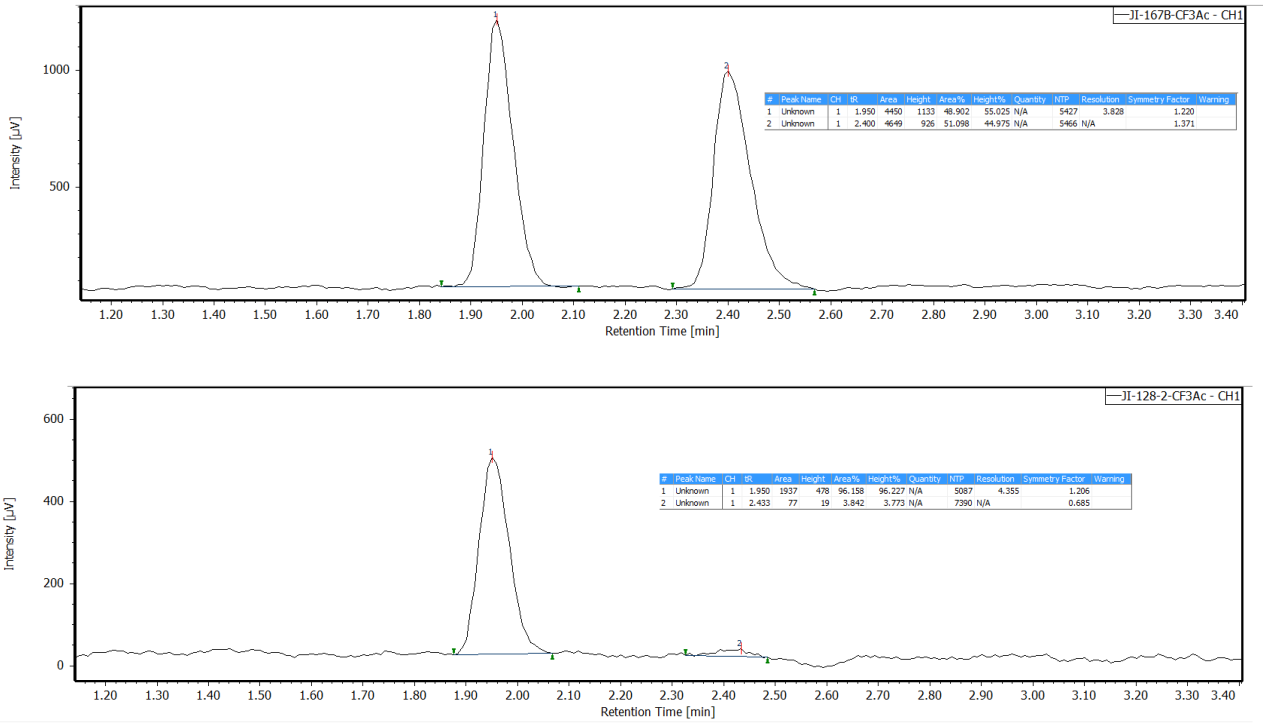

Supplementary Figure 20. SFC traces of the racemic 2,2,2-trifluoro-1-phenylethan-1-ol (top) and the enantioenriched products of the hCAII-catalyzed reduction (bottom).

(S)-1-(pyridin-2-yl)ethan-1-ol (**23**)

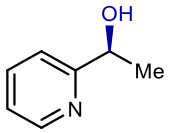

^{1}H NMR (400 MHz, $CDCl_3$) δ 8.53 (dt, J = 4.9, 1.4 Hz, 1H), 7.69 (td, J = 7.7, 1.7 Hz, 1H), 7.33 – 7.26 (m, 1H), 7.20 (ddd, J = 7.4, 4.9, 1.2 Hz, 1H), 4.89 (q, J = 6.6 Hz, 1H), 1.50 (d, J = 6.6 Hz, 3H).
^{13}C NMR (151 MHz, $CDCl_3$) δ 163.20, 148.23, 136.95, 122.35, 119.93, 69.02, 24.32.
Spectral data match those previously reported.[7]

Enantiomer separation: SFC IC column, 2% iPrOH in $scCO_2$, 4.0 mL/min flow rate.

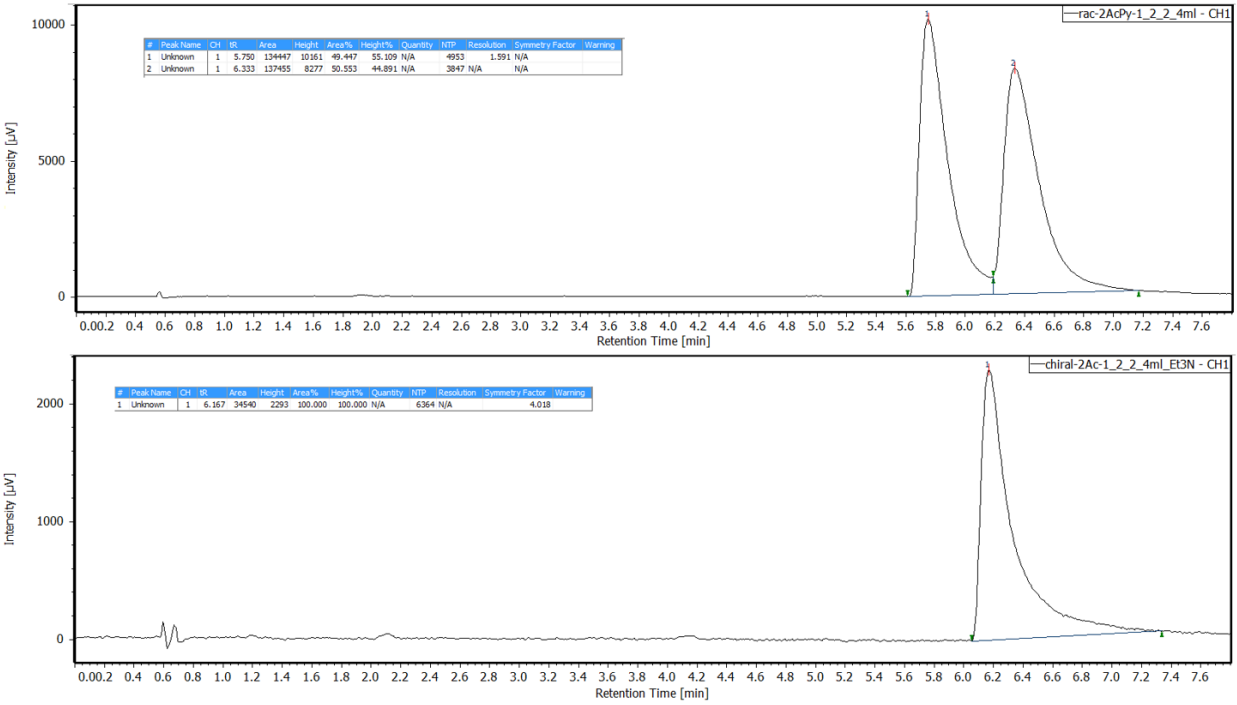

Supplementary Figure 21. SFC traces of the racemic 1-(pyridin-2-yl)ethan-1-ol (top) and the enantioenriched products of the hCAII-catalyzed reduction (bottom).

(S)-1-(pyridin-3-yl)ethan-1-ol (**24**)

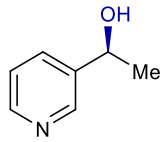

^{1}H NMR (400 MHz, $CDCl_3$) δ 8.53 (d, J = 2.4 Hz, 1H), 8.44 (dd, J = 4.8, 1.7 Hz, 1H), 7.72 (dt, J = 8.0, 1.9 Hz, 1H), 7.26 (q, J = 4.5 Hz, 1H), 4.92 (q, J = 6.5 Hz, 1H), 1.50 (d, J = 6.4 Hz, 3H).
^{13}C NMR (151 MHz, $CDCl_3$) δ 148.21, 147.04, 141.62, 133.77, 123.77, 67.94, 25.30.
Spectral data match those previously reported.[4]

Enantiomer separation: HPLC OJ-H column, 10% iPrOH in Hexane, 0.8 mL/min flow rate.

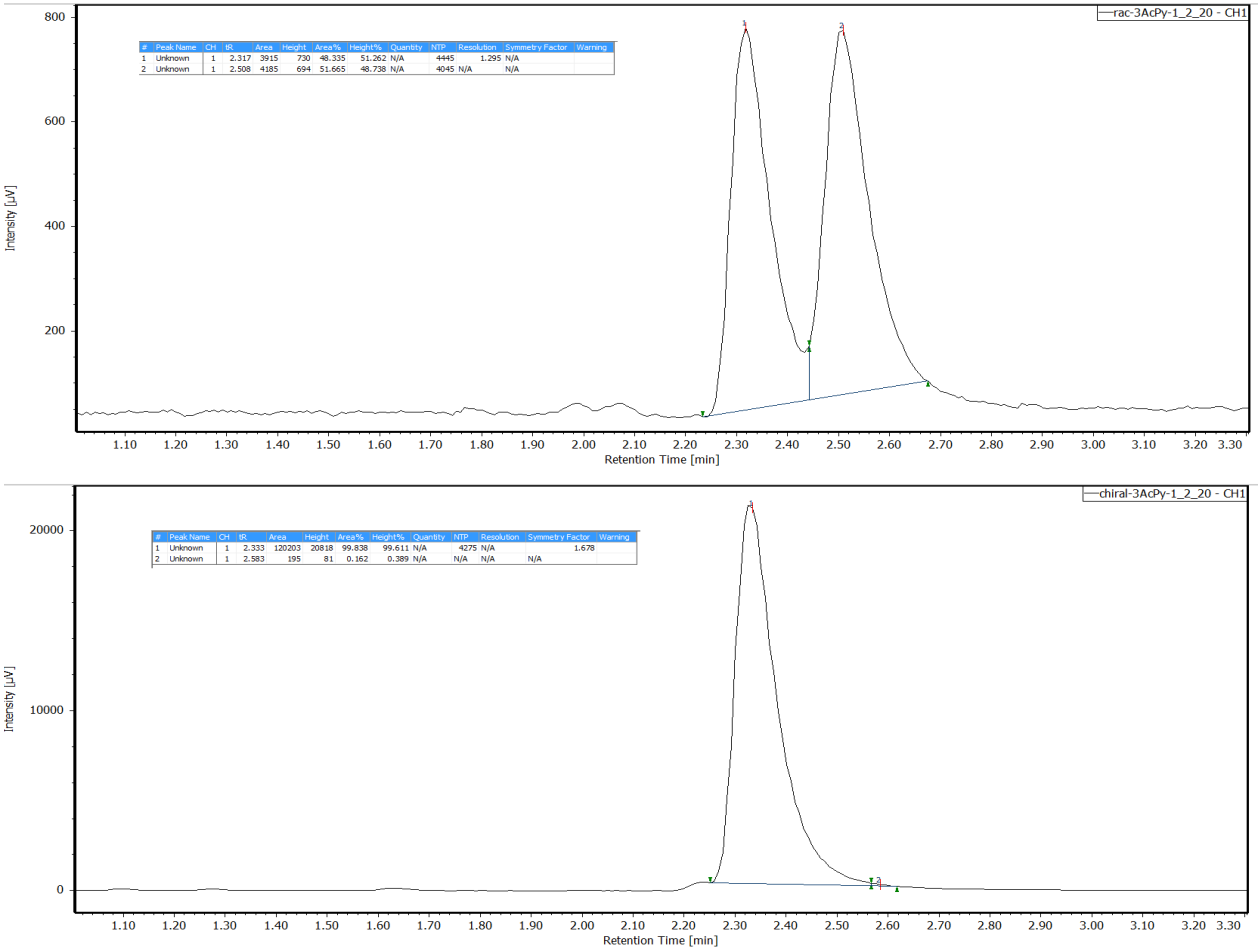

Supplementary Figure 22. SFC traces of the racemic 1-(pyridin-3-yl)ethan-1-ol (top) and the enantioenriched products of the hCAII-catalyzed reduction (bottom).

(S)-1-(pyrazin-2-yl)ethan-1-ol (**25**)

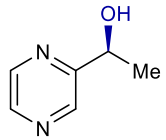

^{1}H NMR (400 MHz, $CDCl_3$) δ 8.72 (s, 1H), 8.56 (m, 2H), 5.04 (q, J = 6.6 Hz, 1H), 1.62 (dd, J = 6.6, 0.8 Hz, 3H).

^{13}C NMR (151 MHz, $CDCl_3$) δ 158.75, 143.50, 143.23, 142.51, 68.07, 24.05.

Spectral data match those previously reported.[12]

Enantiomer separation: SFC OD column, 5% iPrOH in $scCO_2$, 2.5 mL/min flow rate.

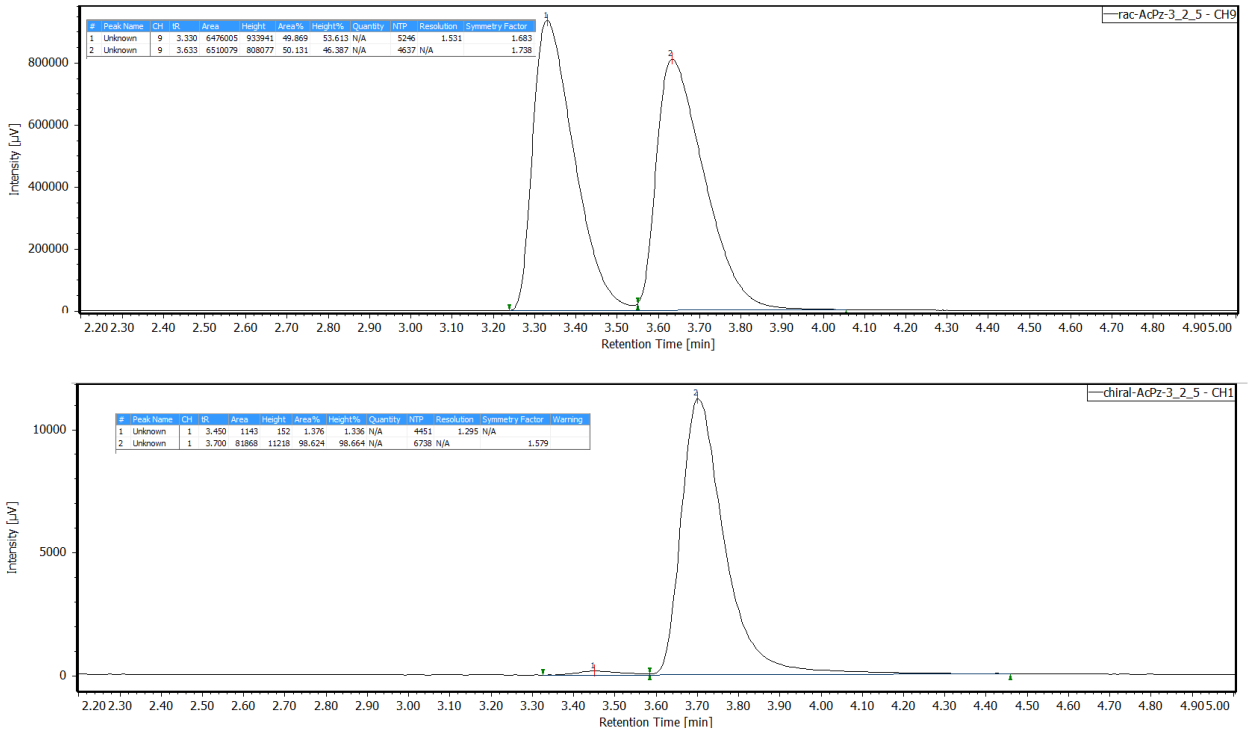

Supplementary Figure 23. SFC traces of the racemic 1-(pyrazin-2-yl)ethan-1-ol (top) and the enantioenriched products of the hCAII-catalyzed reduction (bottom).

(S)-1-(5-bromopyridin-3-yl)ethan-1-ol (**26**)

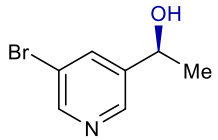

^{1}H NMR (400 MHz, $CDCl_3$) δ 8.55 (d, *J* = 2.2 Hz, 1H), 8.47 (d, *J* = 1.9 Hz, 1H), 7.89 (t, *J* = 2.0 Hz, 1H), 4.93 (q, *J* = 6.5 Hz, 1H), 1.51 (d, *J* = 6.5 Hz, 3H).

^{13}C NMR (151 MHz, $CDCl_3$) δ 149.26, 145.22, 143.66, 136.41, 121.06, 67.08, 25.34.

Spectral data match those previously reported.[13]

Enantiomer separation: SFC OJ-H column, 5% iPrOH in $scCO_2$, 2.5 mL/min flow rate.

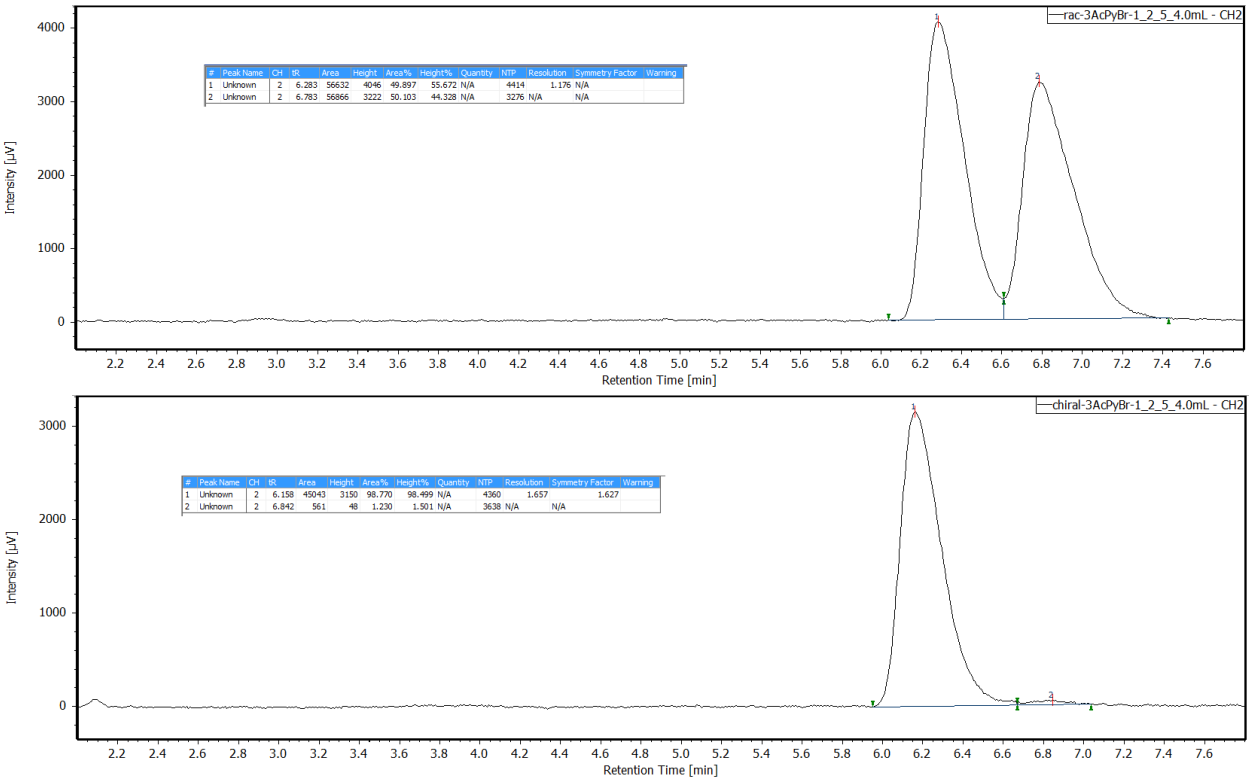

Supplementary Figure 24. SFC traces of the racemic 1-(5-bromopyridin-3-yl)ethan-1-ol (top) and the enantioenriched products of the hCAII-catalyzed reduction (bottom).

(S)-1-(furan-2-yl)ethan-1-ol (**27**)

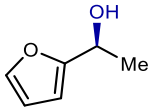

^{1}H NMR (400 MHz, $CDCl_3$) δ 8.55 (d, *J* = 2.2 Hz, 1H), 8.47 (d, *J* = 1.9 Hz, 1H), 7.89 (t, *J* = 2.0 Hz, 1H), 4.93 (q, *J* = 6.5 Hz, 1H), 1.51 (d, *J* = 6.5 Hz, 3H).

^{13}C NMR (151 MHz, $CDCl_3$) δ 157.77, 141.96, 110.22, 105.19, 63.65, 21.36.

Spectral data match those previously reported.[13]

Enantiomer separation: HPLC IF column, 5% iPrOH in hexane, 1.0 mL/min flow rate.

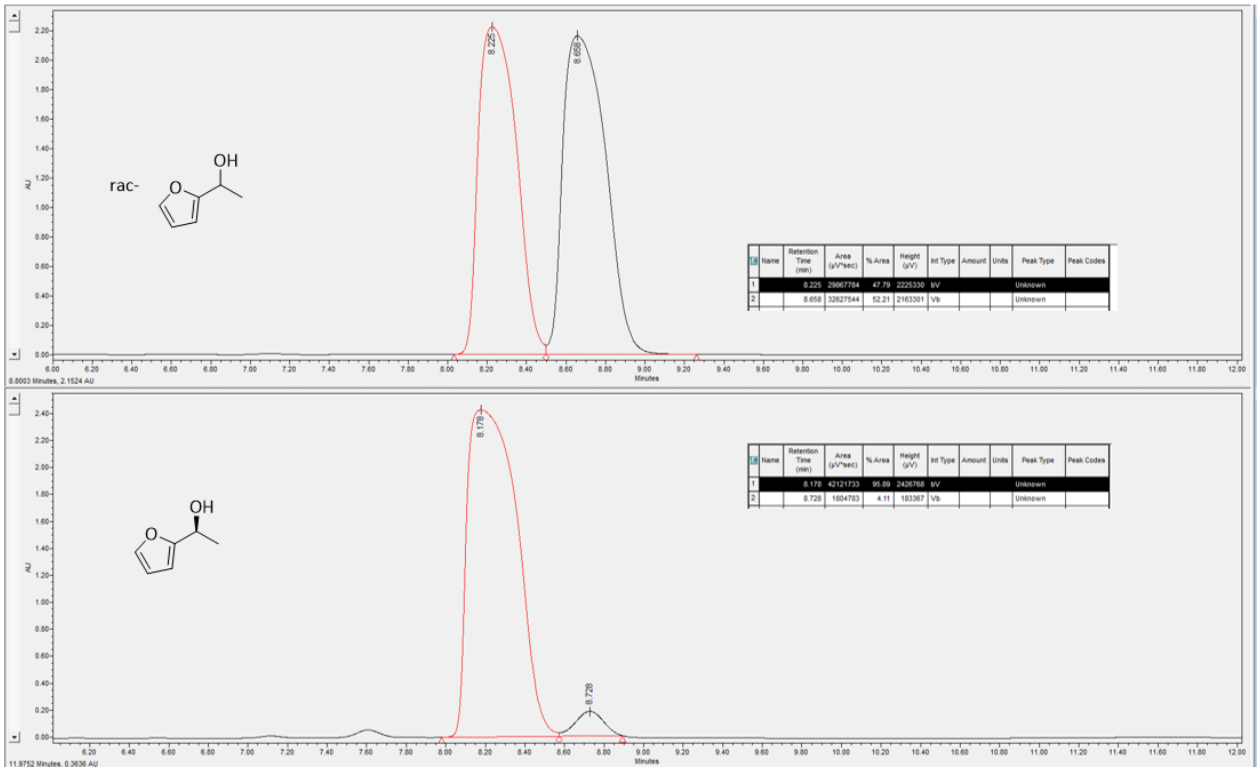

Supplementary Figure 25. HPLC traces of the racemic 1-(furan-2-yl)ethan-1-ol (top) and the enantioenriched products of the hCAII-catalyzed reduction (bottom).

(S,E)-4-(thiophen-2-yl)but-3-en-2-ol (**28**)

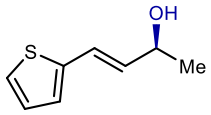

^{1}H NMR (400 MHz, $CDCl_3$) δ 7.16 – 7.10 (m, 1H), 6.96 – 6.88 (m, 2H), 6.67 (dd, J = 15.7, 1.3 Hz, 1H), 6.07 (dd, J = 15.7, 6.3 Hz, 1H), 4.42 (pd, J = 6.4, 1.3 Hz, 1H), 1.33 (d, J = 6.4 Hz, 3H).
^{13}C NMR (151 MHz, $CDCl_3$) δ 141.95, 133.29, 127.47, 125.90, 124.39, 122.71, 68.69, 23.45.
Spectral data match those previously reported.[14]

Enantiomer separation: SFC OJ-H column, 5% iPrOH in $scCO_2$, 2.5 mL/min flow rate.

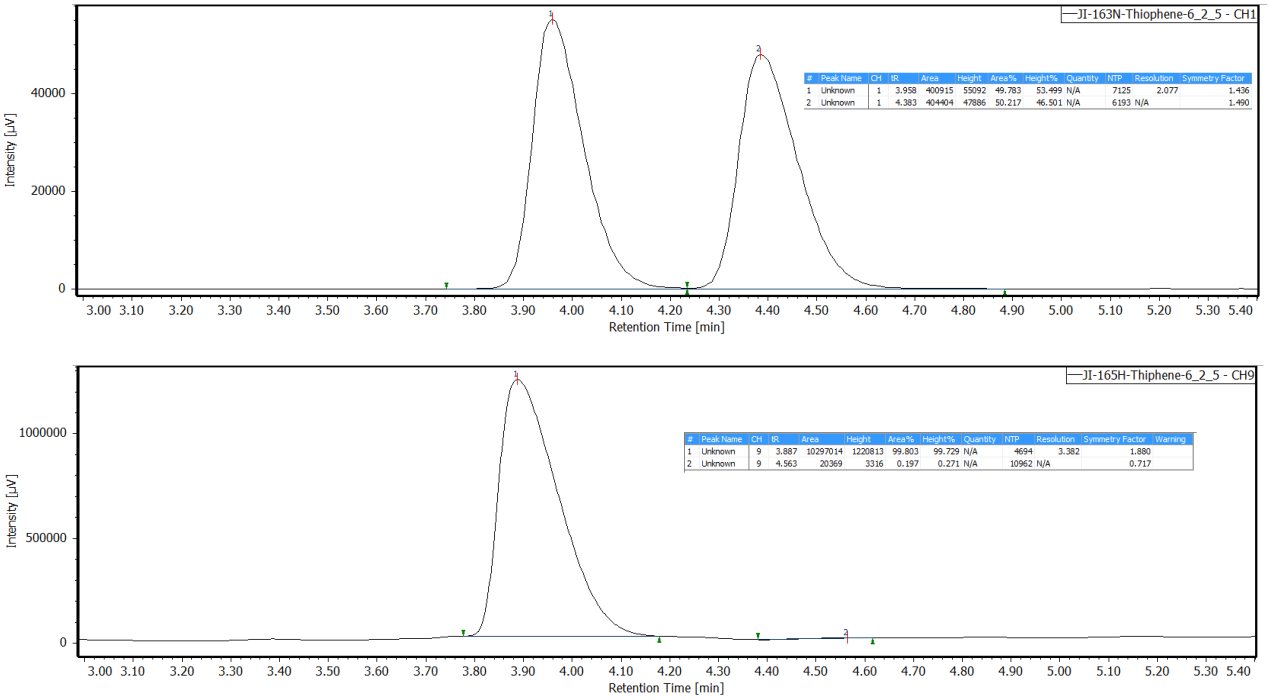

Supplementary Figure 26. SFC traces of the racemic E-4-(thiophen-2-yl)but-3-en-2-ol (top) and the enantioenriched products of the hCAII-catalyzed reduction (bottom).

(S)-3-hydroxy-1-phenylbutan-1-one (**29**)

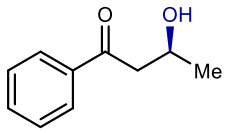

^{1}H NMR (400 MHz, $CDCl_3$) δ 8.01 (dt, *J* = 8.5, 1.1 Hz, 2H), 7.73 – 7.63 (m, 1H), 7.58 – 7.47 (m, 2H), 4.46 (dqd, *J* = 9.3, 6.3, 3.1 Hz, 1H), 3.37 (d, *J* = 3.1 Hz, 1H), 3.23 (ddd, *J* = 17.7, 2.8, 1.0 Hz, 1H), 3.09 (dd, *J* = 17.8, 9.0 Hz, 1H), 1.35 (d, *J* = 6.4 Hz, 3H).
^{13}C NMR (151 MHz, $CDCl_3$) δ 201.00, 136.84, 133.69, 128.83, 128.21, 64.18, 46.63, 22.56.
Spectral data match those previously reported.[15]

Enantiomer separation: SFC OJ-H column, 5% iPrOH in $scCO_2$, 2.5 mL/min flow rate.

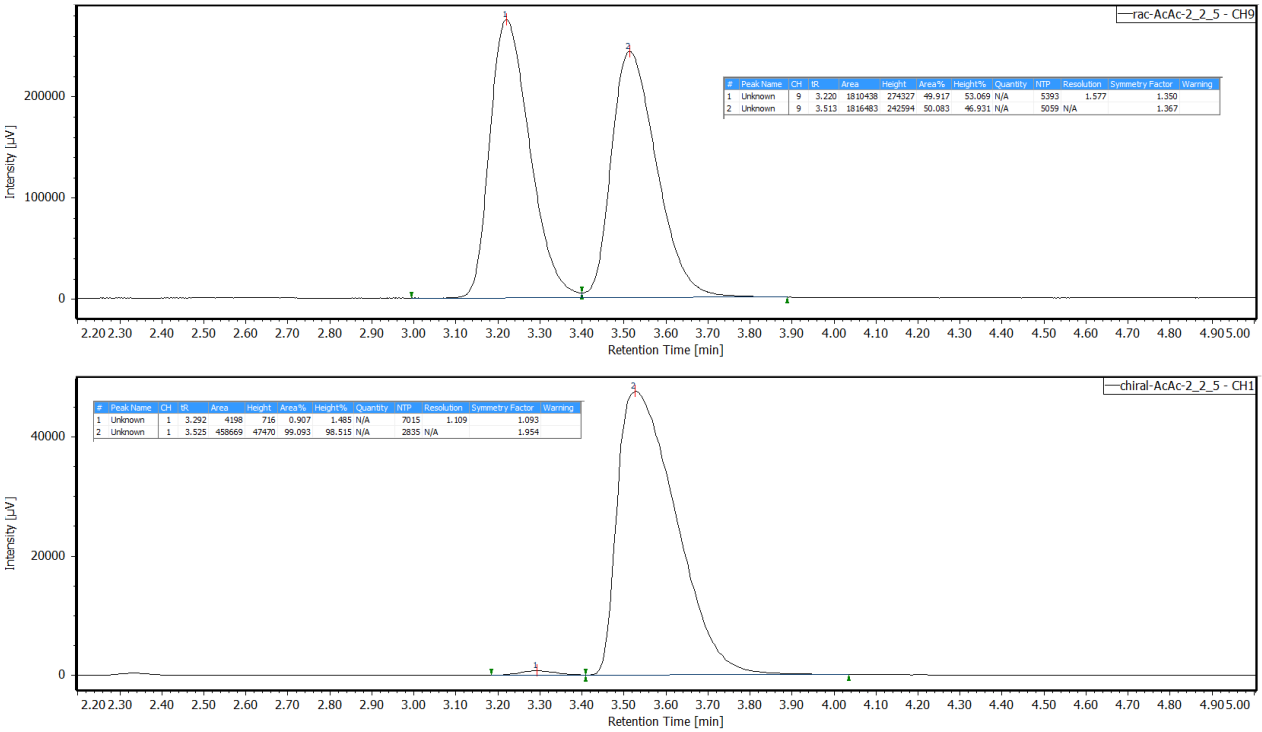

Supplementary Figure 27. SFC traces of the racemic 3-hydroxy-1-phenylbutan-1-one (top) and the enantioenriched products of the hCAII-catalyzed reduction (bottom).

(S)-2-hydroxy-1-phenylpropan-1-one (**30**)

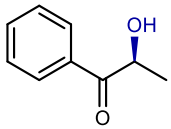

^{1}H NMR (400 MHz, $CDCl_3$) δ 7.93 (dt, *J* = 8.5, 1.8 Hz, 2H), 7.74 – 7.59 (m, 1H), 7.51 (td, *J* = 7.8, 7.3, 1.6 Hz, 2H), 5.26 – 5.12 (m, 1H), 3.79 (d, *J* = 6.3 Hz, 1H), 1.46 (d, *J* = 7.1 Hz, 3H).
^{13}C NMR (151 MHz, $CDCl_3$) δ 202.52, 134.12, 133.48, 129.01, 128.79, 69.46, 22.43.
Spectral data match those previously reported.[16]

Enantiomer separation: SFC OD-H column, 5% iPrOH in $scCO_2$, 2.5 mL/min flow rate.

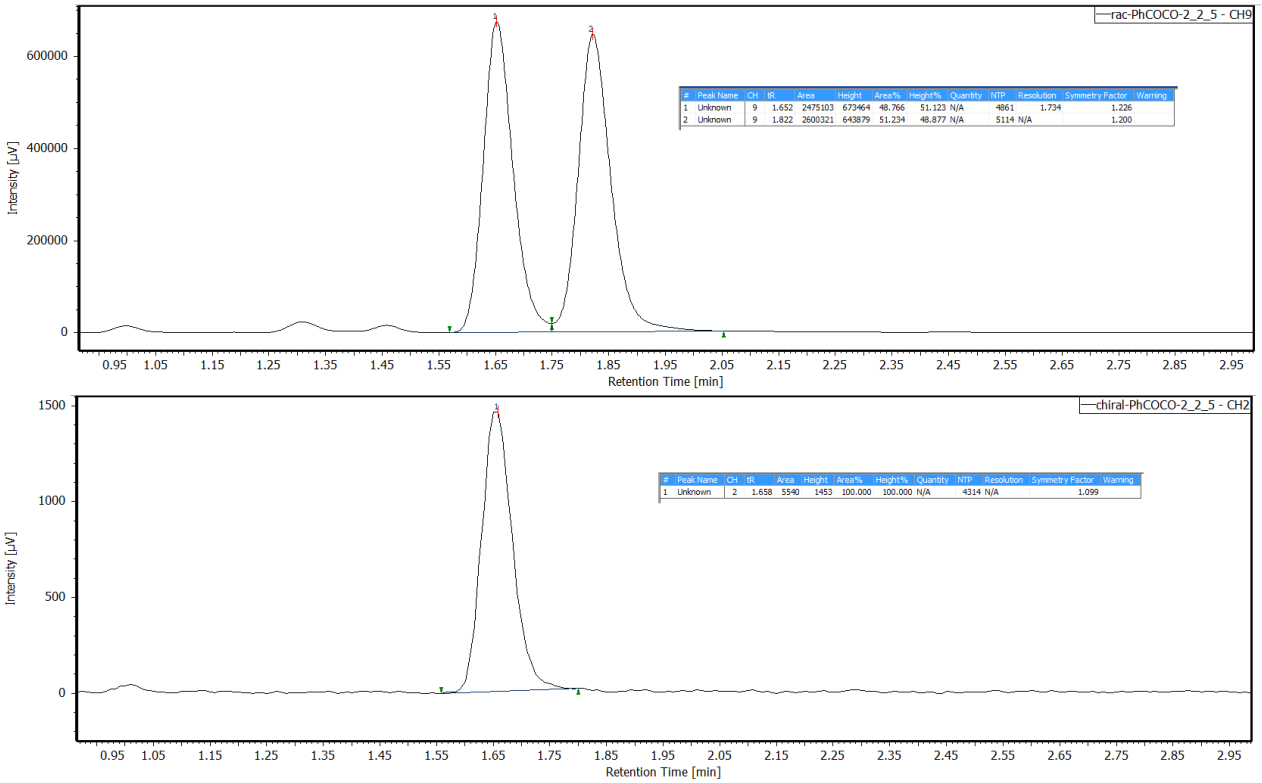

Supplementary Figure 28. SFC traces of the racemic 2-hydroxy-1-phenylpropan-1-one (top) and the enantioenriched products of the hCAII-catalyzed reduction (bottom).

(S)-1-(2-bromophenyl)ethan-1-ol (**32**)

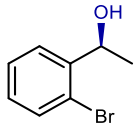

^{1}H NMR (400 MHz, $CDCl_3$) δ 7.63 (dd, *J* = 7.8, 1.8 Hz, 1H), 7.56 (dd, *J* = 8.0, 1.3 Hz, 1H), 7.38 (td, *J* = 7.5, 1.2 Hz, 1H), 7.17 (ddd, *J* = 8.0, 7.3, 1.8 Hz, 1H), 5.28 (q, *J* = 6.4 Hz, 1H), 1.53 (d, *J* = 6.4 Hz, 3H).

^{13}C NMR (151 MHz, $CDCl_3$) δ 144.73, 132.78, 128.89, 127.98, 126.79, 121.84, 69.31, 23.70.

Spectral data match those previously reported.[7]

Enantiomer separation: SFC OJ-H column, 5% iPrOH in $scCO_2$, 2.5 mL/min flow rate.

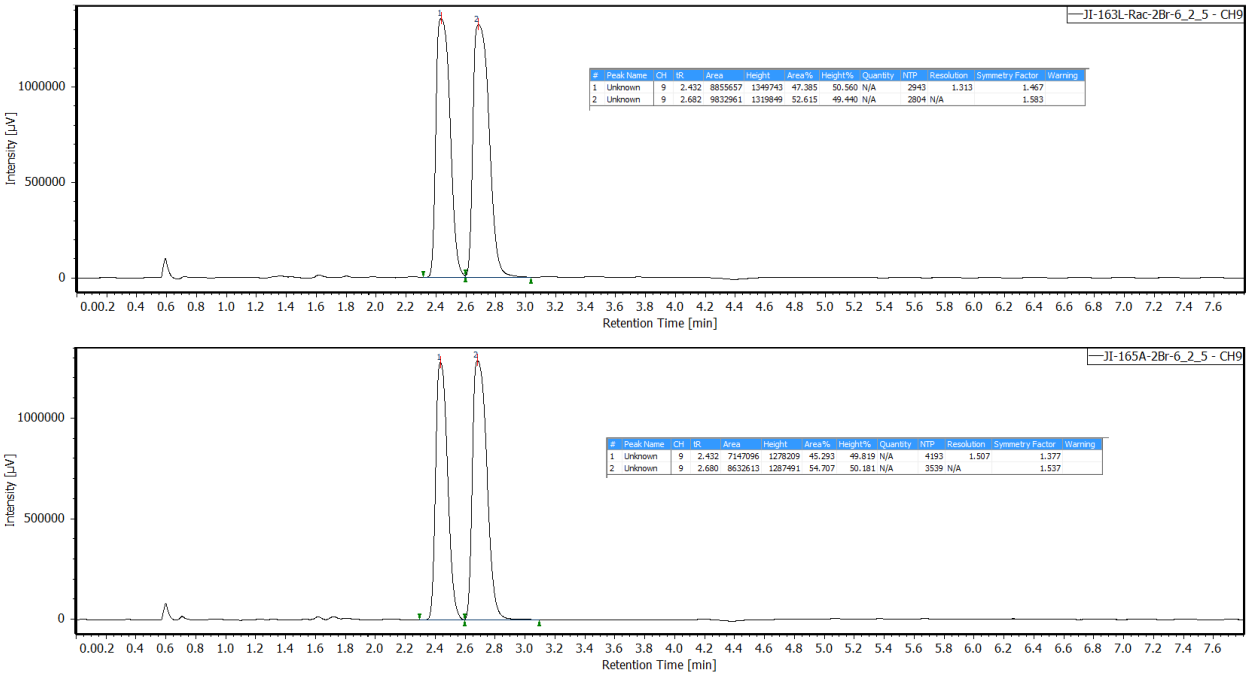

Supplementary Figure 29. SFC traces of the racemic 1-(2-bromophenyl)ethan-1-ol (top) and the enantioenriched products of the hCAII-catalyzed reduction (bottom).

7. QM/MM Study of hCAII Catalytic Intermediates

7.1 Complex of ZnOH-hCAII Docked by Phenylsilane

The binding mode of phenylsilane to the active site in ZnOH-hCAII was simulated in three steps. In step one, the starting structure for phenylsilane-hCAII complex was generated through docking. In step 2, the structure of the docking complex was equilibrated through Molecular Dynamics (MD). In step 3, the most frequent trajectory was further optimized through QM/MM calculations.

Generation of the initial structure with Glide Docking

Protein structure with the PDB code of 1BN1 was used as the starting structure for the calculations. Protein preparation module in Schrödinger [17,18] was used to correct errors in the crystal structure and add hydrogen atoms. The Hg ion coordinating to cysteine was replaced with two protons to ensure accuracy of the structure. Protonation states were simulated at pH of 7.0, and water molecules beyond 5 Å from the protein were deleted for clarity. The hydrogen-bonding interactions within the protein were optimized with the OPLS_2005 force field[19] to generate an accurate structure for the protein receptor. Then, the native sulfamide anion was replaced with a hydroxide group, followed by receptor grid generation with a box length of 20 Å centering at the Zn atom.

The phenylsilane ligand was built and prepared with the same force field with the Ligprep module.[20] Docking of the ligands into the hCAII enzymatic active site was performed using the Glide Dock module in Maestro.[21] For optimization of the structure with the phenylsilane docked, the ligand was set to be flexible, and the docking was performed at the XP (extra precision) level with the same OPLS_2005 force field.[19] The most stable docking complex was exported and used for the MD simulations.

Classical MD Simulations

MD simulations was performed using the Desmond program of the Schrödinger package.[22,23] Each protein was immersed in a pre-equilibrated truncated cubic box with a 10 Å buffer of TIP3P[24] water molecules using the System Builder panel of Desmond,[21] resulting in the addition of around 7,500 solvent molecules. The systems were neutral, therefore do not need the addition of explicit counter ions (Na^+ or Cl^-). All subsequent calculations were done using the OPLS_2005 force field.[19] The system was equilibrated in two stages. In the first stage, the systems were gently heated using six 50-ps steps, incrementing the temperature by 50 K for each step (0–300 K); The system was simulated with a weak restraint of 15 kcal/mol/Å on the solute using the NPT ensemble, [25] at the target temperature of 300 K and target pressure of 1.013 bar. In the second stage, the system was equilibrated for 1.2 ns without constraints. Trajectories were processed and analyzed using the

Trajectory Frame Clustering panel of Desmond.[4] The most populated conformational snapshot extracted from the classical MD trajectory was selected for the subsequence QM/MM simulations.

QM/MM Simulations

QM/MM simulations were performed using the QSite program[26-28] in the Schrödinger package 2020-2. The QM/MM methodology (an additive scheme) with hydrogen caps on boundary QM atoms and electrostatic treatment at the interface between the QM and MM regions using Gaussian charge distributions represented on a grid was employed.[9,10] The QM region has 51 atoms in total, including the Zinc hydroxide (3 atoms), three histidine side chains (33 atoms), and the docked phenylsilane (15 atoms). The QM region was simulated with the (R)B3LYP functional,[29,30] with the Los Alamos National Laboratory effective core potential (LACVP*) basis set.[31,32] In the LACVP* basis set the valence electrons are described by the Pople's split-valence basis set 6-31G(d) augmented by polarization on all atoms.[33] MM calculations were conducted for all other atoms with the OPLS_2005 force field with no cut-offs introduced for nonbonding interactions. No atom in the system was frozen or restrained during the optimization. Convergence thresholds for the energy and gradient change were set to be 5×10^{-5} Hartree and 4.5×10^{-4} Hartree·Bohr^{-1}, respectively. The structure optimization for $PhSiH_3$-ZnOH-hCAII converged with energy change of -3.4628×10^{-5} hartree.

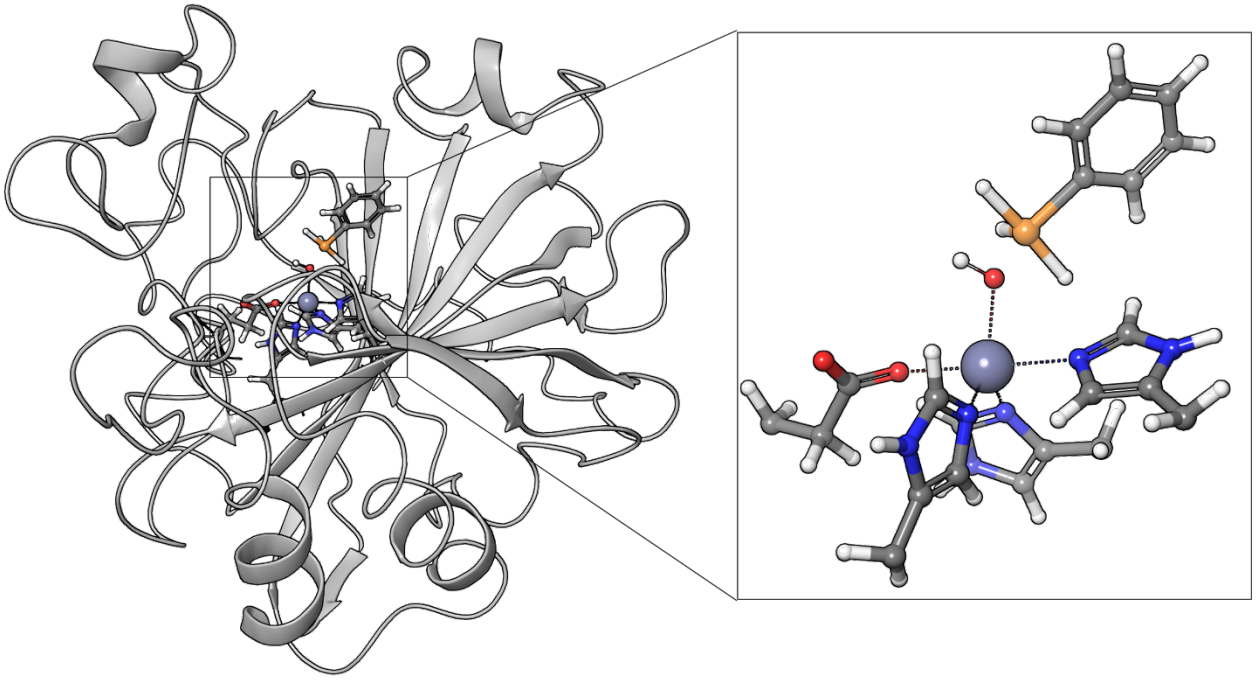

Supplementary Figure 30. Atoms in the QM region were shown in ball-and-stick format. All other atoms are in the MM region. The hanging bonds between Cα and Cβ of histadine were hydrogen-capped for QM/MM simulation.

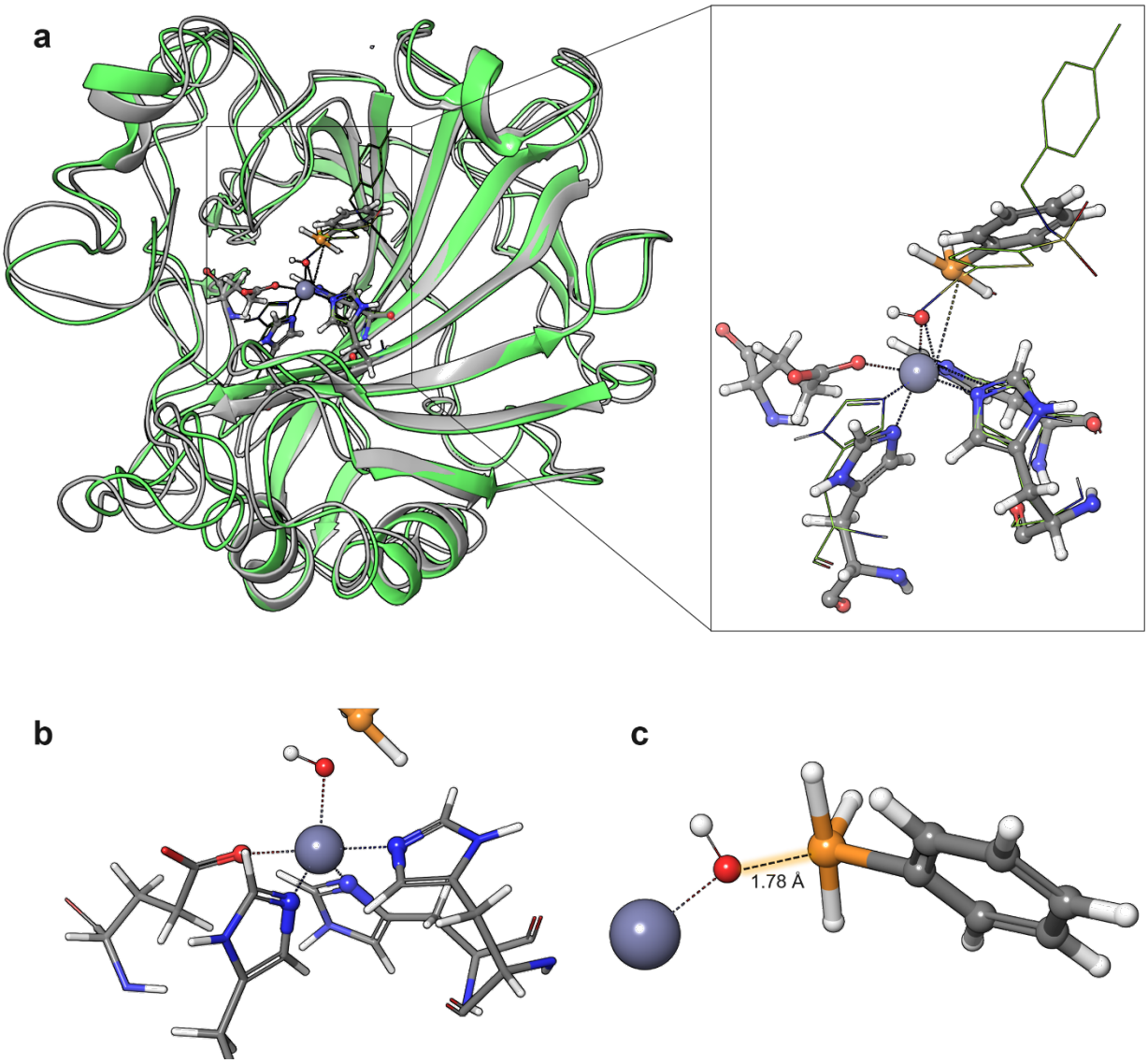

Supplementary Figure 31. (a) The structure of ZnOH-hCAII (gray) docked to phenylsilane optimized by QM/MM overlayed with the structure of hCAII bound by thiophene-2,5-disulfonic acid 2-amide-5-(4-methyl-benzylamide) as inhibitor (pdb 1BN1, green). The protein backbone of the two complexes are almost identical, indicating the QM/MM calculation well reproduced the protein structure. (b) The triagonal bipyramidal geometry around Zn center. (c) The Si atom closely contacts the hydroxide group with a bond distance of 1.78 Å, forming a pentacoordinate trigonal bipyramidal silicon center.

7.2 Complex of ZnH-hCAII docked by acetophenone and 2'-Bromoacetophenone

The binding mode of acetophenones to the active site in ZnH-hCAII was simulated in three steps using almost idental procedure in simulating the complex of phenylsilane with ZnOH-hCAII. In step one, the starting structure for acetophenone-hCAII complex was generated through docking.

In step 2, the structure of the docking complex was equilibrated through Molecular Dynamics (MD). In step 3, the most frequent trajectory was further optimized through QM/MM calculations.

Generation of the initial structure with Glide docking

Protein structure with the PDB code of 1BN1 was used as the starting structure for the calculations. Protein preparation module in Schrödinger [17,18] was used to correct errors in the crystal structure and add hydrogen atoms. The Hg ion coordinating to cysteine was replaced with two protons to ensure accuracy of the structure. Protonation states were simulated at pH of 7.0, and water molecules beyond 5 Å from the protein were deleted for clarity. The hydrogen-bonding interactions within the protein were optimized with the OPLS_2005 force field[19] to generate an accurate structure for the protein receptor. Then, the native sulfamide anion was replaced with a hydride, followed by receptor grid generation with a box length of 20 Å centering at the Zn atom.

The ligand was built and prepared with the same force field with the Ligprep module.[20] Docking of the ligands into the hCAII enzymatic active site was performed using the Glide Dock module in Maestro.[21] For optimization of the structure with the ketone docked, the ligand was set to be flexible, and the docking was performed at the XP (extra precision) level with the same OPLS_2005 force field. The most stable docking complex was exported and used for the MD simulations.

Classical MD Simulations

MD simulations was performed using the Desmond program of the Schrödinger package.[22,23] Each protein was immersed in a pre-equilibrated truncated cubic box with a 10 Å buffer of TIP3P[24] water molecules using the System Builder panel of Desmond, [21] resulting in the addition of around 7,500 solvent molecules. The systems were neutral, therefore do not need the addition of explicit counter ions (Na^+ or Cl^-). All subsequent calculations were done using the OPLS_2005 force field.[19] The system was equilibrated in two stages. In the first stage, the systems were gently heated using six 50-ps steps, incrementing the temperature by 50 K for each step (0–300 K); The system was simulated with a weak restraint of 15 kcal/mol/Å on the solute using the NPT ensemble, [25] at the target temperature of 300 K and target pressure of 1.013 bar. In the second stage, the system was equilibrated for 1.2 ns without constraints. Trajectories were processed and analyzed using the Trajectory Frame Clustering panel of Desmond.[4] The most populated conformational snapshot extracted from the classical MD trajectory was selected for the subsequence QM/MM simulations.

QM/MM Calculations

QM/MM simulations were performed using the QSite program[26-28] in the Schrödinger package 2020-2. The QM/MM methodology (an additive scheme) with hydrogen caps on boundary QM atoms and electrostatic treatment at the interface between the QM and MM regions using

Gaussian charge distributions represented on a grid was employed.[9,10] The QM region has 52 atoms in total, including the Zinc hydride (2 atoms), three histidine side chains (33 atoms), and the docked acetophenone or 2'-bromoacetophenone (17 atoms). The QM region was simulated with the (R)B3LYP functional,[29,30] with the Los Alamos National Laboratory effective core potential (LACVP*) basis set.[31,32] In the LACVP* basis set the valence electrons are described by the Pople's split-valence basis set 6-31G(d) augmented by polarization on all atoms.[33] MM calculations were conducted for all other atoms with the OPLS_2005 force field with no cut-offs introduced for nonbonding interactions. No atom in the system was frozen or restrained during the optimization. Convergence thresholds for the energy and gradient change were set to be 5×10^{-5} Hartree and 4.5×10^{-4} Hartree·Bohr^{-1}, respectively. The structure optimization of acetophenone-ZnH-hCAII converged with energy change of -3.0778×10^{-5} Hartree.

The optimized structure contains a strong hydrogen-bonding interaction of the carbonyl group to the amide N-H of Thr199, with a bond distance of 2.28 Å. The Thr199 amide N-H is the major functional group in the binding site of the the native enzyme ineracting with carbon dioxide, the native substrate. The ketone was placed in an ideal geometry for concerted hydride and proton transfer to form the corresponding (S)-1-phenylethan-1-ol.

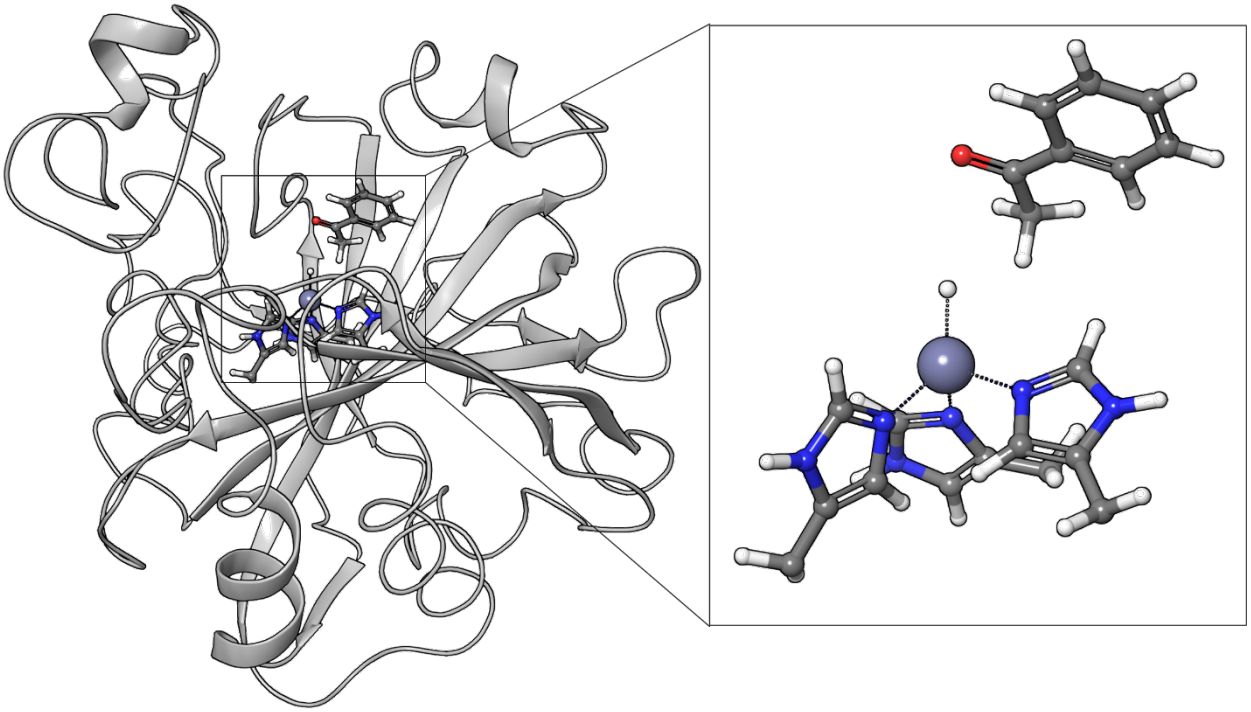

Supplementary Figure 32. Atoms in the QM region were shown in ball-and-stick format. All other atoms are in the MM region. The hanging bonds between Cα and Cβ of histadine were hydrogen-capped for QM/MM simulation.

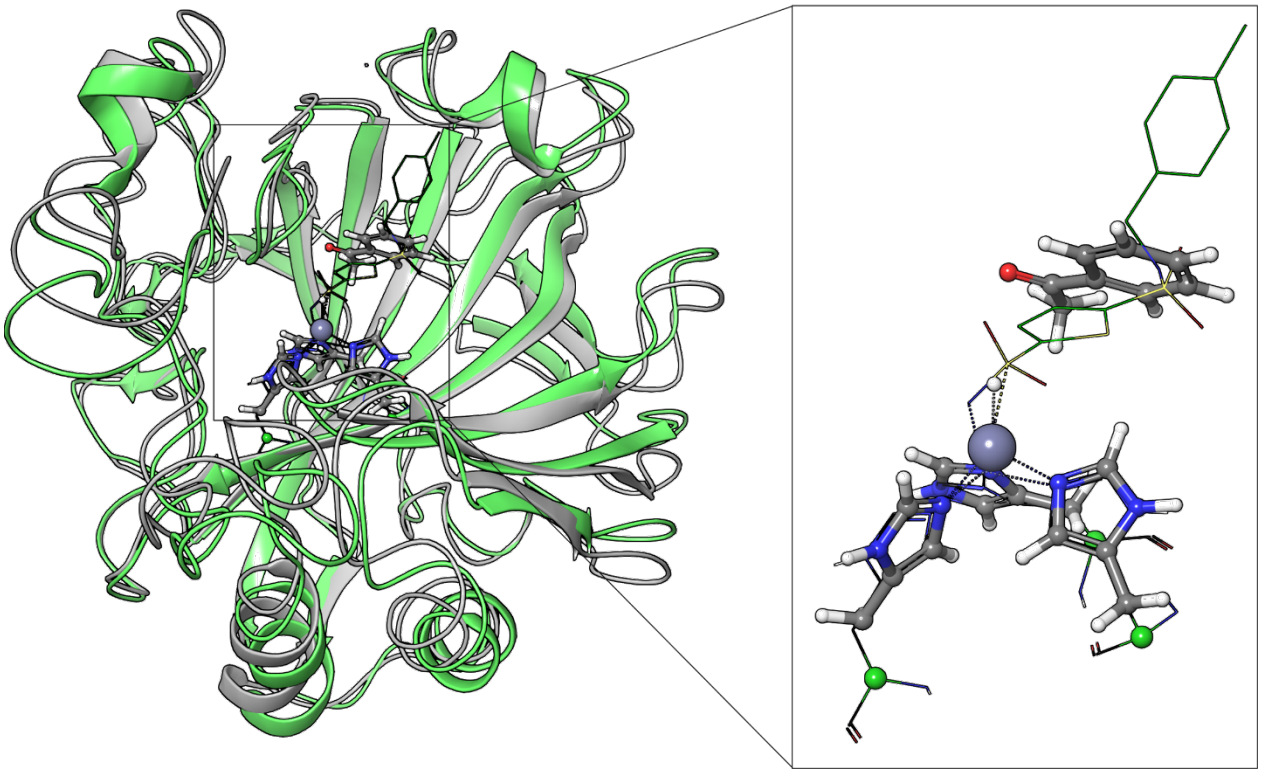

Supplementary Figure 33. The structure of ZnH-hCAII (gray) docked with acetophenone optimized by QM/MM overlayed with hCAII bound by thiophene-2,5-disulfonic acid 2-amide-5-(4-methyl-benzylamide) as inhibitor (pdb 1BN1, green). The protein backbone of the two complexes are almost identical, indicating the QM/MM calculation well reproduced the protein structure. A more detailed figure showing the accurate interactions of acetophenone with neighboring residues was included in Figure 4c.

7.3 Cartesian coordinates QM/MM optimized structures in xyz format

hCAII-ZnOH-PhSiH3 (QM region + Hydrogen Cap)

atom	x	y	z
C1	-1.5314610264	5.8304157448	0.4568552644
N2	-0.7843192035	4.8768752071	1.0313055561
C3	-0.4676158868	4.7822335896	2.4511338982
C4	0.8552285102	4.0204787740	2.6249591689

O5	1.0867675528	3.0165166717	1.9497163765
C6	-1.6609016778	4.1377648453	3.2107019052
C7	-1.9923868313	2.7174595248	2.8820810344
N8	-2.9190803073	2.3083663789	1.9412669331
C9	-1.5180298326	1.5608950171	3.4416086306
C10	-2.9662664827	0.9536923342	1.9629384733
N11	-2.1193531924	0.4651156189	2.8618318281
H12	-0.3701994312	4.1801496571	0.4269236446
H13	-0.3126357305	5.7949576168	2.8352979578
H14	-2.5201590685	4.7912785717	3.0499873457
H15	-1.4340279382	4.1883231570	4.2813733936
H16	-3.4576094406	2.9275411720	1.3300132842
H17	-0.7647367535	1.4606132328	4.2050998392
H18	-3.6040528443	0.3642000452	1.3213125679
N19	1.6992533204	4.4680469558	3.5640807953
C20	2.6521581224	2.8896609780	5.2111243979
N21	3.6460030506	2.0467670367	5.5296870068
C22	3.7099107531	1.1581279496	6.6831787798
C23	5.1084691383	1.2152789807	7.3079014872
O24	6.0777518744	1.5271443158	6.6201628218
C25	3.2898266710	-0.2892639666	6.3009935436
C26	1.8702569535	-0.4503909674	5.8547471217
N27	0.7802405819	-0.3248088764	6.6987284735
C28	1.3444259710	-0.7659021605	4.6260345674
C29	-0.3371399329	-0.5446389084	5.9842626578
N30	-0.0360464960	-0.8168559816	4.7211233355
H31	4.4791738340	2.0860144471	4.9582526301
H32	3.0289766683	1.5370743808	7.4466188687
H33	3.4934817755	-0.9556798838	7.1513084904
H34	3.9439893911	-0.6123158755	5.4880385490
H35	0.7875290200	-0.0437533587	7.6810347531
H36	1.8696158050	-0.9537638964	3.6982841286
H37	-1.3260146658	-0.4964552164	6.4153022776
N38	5.1921026496	0.9520490674	8.6198880561
C39	4.9046627121	-5.6458877334	5.8816846207
N40	3.7715354592	-5.5719635593	5.1576695325
C41	2.6434094720	-6.5006629376	5.2267414137

C42	3.0409920951	-7.8534881991	4.5950895561
O43	2.9330448899	-8.8945789150	5.2427744841
C44	1.3972534336	-5.8855270874	4.5204647796
C45	1.0092116223	-4.3984818441	4.7800374862
C46	-0.4993555044	-4.2534165670	5.1611658791
O47	-1.1942682585	-3.3692261387	4.5555468261
O48	-0.9204610105	-5.0256422158	6.0543477902
H49	3.6756453832	-4.8224837414	4.4925504881
H50	2.4019782095	-6.6491303333	6.2797781003
H51	0.5500161207	-6.5047063894	4.8411884669
H52	1.5063724490	-6.0238040612	3.4346782643
H53	1.2590617196	-3.7811427326	3.9149538084
H54	1.5679199083	-3.9616591070	5.6117918132
N55	3.6017893529	-7.8201664038	3.3711252386
C56	3.0448604756	0.7479247978	-0.3807262343
N57	1.7958230280	1.2414522984	-0.4028803808
C58	0.5921942528	0.6412779571	-0.9683609103
C59	-0.1860545701	1.7318681208	-1.7126027206
O60	-1.0161949473	2.4153897473	-1.1144846852
C61	-0.2253921058	-0.0618774577	0.1520690582
C62	0.1396968764	-1.4866150803	0.4485172765
N63	-0.4220338883	-2.1651647100	1.5321271432
C64	0.9496522200	-2.3620435817	-0.2147268149
C65	0.0733898314	-3.4006885937	1.5036674871
N66	0.8848323551	-3.5542459552	0.4519673057
H67	1.6741989679	2.1665693447	-0.0137022288
H68	0.8686045848	-0.0854087192	-1.7353930184
H69	-1.2906846091	-0.0316965295	-0.1181720076
H70	-0.1281201202	0.5588298231	1.0477136492
H71	1.6392134772	-2.2379512203	-1.0274256808
H72	-0.1734830150	-4.1718879211	2.2135040122
H73	1.5650742687	-4.2985729853	0.2890593785
N74	0.1016383851	1.8785959728	-3.0170923385
Zn75	-1.4114996316	-1.6091719965	3.2739904247
Si76	-4.8627898768	-2.5978670959	2.1114259364
C77	-6.5172157269	-1.6964923583	1.7029687100
C78	-7.5660650157	-1.5654471651	2.6299451749

C79	-8.7567441106	-0.9095664113	2.3048114182
C80	-8.9393951509	-0.3886110665	1.0214805854
C81	-7.9186878135	-0.5166716365	0.0741144904
C82	-6.7207523606	-1.1471475048	0.4234149414
H83	-9.8695965564	0.1136876031	0.7626188687
O84	-3.5116283747	-2.1465517146	3.1665495528
H85	-4.8828209006	-4.0454239207	1.4869064172
H86	-4.0971260514	-2.0024361866	0.9375294696
H87	-5.5210087969	-3.2039753515	3.4360986800
H88	-7.4562269855	-1.9817380372	3.6267822681
H89	-9.5383157411	-0.8115570748	3.0552508564
H90	-8.0595461314	-0.1293610103	-0.9322223567
H91	-5.9218678904	-1.2240491034	-0.3120336923
H92	-3.6237168244	-2.5942901038	4.0211783563
H93	-0.8102270199	4.5971964691	2.6692178287
H94	3.5892980010	0.7425589483	6.5734473828
H95	2.2856184587	-6.3240477527	5.0239582752
H96	0.3574523404	0.4393909697	-0.6466678307

hCAII-ZnH-PhC(O)Me (QM region + Hydrogen cap)

atom	x	y	z
C1	-3.7127176766	4.6581194448	6.5755158970
N2	-3.9698714984	3.7918261017	5.5851812576
C3	-5.1905959921	3.7747175717	4.7917369740
C4	-5.4496887446	2.3909997381	4.1848373791
O5	-4.5174479155	1.7062407733	3.7650462567
C6	-5.1822941475	4.8840690485	3.7050346097
C7	-4.0610223285	4.8127964759	2.7213690152
N8	-2.8818851787	5.5155723652	2.8745848791
C9	-3.9015987791	4.0865545869	1.5700987092
C10	-2.0692165181	5.1958650537	1.8444472132
N11	-2.6542557790	4.3261215050	1.0362006669
H12	-3.2907018993	3.0632714230	5.4089448668
H13	-6.0273636038	3.9695146157	5.4700540448
H14	-5.1449379134	5.8352722078	4.2350026279
H15	-6.1418946871	4.8475176080	3.1809973502

H16	-2.6700323419	6.1951316503	3.6099858001
H17	-4.5922139247	3.3987565177	1.1059227777
H18	-1.0850161018	5.6175425699	1.7082825989
N19	-6.7323546432	2.0334783113	4.0472689467
C20	-7.3122360132	1.1258844686	1.8290921326
N21	-7.3093232607	0.0412035911	1.0394632889
C22	-7.7510512642	0.0026595750	-0.3492929400
C23	-8.6142149069	-1.2492949590	-0.5275322018
O24	-8.1590407056	-2.3440646945	-0.2081170024
C25	-6.5898110841	0.0150131132	-1.3777282695
C26	-5.7065444532	1.2231621491	-1.3795367941
N27	-5.8285971527	2.2567980054	-2.2815373474
C28	-4.5302176860	1.4652970800	-0.7212438289
C29	-4.7523528782	3.0531455648	-2.1774364921
N30	-3.9304758710	2.6070319709	-1.2308322127
H31	-7.2296881860	-0.8536836774	1.5041778299
H32	-8.3926269325	0.8661177310	-0.5375749493
H33	-6.9917467654	-0.1210644669	-2.3846529661
H34	-5.9608391525	-0.8582037258	-1.1822331143
H35	-6.5773243043	2.3842657227	-2.9698971443
H36	-4.0526428888	0.8480674285	0.0229992702
H37	-4.6065677251	3.9300191028	-2.7882775744
N38	-9.8356477739	-1.0771639628	-1.0472565440
C39	-2.8314372725	-1.7458117840	3.8594039760
N40	-2.4929948439	-0.4440190885	3.8809640573
C41	-1.1521409103	0.1321181767	3.7558079517
C42	-0.8431143073	0.8774408530	5.0635291901
O43	-1.5516241605	1.8265946142	5.4010164282
C44	-1.1202118718	1.1730502115	2.5999376855
C45	-1.1850430475	0.5377630325	1.2349701095
N46	-1.3835353463	1.2873933541	0.0738288270
C47	-1.1473795901	-0.7867140165	0.8735665420
C48	-1.4939520478	0.3990361251	-0.9244123625
N49	-1.3410222852	-0.8445197004	-0.4771190785
H50	-3.2224449979	0.2052948750	4.1409511425
H51	-0.3919028175	-0.6359343003	3.6024882052
H52	-0.2082496273	1.7867427294	2.6937819688

H53	-1.9683812120	1.8534909510	2.7315850559
H54	-1.0393115596	-1.6923892534	1.4446960741
H55	-1.7575065597	0.6094122348	-1.9496519258
H56	-1.5886109458	-1.7420670245	-1.0078123973
N57	0.2306798999	0.4757761172	5.7620533975
Zn58	-1.9804515576	3.1799464883	-0.6752167282
C59	1.5220417874	6.0163179244	-1.5476720056
C60	1.4236996431	7.3618600603	-0.9009273805
C61	1.6947827242	7.5696998127	0.4614906501
C62	1.6373498868	8.8533846555	1.0036575743
C63	1.3036476528	9.9414919148	0.1937287153
C64	1.0244628624	9.7424404032	-1.1623275970
C65	1.0892332919	8.4635000250	-1.7076566669
H66	1.2667911944	10.9413826559	0.6191099958
H67	-0.8095141582	4.0898925381	-1.5030152020
O68	1.2484556523	5.8829843508	-2.7363909792
H69	1.9533781157	6.7368636339	1.1065316020
H70	1.8749419228	9.0042610377	2.0532373319
H71	0.7551209538	10.5818678484	-1.7970409245
H72	0.8857612319	8.3037209295	-2.7605884990
C73	1.9589059409	4.8176300615	-0.7414105142
H74	1.0447350097	4.3286886887	-0.3749074801
H75	2.4494075518	4.0979285723	-1.4030034433
H76	2.6204905867	5.0533639827	0.0942763238
H77	-5.1882124018	4.0932298420	4.4797276204
H78	-7.4176409305	0.0062064703	-0.6445729108
H79	-1.1429735808	0.4309861483	3.4239394047

hCAII-ZnH-2BrPhC(O)Me conformation 1 (QM region + Hydrogen cap)

atom	x	y	z
C1	-3.8155947354	4.3345596147	6.6496642754
N2	-4.0829396701	3.4330615034	5.6917719480
C3	-5.3019934282	3.4127239276	4.8897602422
C4	-5.5655529126	2.0267223836	4.2798730665
O5	-4.6372773768	1.3554645627	3.8282447650
C6	-5.2978445031	4.5227743244	3.8039264083

C7	-4.1340643160	4.5110144007	2.8706064122
N8	-3.0291156699	5.3240664155	3.0396555015
C9	-3.8852754429	3.7900299324	1.7334367678
C10	-2.1696922769	5.0709832566	2.0270777860
N11	-2.6577332128	4.1446139871	1.2179121745
H12	-3.4356159905	2.6644737047	5.5764881357
H13	-6.1392742896	3.6093604755	5.5669851135
H14	-5.3150026115	5.4723249513	4.3371971388
H15	-6.2323976080	4.4480480575	3.2361700016
H16	-2.8879913487	6.0111740446	3.7820880333
H17	-4.4947147294	3.0280912183	1.2707195256
H18	-1.2206848031	5.5733611093	1.9117833852
N19	-6.8496128915	1.6526206897	4.1733100514
C20	-7.5194169616	0.7665318551	1.9609979744
N21	-7.6979535116	-0.3029654928	1.1675427992
C22	-7.8514047782	-0.3093989757	-0.2859874336
C23	-8.7443620977	-1.4944371460	-0.6885805715
O24	-8.2378340254	-2.5221759920	-1.1384206239
C25	-6.4631334361	-0.3012066344	-1.0028611846
C26	-5.6474609063	0.9531694187	-1.0113800483
N27	-5.9421266744	2.0990688560	-1.7272068366
C28	-4.3616487856	1.1338341429	-0.5754982193
C29	-4.8659133630	2.9060563891	-1.7271637781
N30	-3.8718556332	2.3540313371	-1.0316855577
H31	-7.7906156831	-1.1983747108	1.6284707148
H32	-8.4014937801	0.5859943620	-0.5726787374
H33	-6.5791209189	-0.6135376859	-2.0435887120
H34	-5.8449069868	-1.0875465684	-0.5739272543
H35	-6.8130731494	2.3097714456	-2.2167000333
H36	-3.7600165208	0.4001273249	-0.0639988905
H37	-4.8503759947	3.8652979155	-2.2227251393
N38	-10.0629858389	-1.3318973147	-0.5052117618
C39	-2.7761025601	-1.9415758827	3.8678628208
N40	-2.4397833893	-0.6426023551	3.9738235229
C41	-1.1065234827	-0.0426557224	3.8558621593
C42	-0.8272569340	0.6708506934	5.1898715593
O43	-1.5045851069	1.6503724294	5.5015262962

C44	-1.0852194891	1.0283302397	2.7240109230
C45	-1.0370655639	0.4479771879	1.3347974828
N46	-1.2235575530	1.2355574627	0.1929663694
C47	-0.9503511798	-0.8575973129	0.9270046136
C48	-1.3004892791	0.3739409077	-0.8316954766
N49	-1.1053773546	-0.8757470977	-0.4307686801
H50	-3.1456875544	-0.0324273293	4.3632556899
H51	-0.3320724599	-0.7965696762	3.6972972445
H52	-0.2338476827	1.7112684367	2.8886515881
H53	-1.9914071405	1.6352707555	2.8317292633
H54	-0.8652513014	-1.7838471116	1.4664277500
H55	-1.6003978912	0.5940660174	-1.8442990845
H56	-1.4774663128	-1.7274301460	-0.9629189081
N57	0.1754623141	0.2021177506	5.9500506863
Zn58	-1.9492263289	3.0699567478	-0.5360783022
C59	1.4300982982	6.3198351821	-1.7150383599
C60	1.3818660929	7.7943118433	-1.3685054215
C61	1.4590125057	8.4062481932	-0.1075969494
C62	1.4489614672	9.7930878790	0.0438122866
C63	1.3570772257	10.6121012484	-1.0797828486
C64	1.2632369812	10.0400306973	-2.3486665559
C65	1.2777660246	8.6575522139	-2.4799071511
H66	1.3423473995	11.6914291973	-0.9526184837
H67	-0.8234096728	4.0915060053	-1.3456285891
O68	1.0737653041	5.9893720814	-2.8388772354
Br69	1.5078659323	7.4043997594	1.5818461559
H70	1.5036551836	10.2250772740	1.0370818699
H71	1.1580516965	10.6580028095	-3.2339287506
H72	1.1952720017	8.2060058341	-3.4612000823
C73	1.9631612271	5.2628529692	-0.7810337729
H74	1.1316267689	4.8815865173	-0.1744036973
H75	2.3043375165	4.4207459629	-1.3882381054
H76	2.7656639095	5.6115003741	-0.1286632559
H77	-5.3008022065	3.7314368688	4.5780002574
H78	-7.4528102244	-0.3070468256	-0.4918131712
H79	-1.1004067708	0.2648412047	3.5308898539

hCAII-ZnH-2BrPhC(O)Me conformation 2 (QM region + Hydrogen cap)

atom	x	y	z
C1	-11.9466917703	0.6806996591	10.4684354225
N2	-11.3898287262	-0.3519444007	11.1082217024
C3	-10.5084661439	-1.3504828606	10.5203097741
C4	-10.6872963461	-2.7032393347	11.2252031395
O5	-11.2173774842	-2.7552940132	12.3360286561
C6	-9.0410813809	-0.8543210853	10.4950051538
C7	-8.4102723944	-0.6390898478	11.8271348590
N8	-8.5163957171	0.5588028760	12.5054142442
C9	-7.6680593603	-1.4517701307	12.6440120220
C10	-7.8521183469	0.4448350178	13.6774895562
N11	-7.3339253908	-0.7705173696	13.7985930754
H12	-11.6183996526	-0.4868978784	12.0932416842
H13	-10.8342563121	-1.5069007343	9.4883414064
H14	-9.0524293638	0.0842605634	9.9383922725
H15	-8.4454072714	-1.5527478588	9.9083286539
H16	-8.9712449299	1.4036984523	12.1427814614
H17	-7.3686577792	-2.4773264625	12.4872619322
H18	-7.7659678497	1.2409828922	14.4029417811
N19	-10.2318372966	-3.7882075166	10.5932185447
C20	-8.8256942756	-5.6535482317	11.3137003858
N21	-8.6054039146	-6.4690670286	12.3464781814
C22	-7.4625413812	-7.3557399940	12.5170208531
C23	-7.9817134502	-8.7967402447	12.3719715511
O24	-9.1211646947	-9.0623896821	12.7597255628
C25	-6.8584479851	-7.1892733296	13.9377457713
C26	-6.3290663765	-5.8014400548	14.1547354946
N27	-5.0430064782	-5.3903705375	13.8565619295
C28	-6.9560648804	-4.6699734211	14.6120454837
C29	-4.9336379856	-4.0749484735	14.1362579891
N30	-6.0810979730	-3.5997038874	14.5953755370
H31	-9.3704843382	-6.6121377233	13.0060125152
H32	-6.7152630035	-7.1586942269	11.7527203847
H33	-6.0731659039	-7.9378980034	14.0945605666
H34	-7.6475768731	-7.3895148968	14.6687210221

H35	-4.2642870258	-5.9618019615	13.5335869992
H36	-7.9793117476	-4.5637731780	14.9402587358
H37	-4.0173657942	-3.5176005306	14.0200870241
N38	-7.1824476206	-9.7111631252	11.8136433323
C39	-12.7677366540	-3.8816939440	15.4110190448
N40	-12.0436335212	-2.8444225877	14.9870224345
C41	-11.7384054957	-1.6412535308	15.7391637418
C42	-12.4283866107	-0.4665941974	15.0320323396
O43	-12.0846797582	-0.1393343553	13.8958975926
C44	-10.2041722691	-1.4227534682	15.7351396790
C45	-9.4744619789	-2.3610235835	16.6563170604
N46	-8.0889945292	-2.3856193736	16.7106565138
C47	-9.9510552323	-3.2648514239	17.5730303583
C48	-7.7571582272	-3.2730515230	17.6437244303
N49	-8.8568317381	-3.8213112016	18.1879714299
H50	-11.7494494935	-2.8382244943	14.0085374389
H51	-12.1079331886	-1.6948095358	16.7644008926
H52	-9.9705082821	-0.3861952192	16.0107877807
H53	-9.8518873133	-1.5518484327	14.7063771267
H54	-10.9480412843	-3.5637483534	17.8453245747
H55	-6.7496071348	-3.5124453600	17.9429368687
H56	-8.9292628712	-4.5866894776	18.8924372455
N57	-13.4055751196	0.1561214931	15.6948607905
Zn58	-6.3973880593	-1.6812143995	15.5192783051
C59	-6.1479869174	2.4664472022	16.5138472244
C60	-5.2776332204	3.4026580137	15.7067997745
C61	-5.7520945047	4.7188263490	15.5749527425
C62	-5.0302828527	5.6867365747	14.8848735587
C63	-3.8105758295	5.3468995377	14.2959474932
C64	-3.3297978333	4.0405896073	14.3885555811
C65	-4.0626490932	3.0795681790	15.0864537892
H66	-3.2412127313	6.0915441925	13.7461362684
H67	-5.3536838064	-0.8505845712	16.4287502627
O68	-7.3455199402	2.4159071998	16.2759453192
H69	-6.6950507686	4.9697362968	16.0458053511
H70	-5.4266412873	6.6926591528	14.7958741881
H71	-2.3984854045	3.7525344118	13.9136358203

Br72	-3.4233818903	1.2458494814	15.0587905143
C73	-5.5871104662	1.7412053680	17.7171859323
H74	-6.0547711879	0.7592289150	17.8043558392
H75	-4.5059835723	1.6129500582	17.6746537039
H76	-5.8593832941	2.3486577072	18.5925387499
H77	-10.0871568817	-1.2080270053	10.5130444193
H78	-7.2890966587	-7.3079447945	12.9249333395
H79	-11.2979029873	-1.5785187236	15.7380083700

8. NMR Spectra

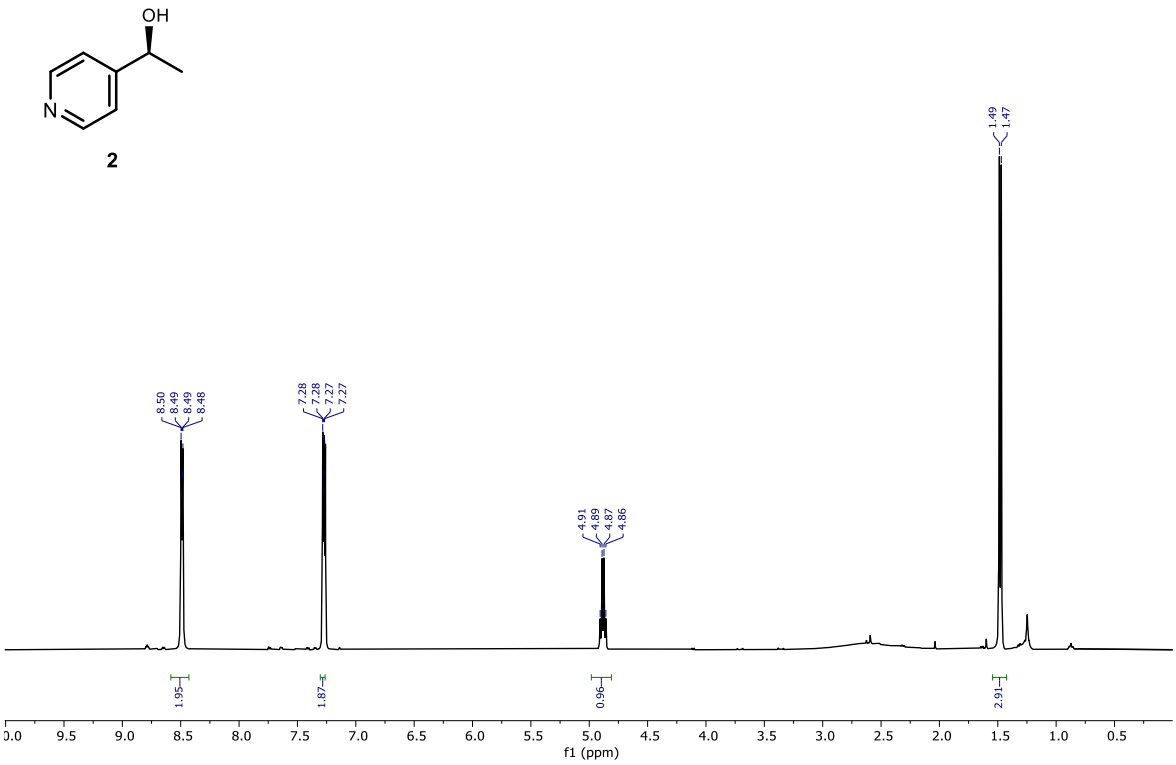

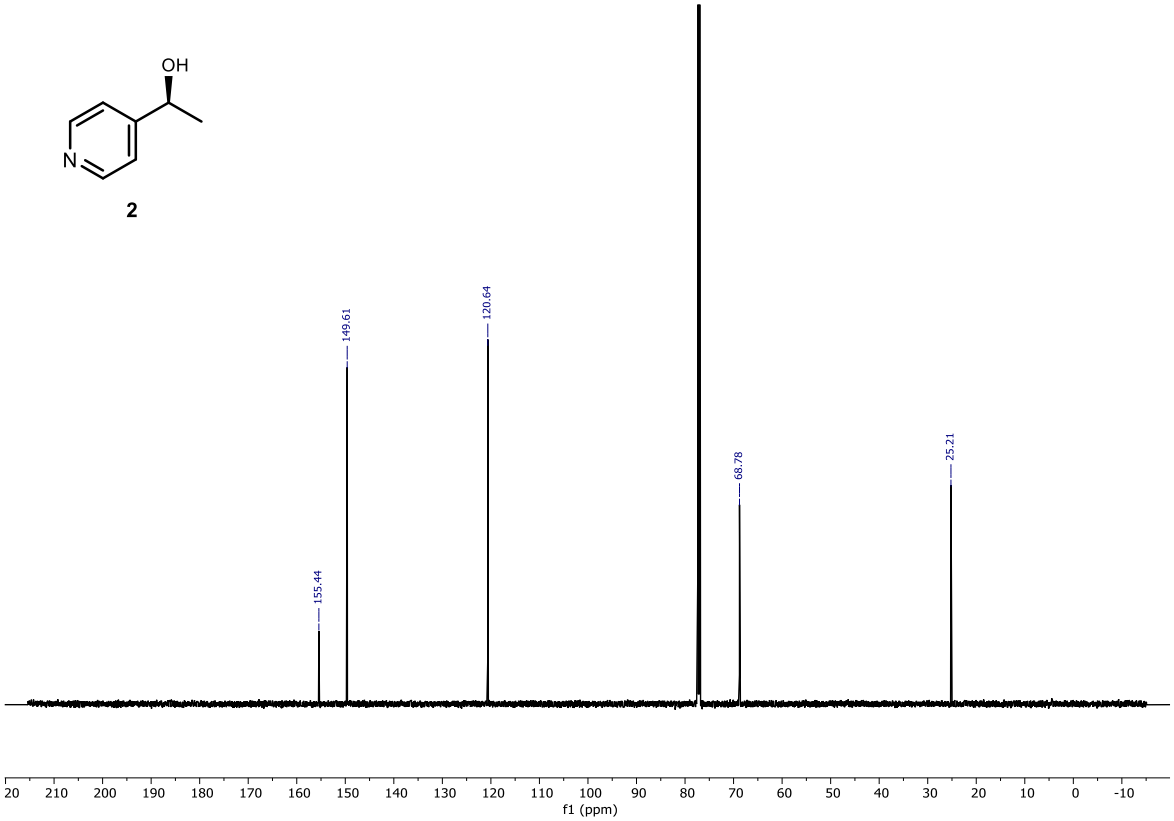

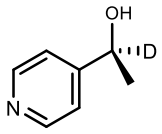

4

^{1}H NMR

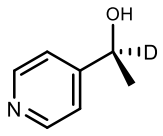

4

^{2}H NMR

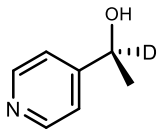

4

^{13}C NMR

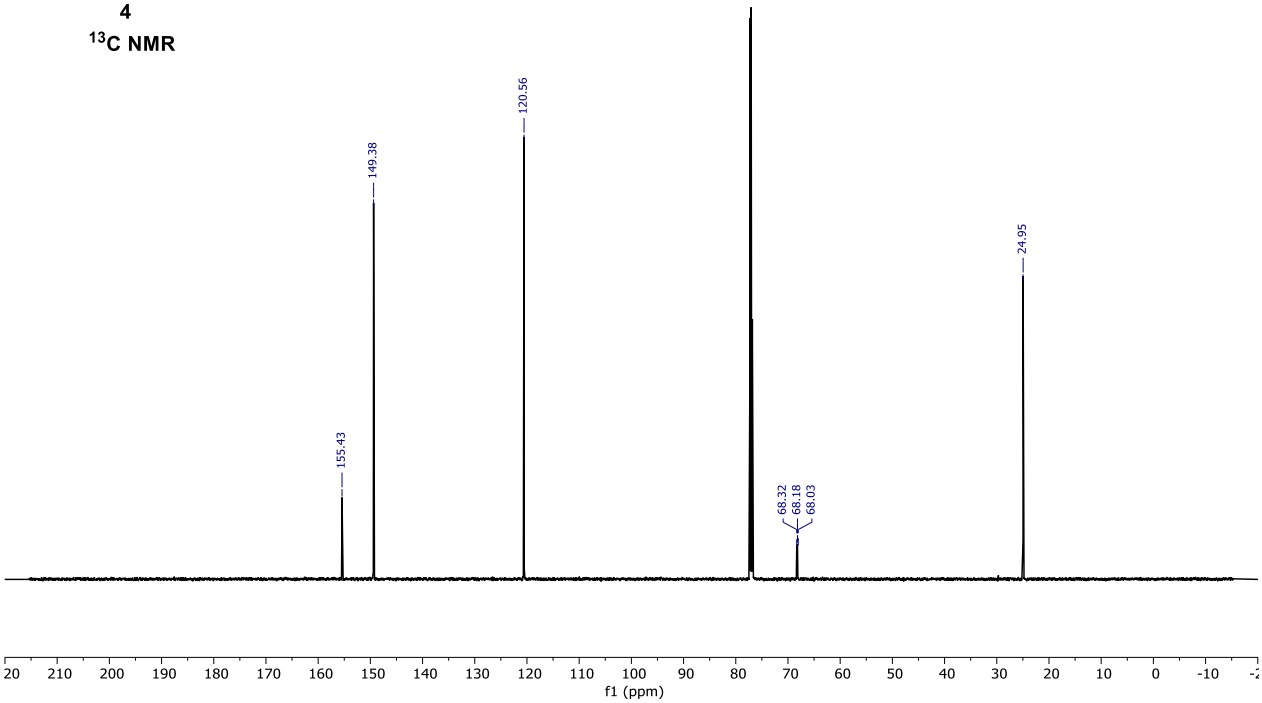

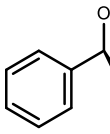

6

^{1}H NMR

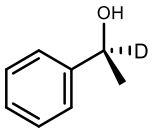

6

^{2}H NMR

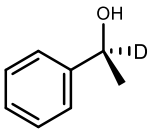

6

^{13}C NMR

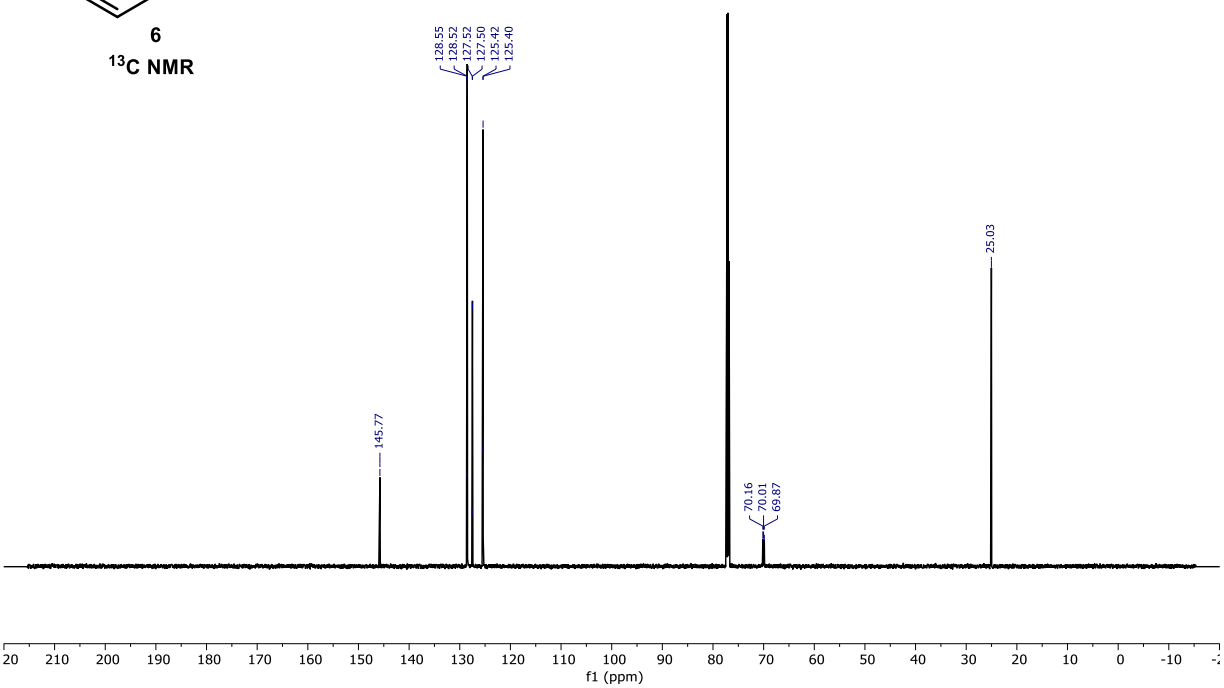

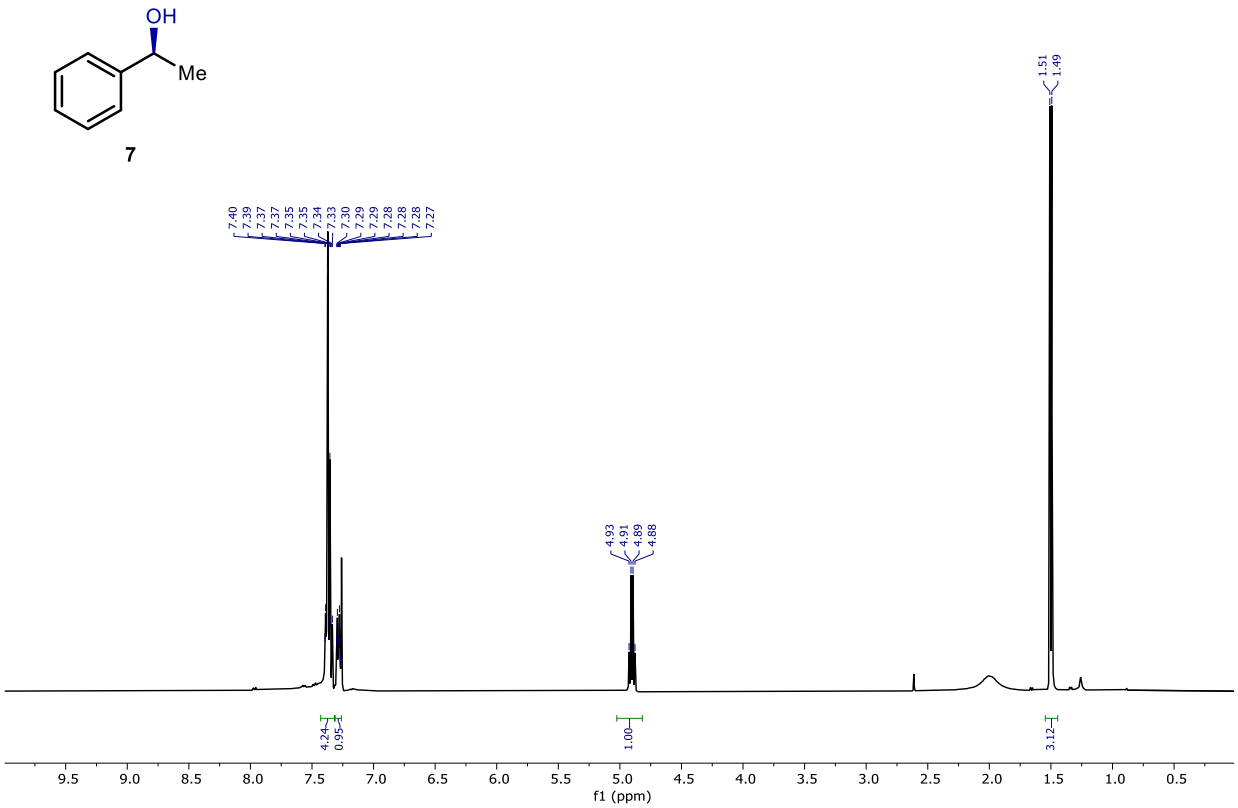
OH
Me
7
7.40
7.39
7.37
7.37
7.35
7.35
7.34
7.33
7.30
7.29
7.29
7.28
7.28
7.28
7.27
4.93
4.91
4.89
4.88
1.51
1.49
4.24
0.95
1.00
3.12
f1 (ppm)

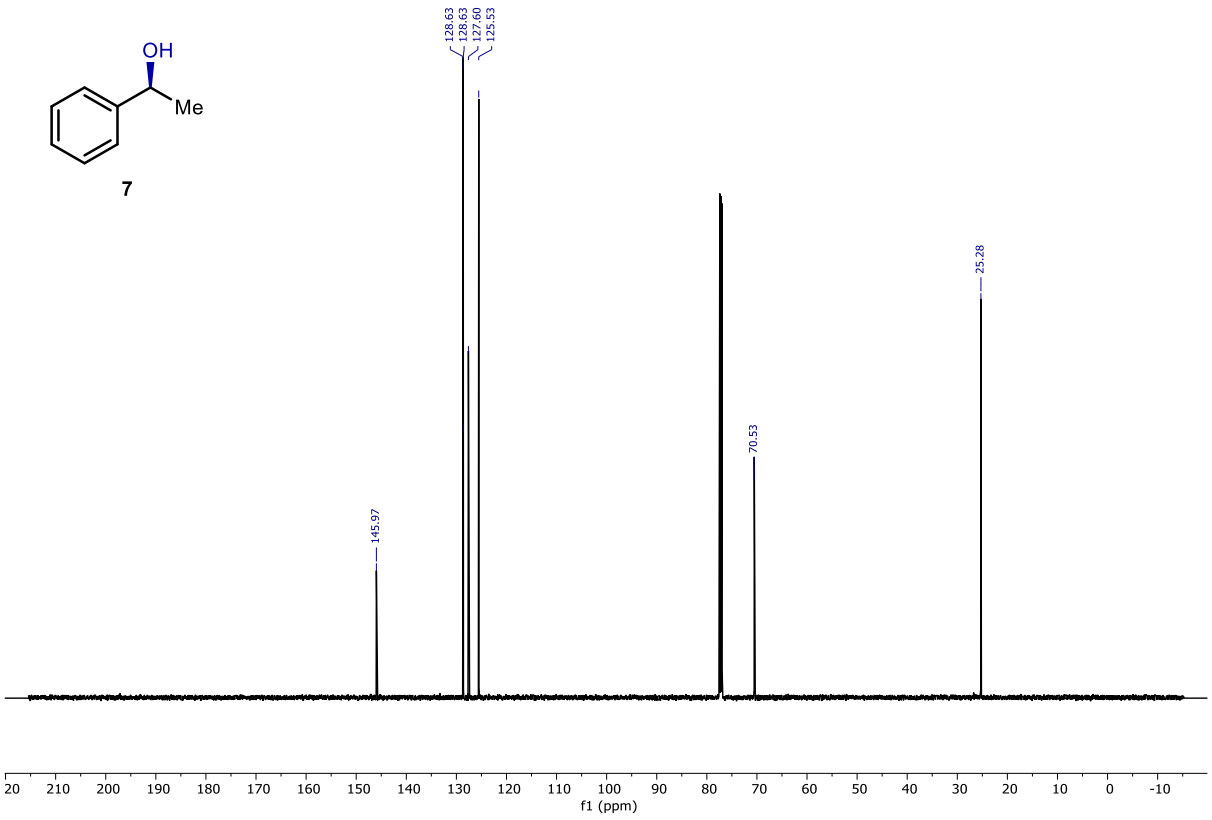
OH
Me
7
128.63
128.63
127.60
125.53
145.97
70.53
25.28
f1 (ppm)

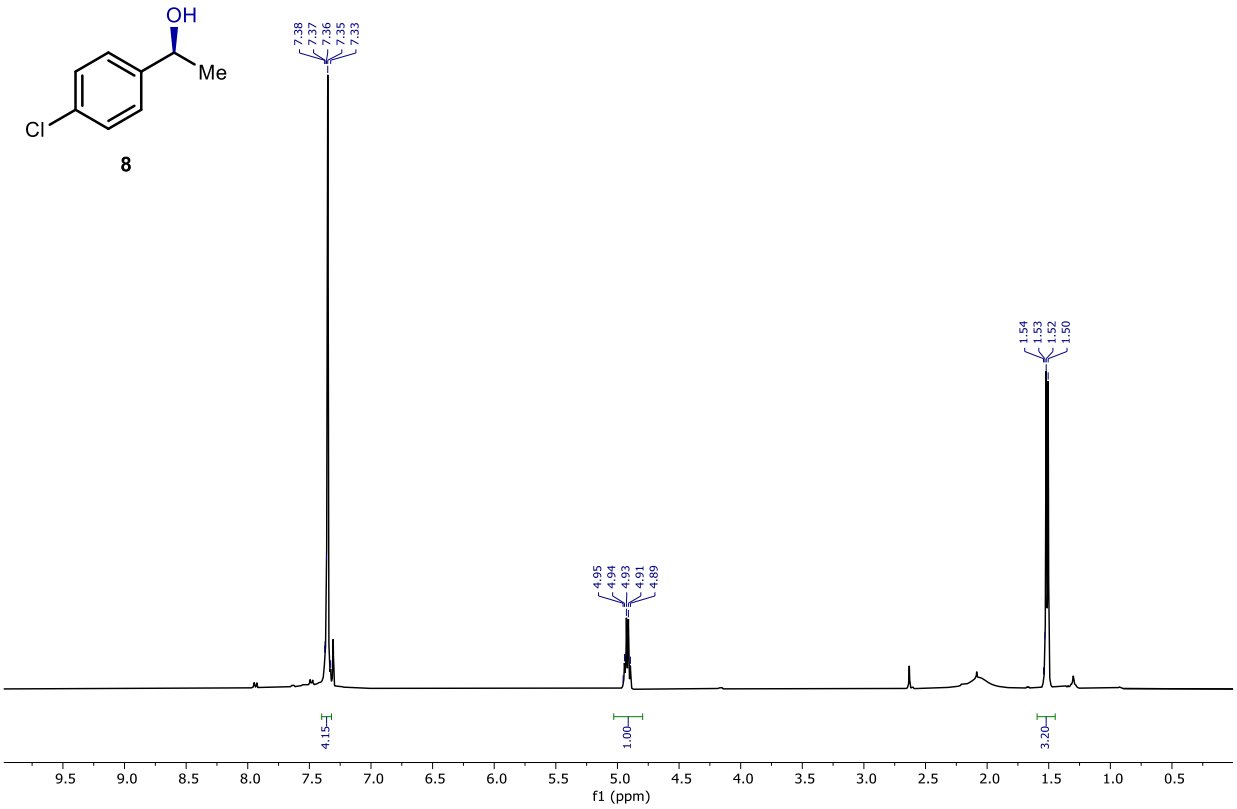
OH
Me
Cl
8
7.38
7.37
7.36
7.35
7.33
4.95
4.94
4.93
4.91
4.89
1.54
1.53
1.52
1.50
4.15
1.00
3.20
f1 (ppm)

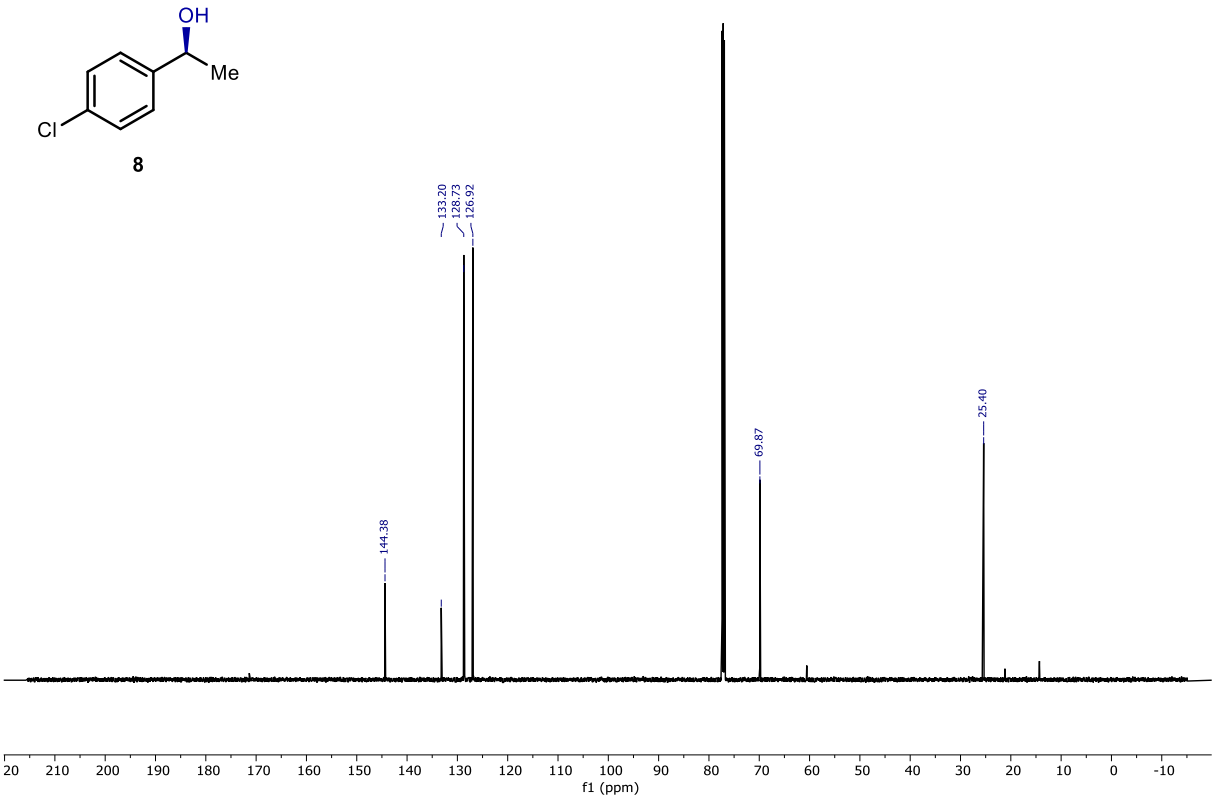
OH
Me
Cl
8
133.20
128.73
126.92
144.38
69.87
25.40
f1 (ppm)

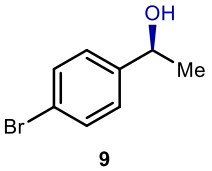
OH
Me
Br

9

1.48
1.46
7.48
7.46
7.26
7.24
4.89
4.88
4.86
4.85
2.05
2.35
1.00
3.11
9.5 9.0 8.5 8.0 7.5 7.0 6.5 6.0 5.5 5.0 4.5 4.0 3.5 3.0 2.5 2.0 1.5 1.0 0.5
f1 (ppm)

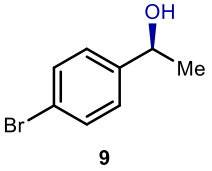
OH
Me
Br

9

131.66
127.27
144.88
121.27
69.88
25.34
170 160 150 140 130 120 110 100 90 80 70 60 50 40 30 20 10 0 -10
f1 (ppm)

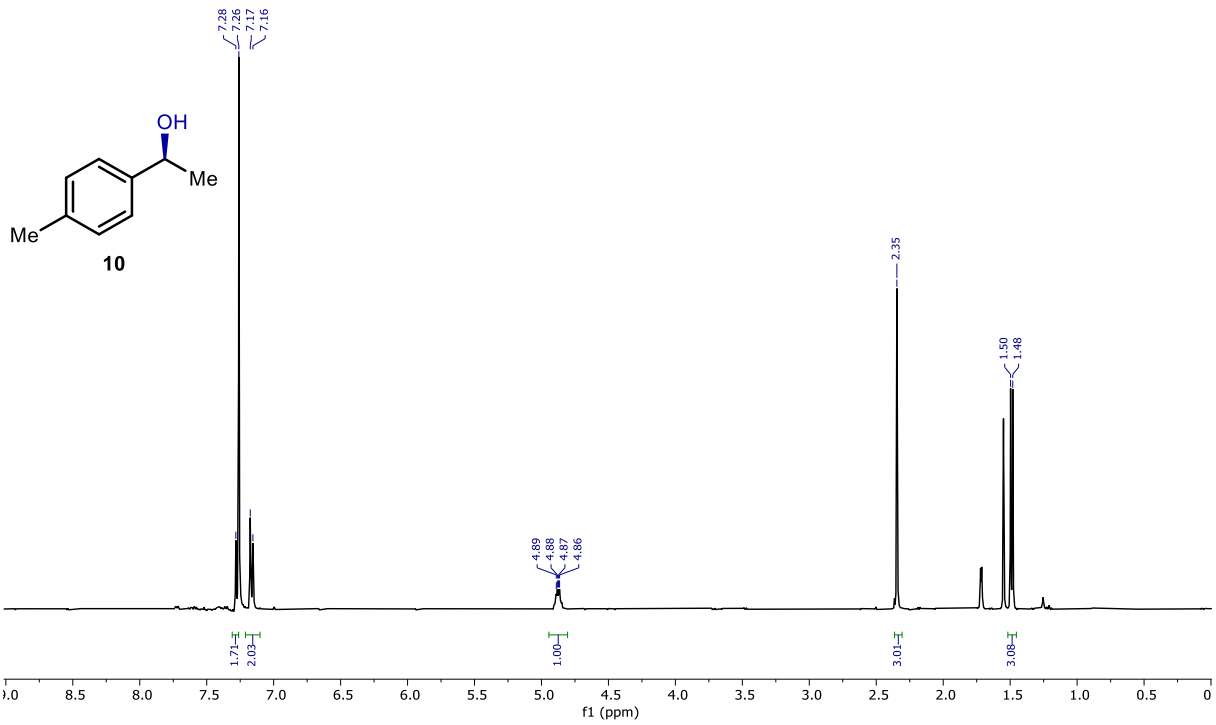
OH
Me
Me
10
7.28
7.26
7.17
7.16
4.89
4.88
4.87
4.86
2.35
1.50
1.48
1.71
2.03
1.00
3.01
3.08
f1 (ppm)

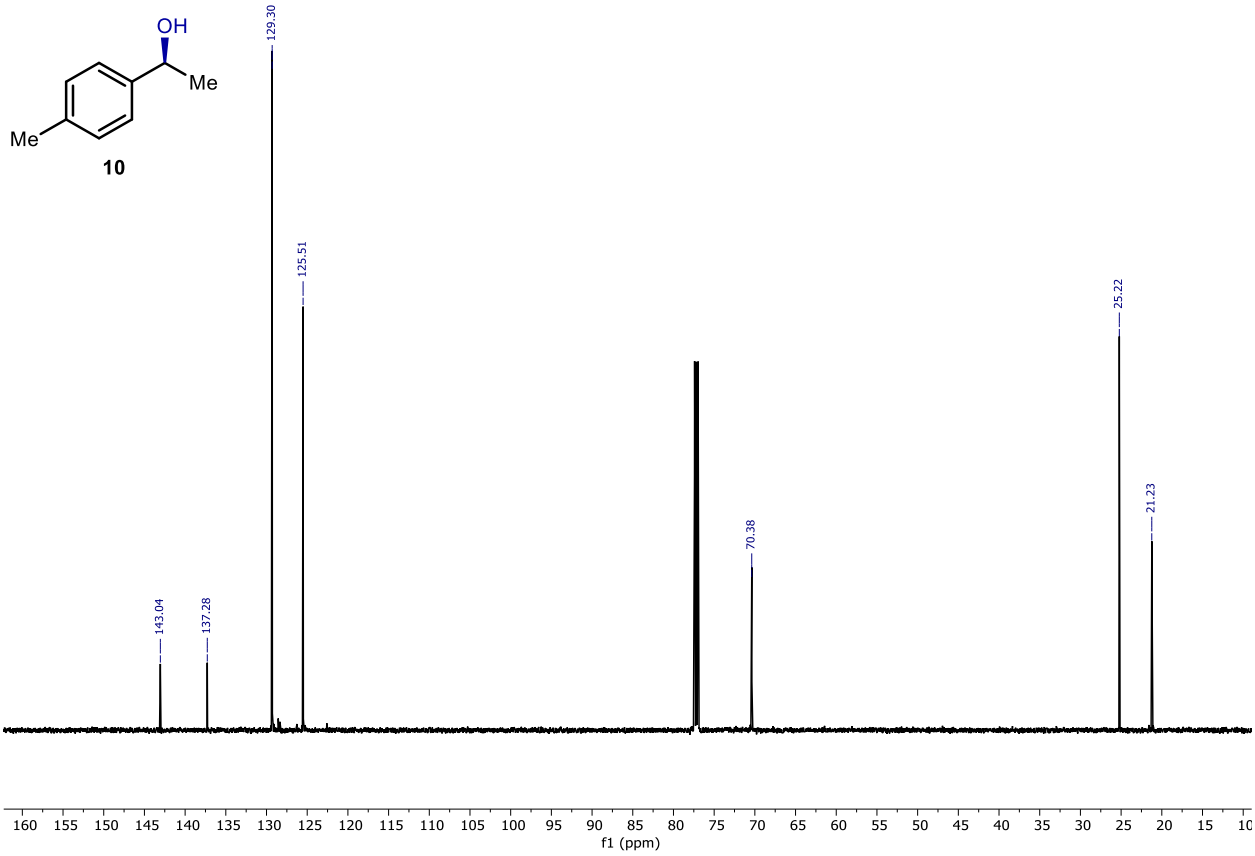
OH
Me
Me
10
129.30
125.51
143.04
137.28
70.38
25.22
21.23
f1 (ppm)

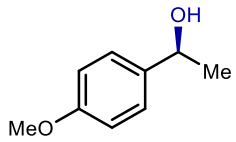
OH
Me
MeO

11

3.81
1.49
1.47
7.32
7.31
7.29
6.95 Ketone SM
6.90
6.89
6.88
7.93 Ketone SM
4.89
4.87
4.85
4.84
2.56 Ketone SM
2.02
1.98
1.00
3.08
3.08
f1 (ppm)

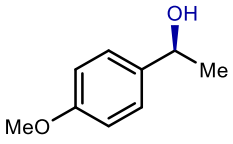
OH
Me
MeO

11

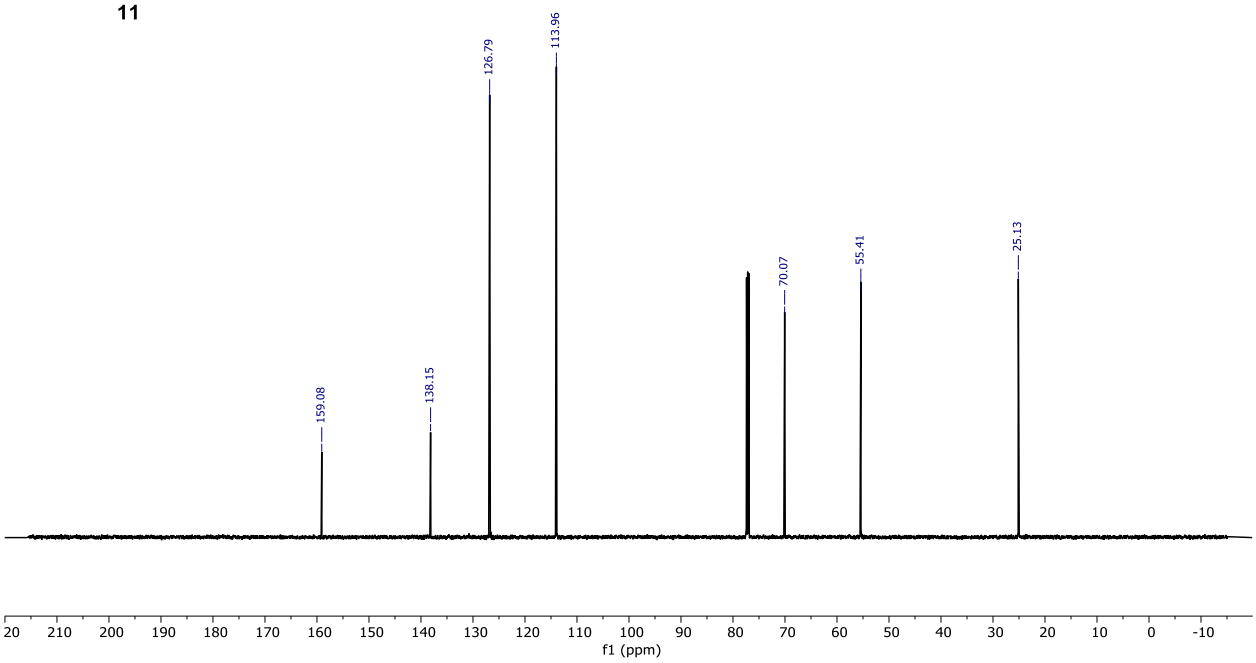
126.79
113.96
159.08
138.15
70.07
55.41
25.13
f1 (ppm)

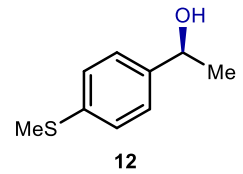
OH
Me
MeS

12

D (d)
7.25
C (d)
7.30
A (q)
4.87
B (s)
2.48
B (d)
1.48
7.31
7.31
7.30
7.29
7.26
7.25
7.24
7.24
4.90
4.88
4.86
4.85
2.48
1.49
1.47
1.91
2.06
0.98
3.00
3.00
9.5 9.0 8.5 8.0 7.5 7.0 6.5 6.0 5.5 5.0 4.5 4.0 3.5 3.0 2.5 2.0 1.5 1.0 0.5 0.
f1 (ppm)

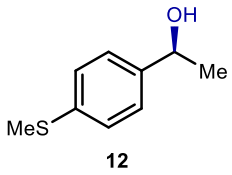
OH
Me
MeS

12

127.00
126.12
142.94
137.57
70.13
25.22
16.16
20 210 200 190 180 170 160 150 140 130 120 110 100 90 80 70 60 50 40 30 20 10 0 -10
f1 (ppm)

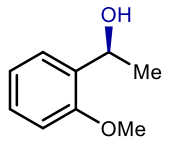
OH
Me
OMe

13

7.35
7.35
7.33
7.33
7.27
7.27
7.27
7.26
7.25
7.25
7.25
7.23
7.23
7.23
6.99
6.98
6.98
6.98
6.97
6.97
6.96
6.95
6.95
6.94
6.90
6.90
6.90
6.88
6.88
5.12
5.10
5.09
5.07
1.52
1.52
1.50
1.50
1.06
1.66
0.99
0.97
1.00
3.08
3.12
f1 (ppm)

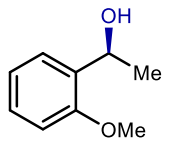
OH
Me
OMe

13

156.69
133.59
128.43
126.23
120.94
110.58
66.65
55.40
23.00
f1 (ppm)

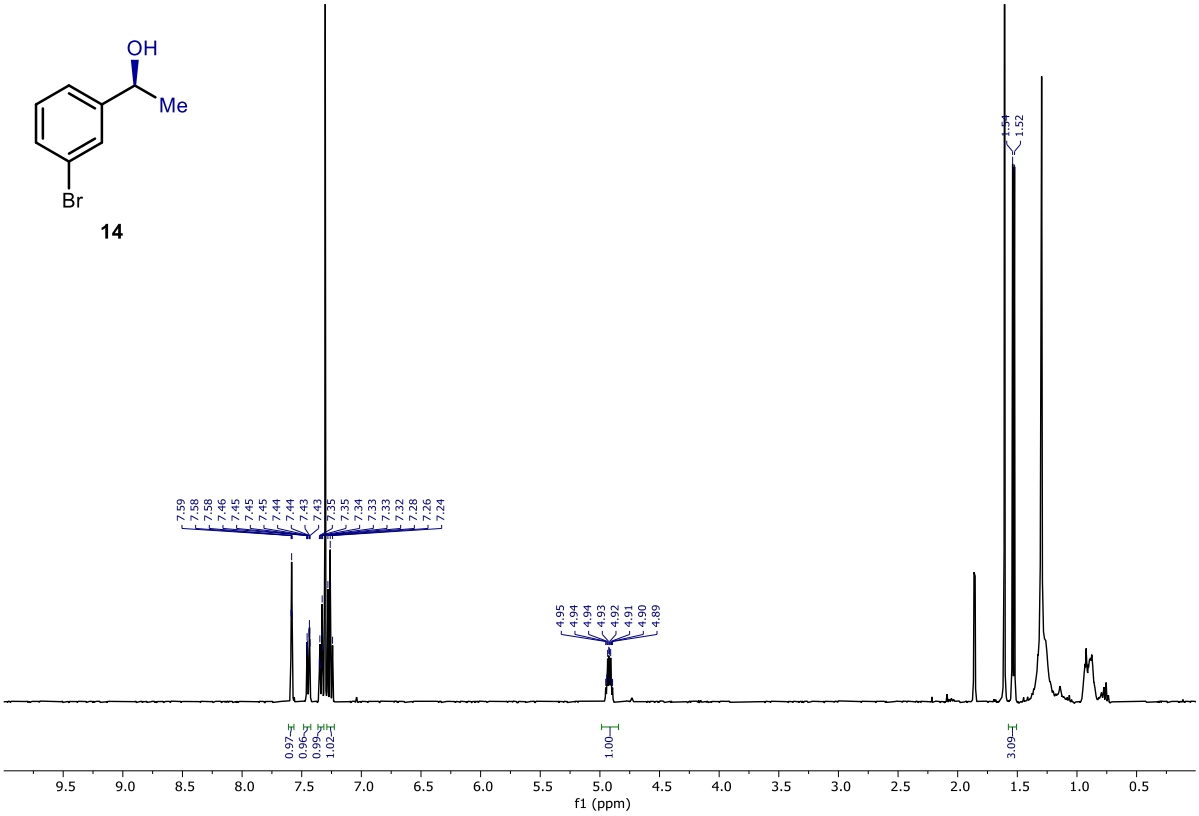
OH
Me
Br
14
7.59
7.58
7.58
7.46
7.45
7.45
7.45
7.44
7.44
7.43
7.43
7.35
7.35
7.34
7.33
7.33
7.32
7.28
7.26
7.24
4.95
4.94
4.94
4.93
4.92
4.91
4.90
4.89
1.54
1.52
0.97
0.96
0.99
1.02
1.00
3.09
f1 (ppm)

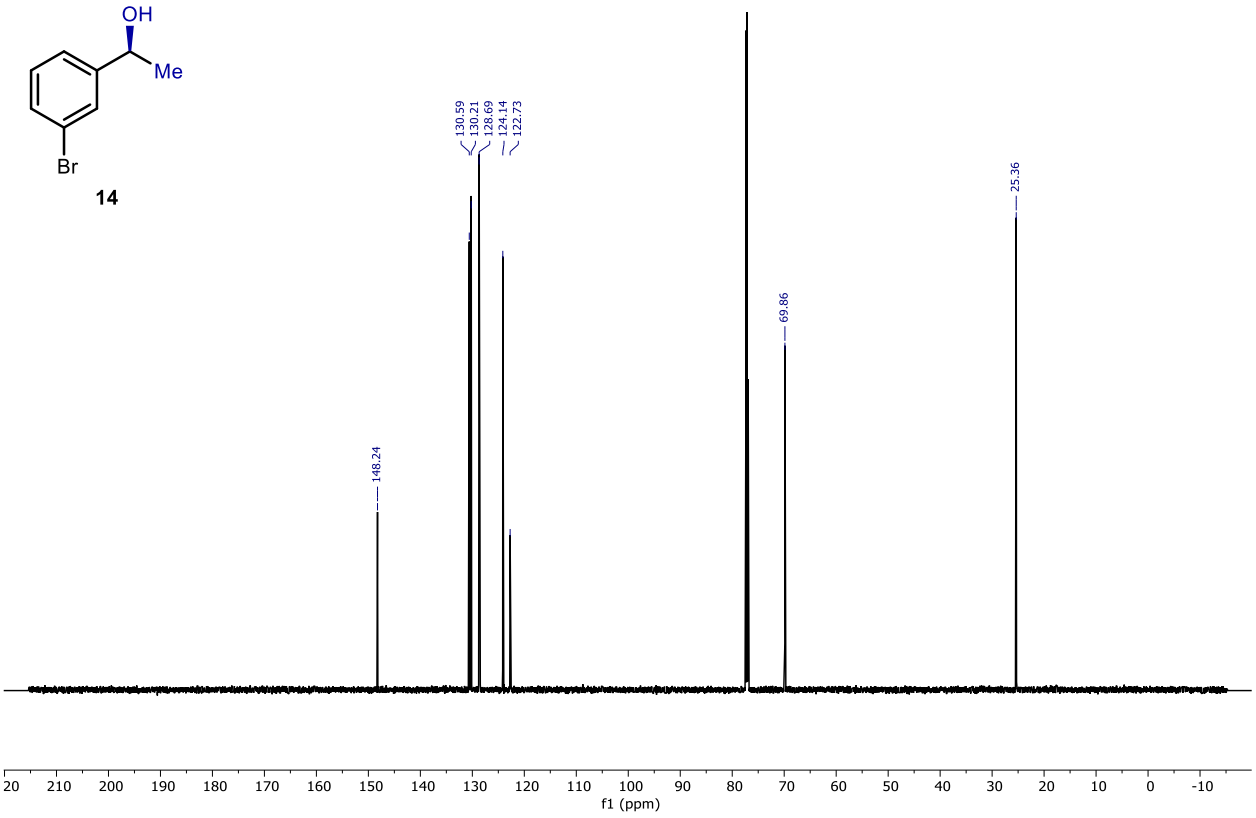
OH
Me
Br
14
130.59
130.21
128.69
124.14
122.73
148.24
69.86
25.36
f1 (ppm)

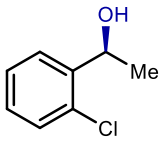
OH
Me
Cl

15

1.50
1.49
7.34
7.34
7.32
7.32
7.30
7.30
7.28
7.22
7.22
7.20
7.20
7.19
7.18
7.61
7.60
7.59
7.58
5.33
5.32
5.31
5.30
5.29
5.29
5.28
5.27
0.99
2.00
0.99
1.00
3.16
9.5 9.0 8.5 8.0 7.5 7.0 6.5 6.0 5.5 5.0 4.5 4.0 3.5 3.0 2.5 2.0 1.5 1.0 0.5
f1 (ppm)

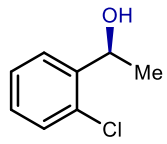
OH
Me
Cl

15

23.63
67.08
131.76
129.52
128.52
127.34
126.55
143.20
20 210 200 190 180 170 160 150 140 130 120 110 100 90 80 70 60 50 40 30 20 10 0 -10
f1 (ppm)

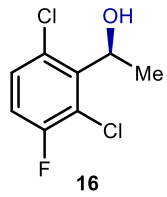

16

^{1}H NMR

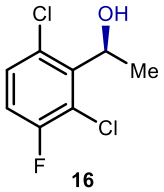

16

^{13}C NMR

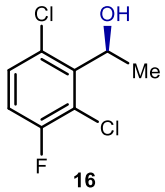

16

^{19}F NMR

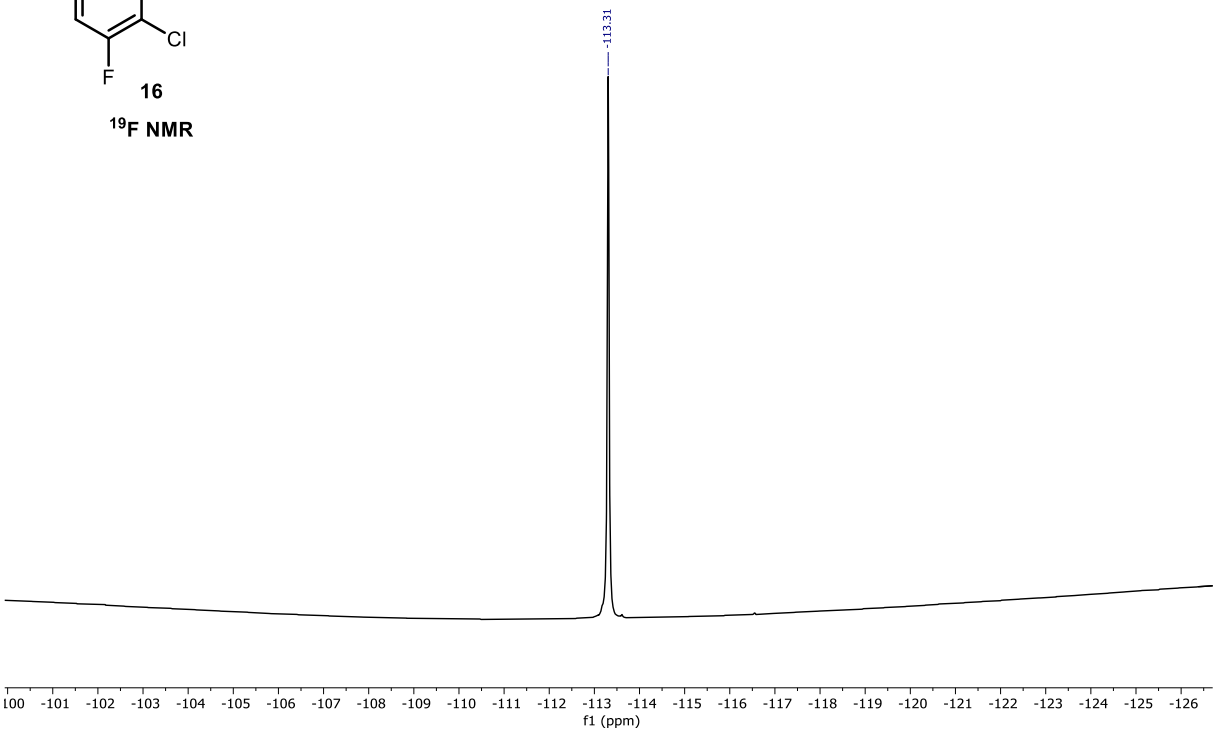

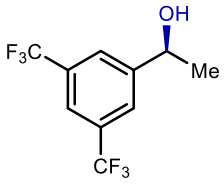

17

^{1}H NMR

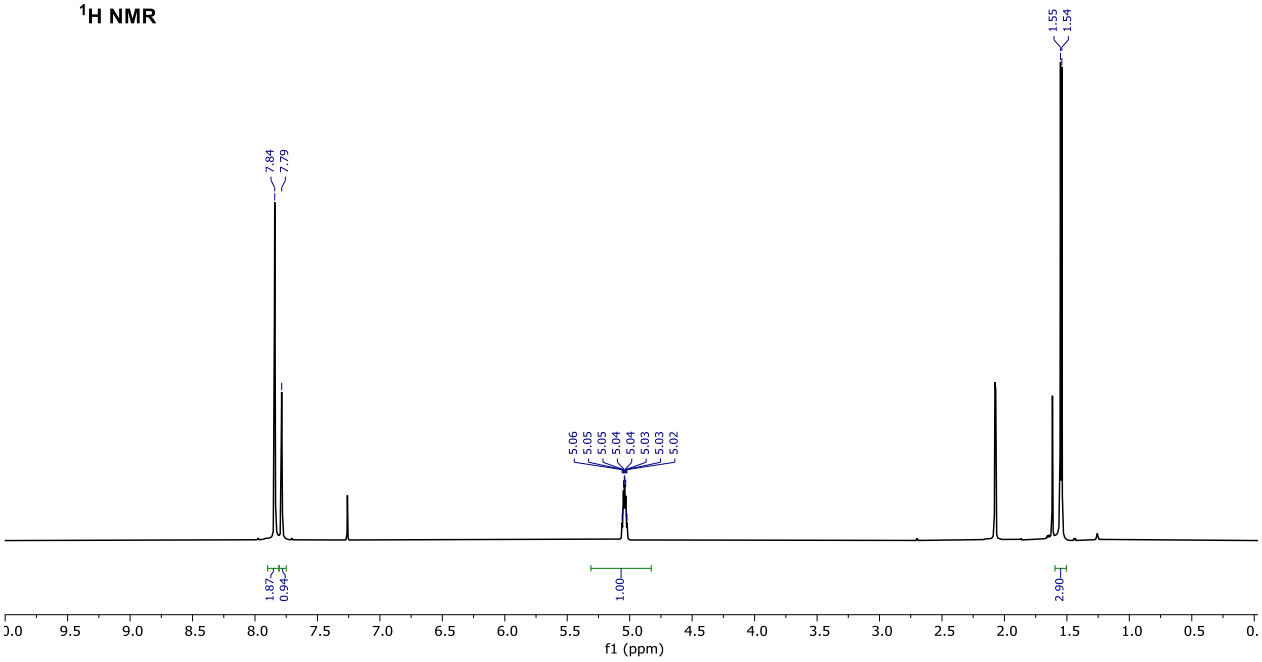

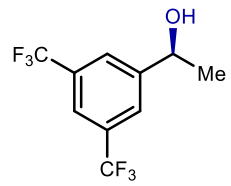

17

^{2}H NMR

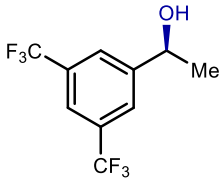

17

^{19}F NMR

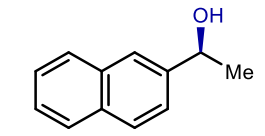
OH
Me

18

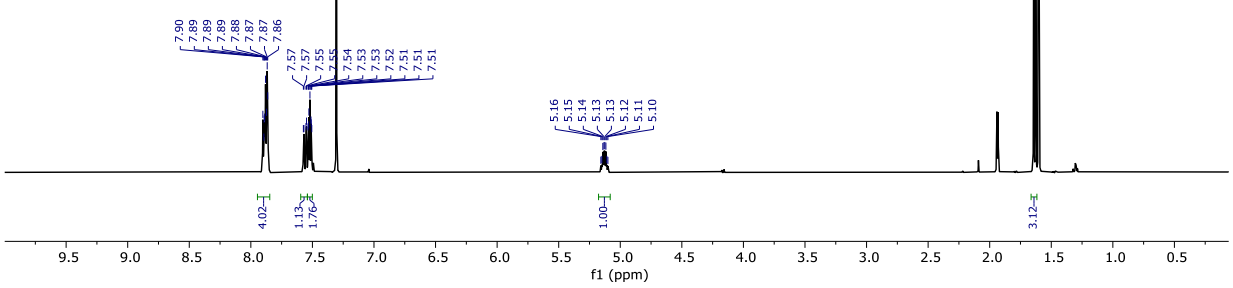
7.90
7.89
7.89
7.89
7.88
7.87
7.87
7.86
7.57
7.57
7.55
7.55
7.54
7.53
7.53
7.52
7.51
7.51
7.51
5.16
5.15
5.14
5.13
5.13
5.12
5.11
5.10
1.64
1.63
4.02
1.13
1.76
1.00
3.12
9.5
9.0
8.5
8.0
7.5
7.0
6.5
6.0
5.5
5.0
4.5
4.0
3.5
3.0
2.5
2.0
1.5
1.0
0.5
f1 (ppm)

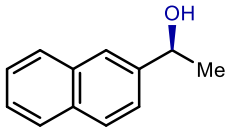
OH
Me

18

133.46
133.05
128.44
128.06
127.80
126.28
125.92
123.94
123.93
143.30
70.66
25.25
20
210
200
190
180
170
160
150
140
130
120
110
100
90
80
70
60
50
40
30
20
10
0
-10
f1 (ppm)

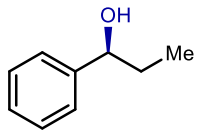
OH
Me

19

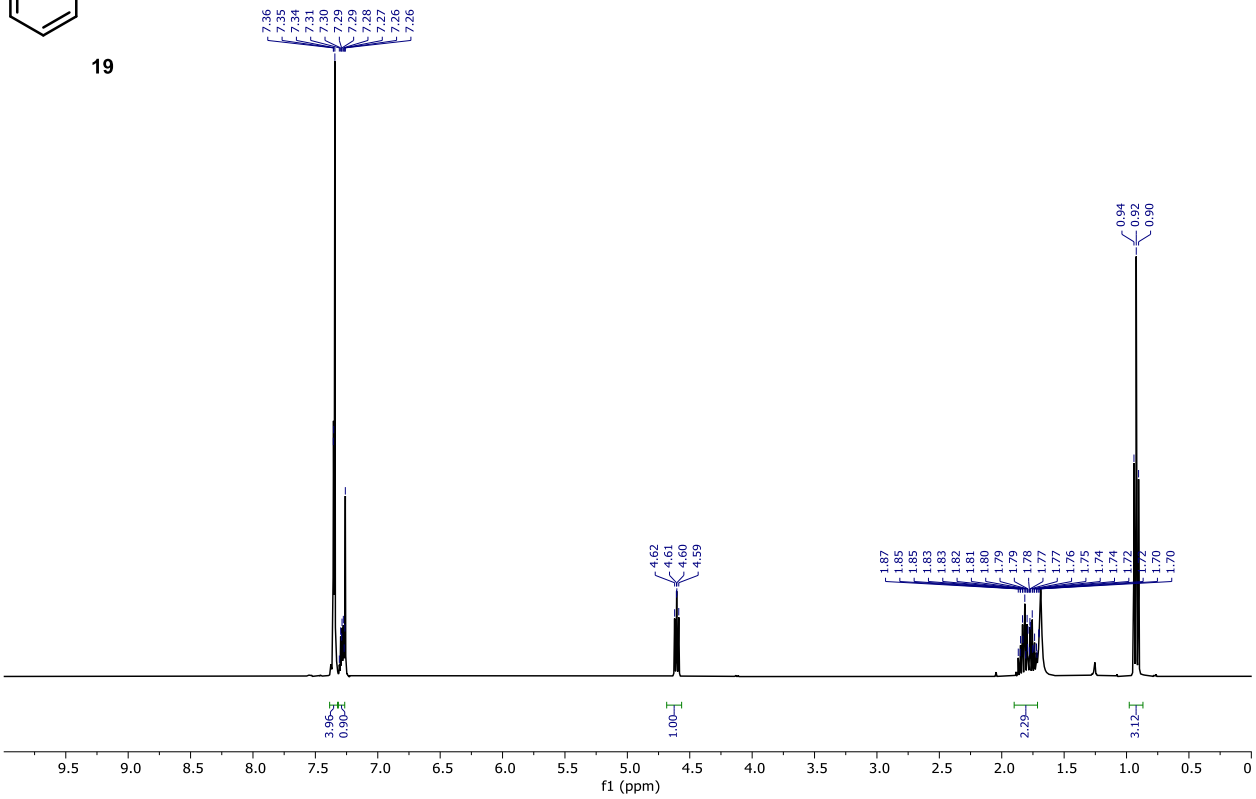
7.36
7.35
7.34
7.31
7.30
7.29
7.29
7.28
7.27
7.26
7.26
4.62
4.61
4.60
4.59
1.87
1.85
1.85
1.83
1.83
1.82
1.81
1.80
1.79
1.79
1.78
1.77
1.77
1.76
1.75
1.74
1.74
1.72
1.72
1.70
1.70
0.94
0.92
0.90
3.96
0.90
1.00
2.29
3.12
f1 (ppm)

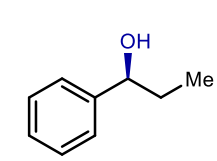
OH
Me

19

128.51
127.59
126.12
144.75
76.11
31.99
10.26
f1 (ppm)

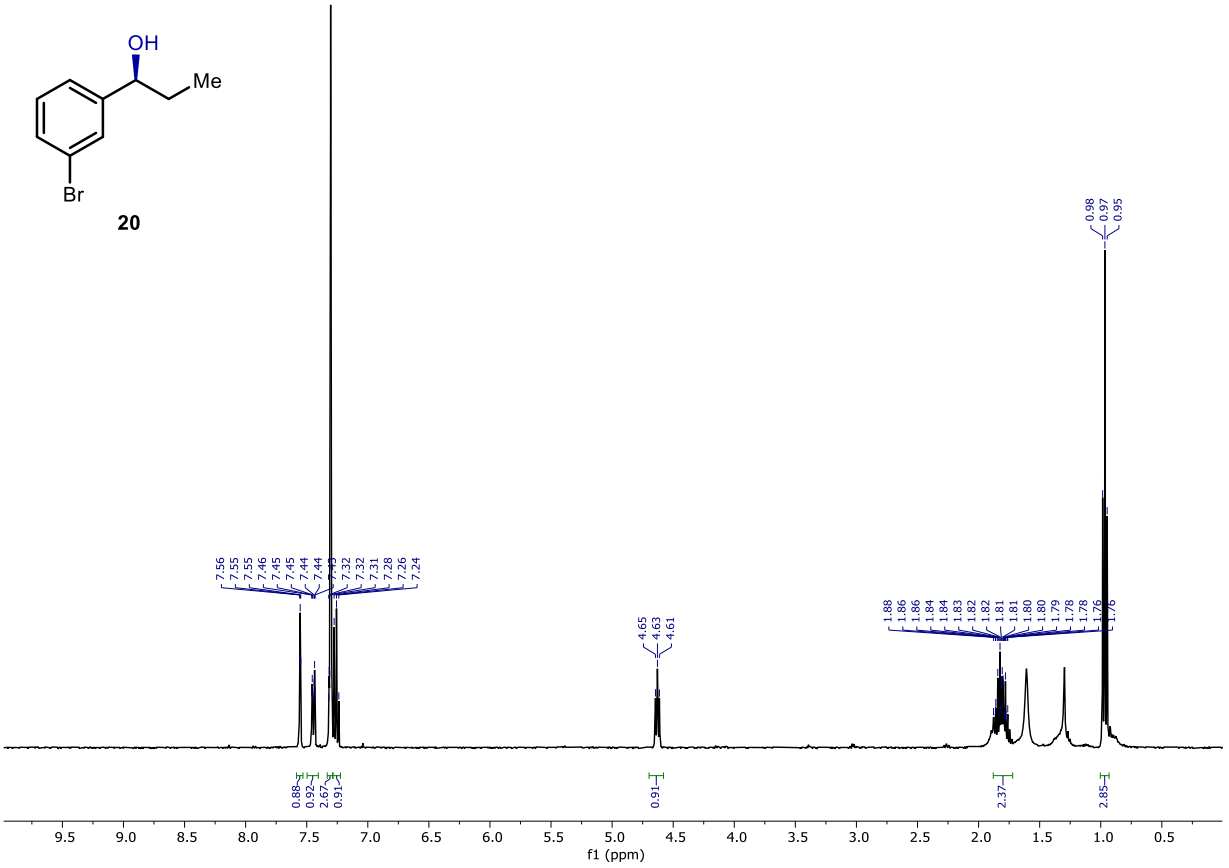
OH
Me
Br
20
7.56
7.55
7.55
7.46
7.45
7.45
7.44
7.44
7.43
7.32
7.32
7.31
7.28
7.26
7.24
4.65
4.63
4.61
1.88
1.86
1.86
1.84
1.84
1.83
1.82
1.82
1.81
1.81
1.80
1.80
1.79
1.78
1.78
1.76
1.76
0.98
0.97
0.95
0.88
0.92
2.67
0.91
0.91
2.37
2.85
9.5
9.0
8.5
8.0
7.5
7.0
6.5
6.0
5.5
5.0
4.5
4.0
3.5
3.0
2.5
2.0
1.5
1.0
0.5
f1 (ppm)

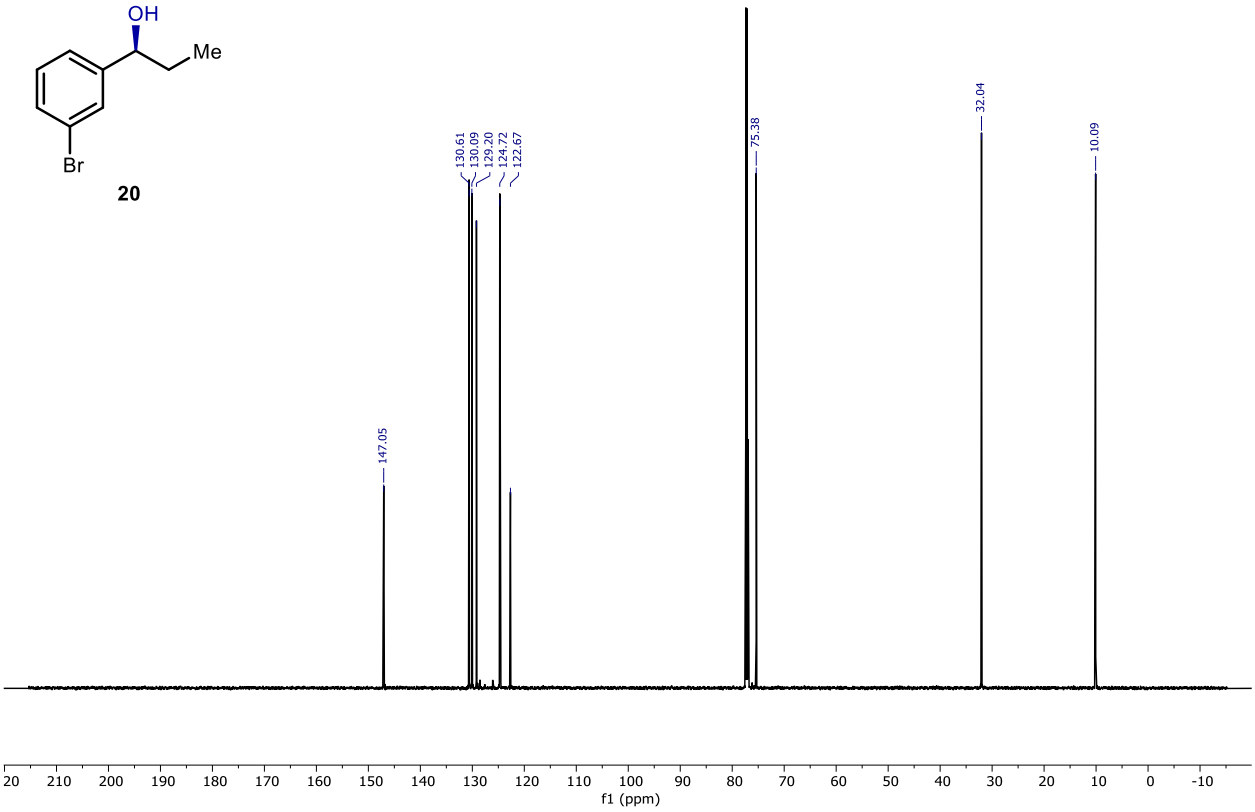
OH
Me
Br
20
147.05
130.61
130.09
129.20
124.72
122.67
75.38
32.04
10.09
20
210
200
190
180
170
160
150
140
130
120
110
100
90
80
70
60
50
40
30
20
10
0
-10
f1 (ppm)

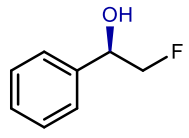

21

^{1}H NMR

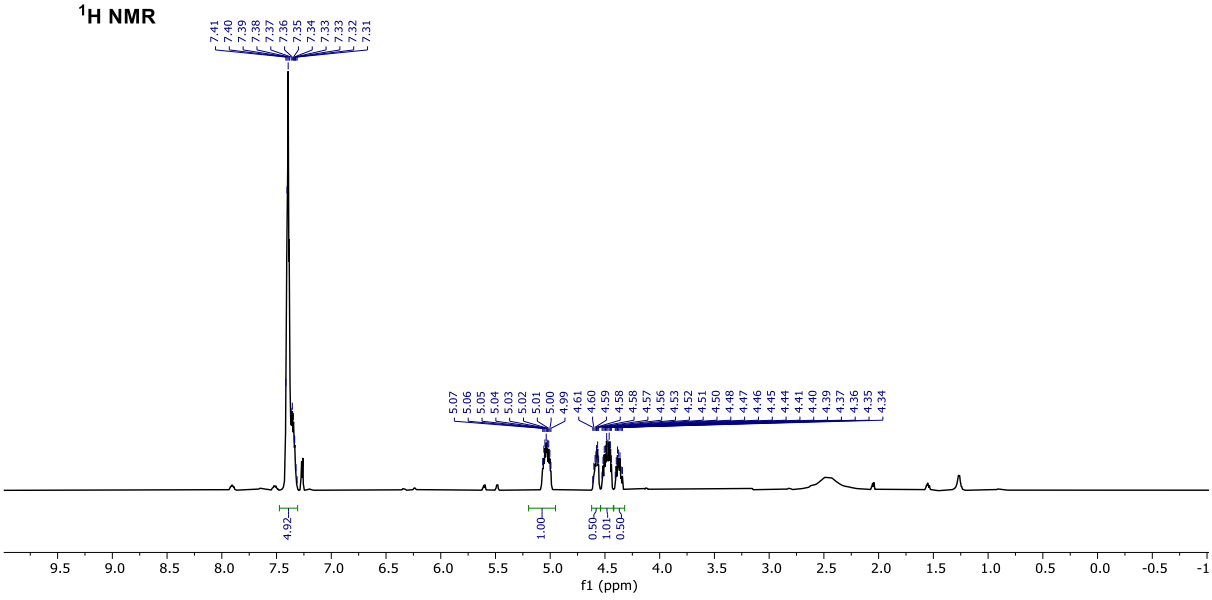

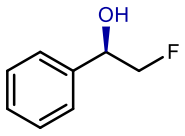

21

^{13}C NMR

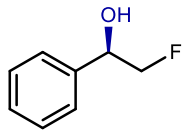

21

^{19}F NMR

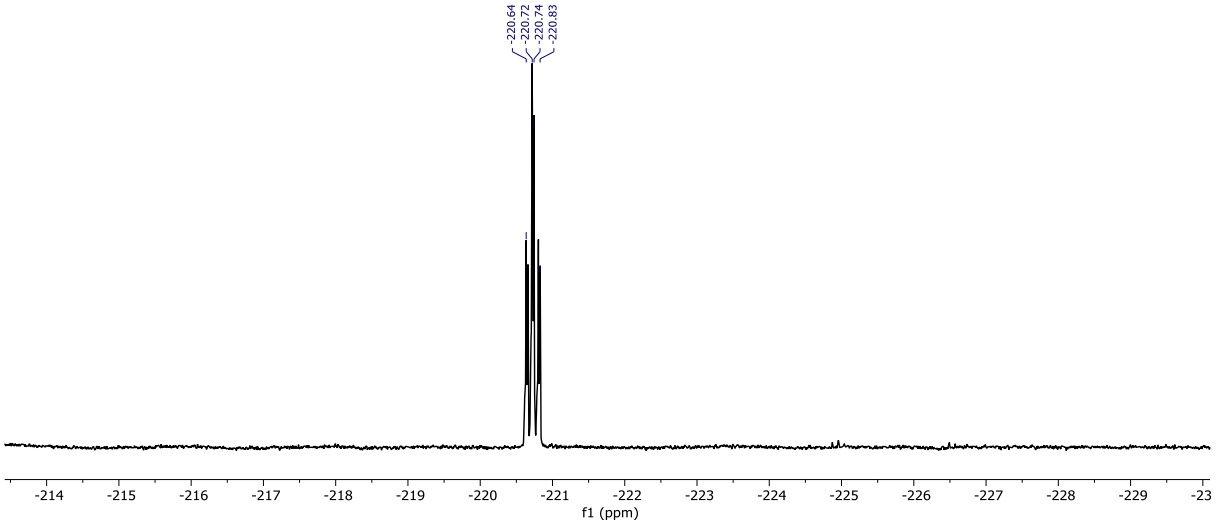

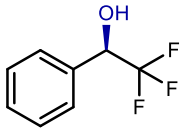

22

^{1}H NMR

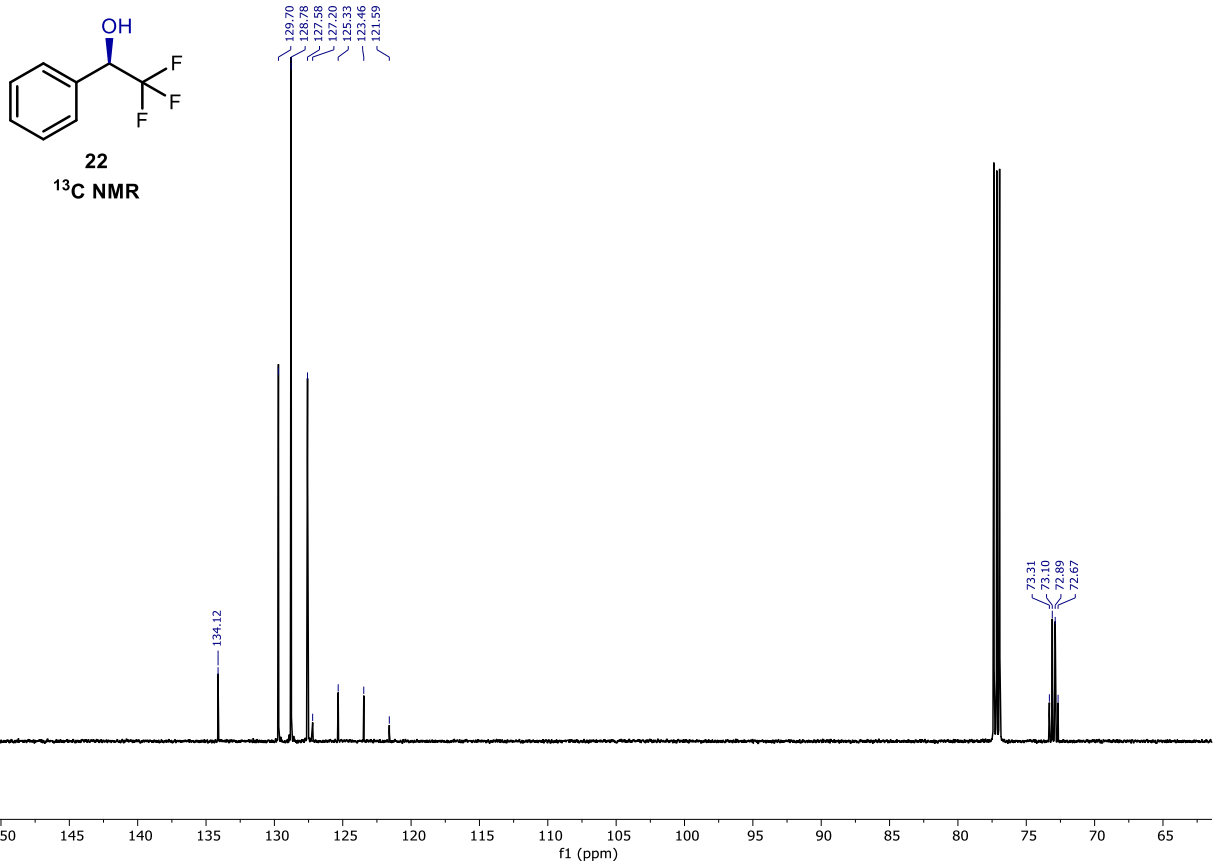
OH
F
F
F
22
13C NMR
129.70
128.78
127.58
127.20
125.33
123.46
121.59
134.12
73.31
73.10
72.89
72.67
150 145 140 135 130 125 120 115 110 105 100 95 90 85 80 75 70 65
f1 (ppm)

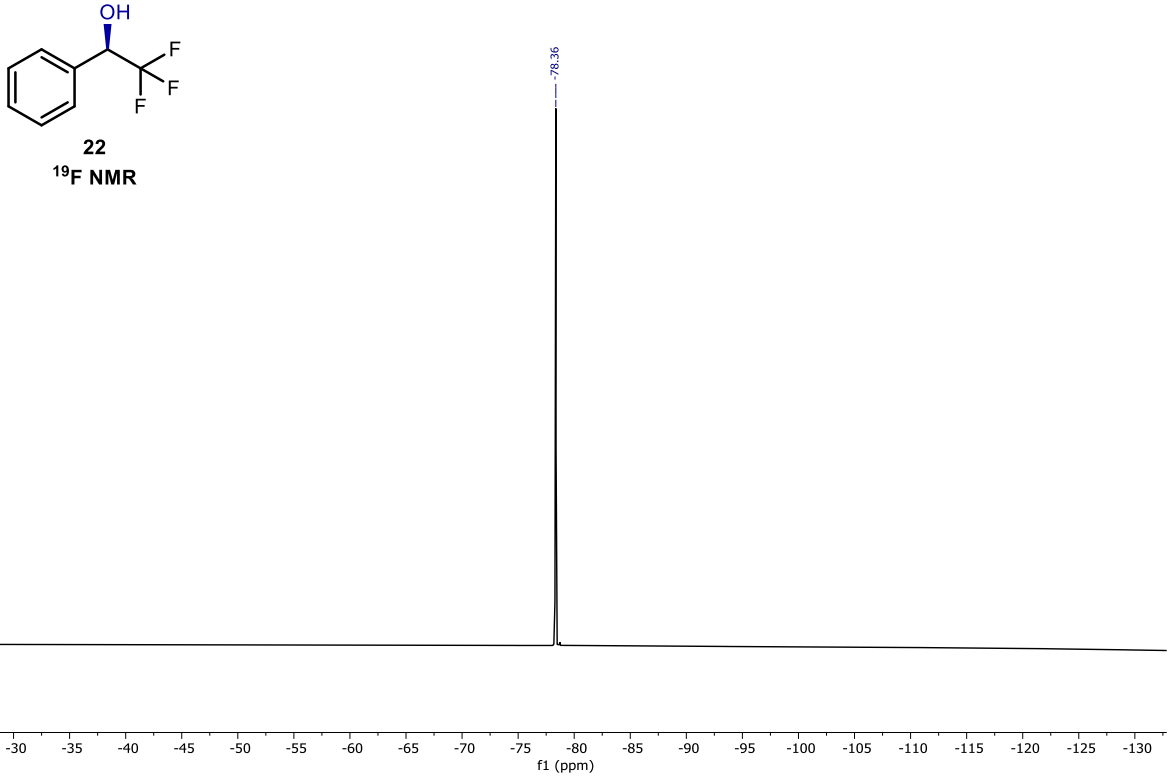
OH
F
F
F
22
19F NMR
-78.36
-30 -35 -40 -45 -50 -55 -60 -65 -70 -75 -80 -85 -90 -95 -100 -105 -110 -115 -120 -125 -130
f1 (ppm)

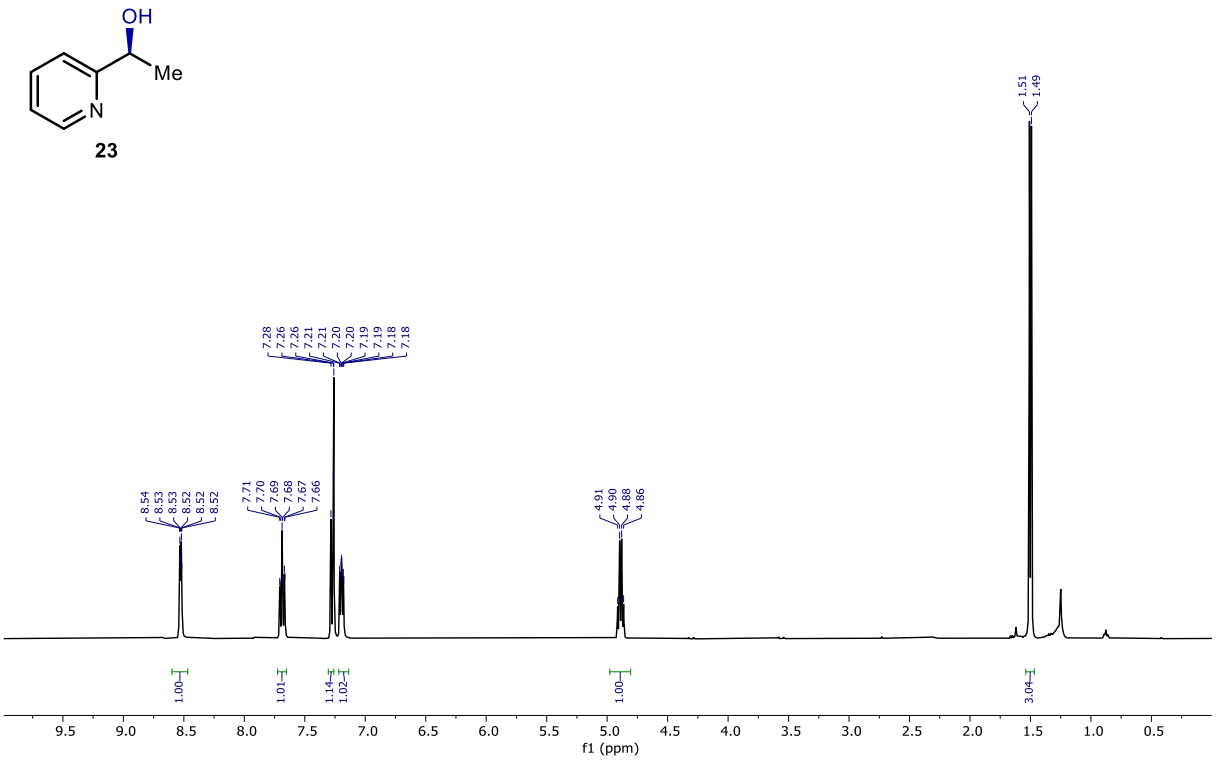
OH
Me
N
23
8.54
8.53
8.53
8.52
8.52
8.52
7.71
7.70
7.69
7.68
7.67
7.66
7.28
7.26
7.26
7.21
7.21
7.20
7.20
7.19
7.19
7.18
7.18
4.91
4.90
4.88
4.86
1.51
1.49
1.00
1.01
1.14
1.02
1.00
3.04
f1 (ppm)

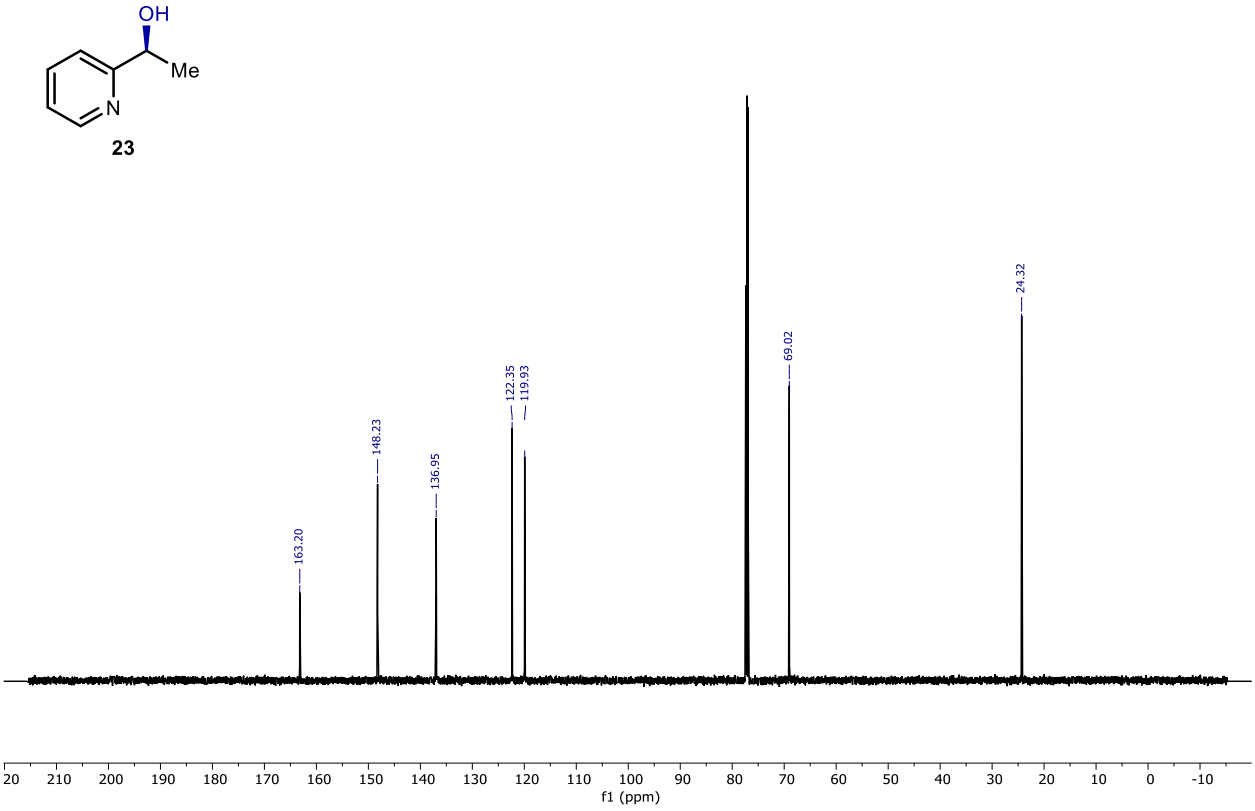
OH
Me
N
23
163.20
148.23
136.95
122.35
119.93
69.02
24.32
f1 (ppm)

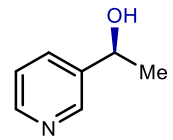
OH
Me
N

24

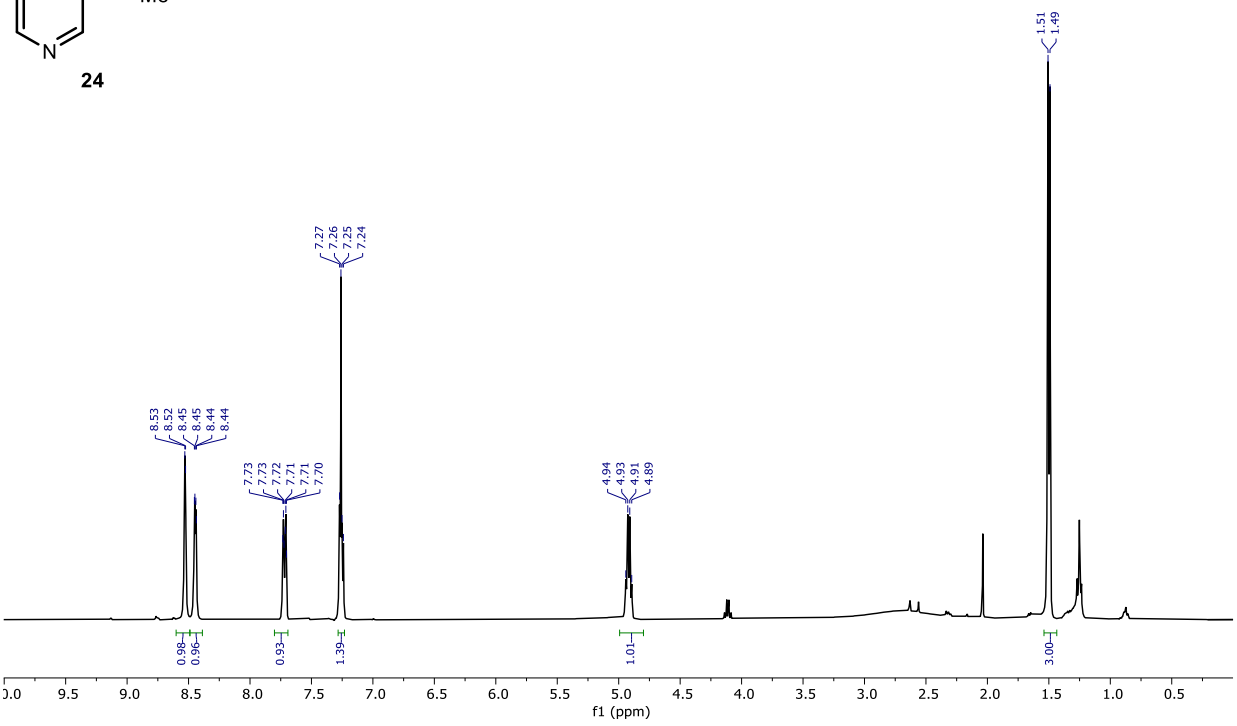
8.53
8.52
8.45
8.45
8.44
8.44
7.73
7.73
7.72
7.71
7.71
7.70
7.27
7.26
7.25
7.24
4.94
4.93
4.91
4.89
1.51
1.49
0.98
0.96
0.93
1.39
1.01
3.00
f1 (ppm)

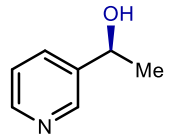
OH
Me
N

24

148.21
147.04
141.62
133.77
123.77
67.94
25.30
f1 (ppm)

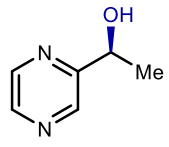
OH
N
Me
N

25

1.57
1.56
8.67
8.67
8.51
8.51
8.51
5.01
5.00
4.99
4.97
0.97
1.98
1.00
3.18
f1 (ppm)

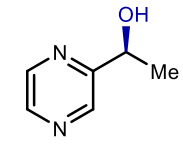
OH
N
Me
N

25

143.50
143.23
142.51
158.75
68.07
24.05
f1 (ppm)

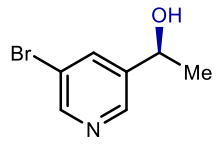
OH
Br
Me
N

26

8.55
8.55
8.48
8.47
7.89
7.89
7.88
4.95
4.94
4.92
4.90
1.52
1.50
0.98
0.97
0.96
1.00
3.01
f1 (ppm)

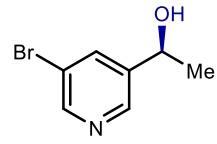
OH
Br
Me
N

26

149.26
145.22
143.66
136.41
121.06
67.08
25.34
f1 (ppm)

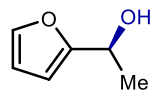
O
OH
Me

27

7.43
7.42
7.42
6.38
6.38
6.37
6.37
6.37
6.28
6.27
4.96
4.94
4.93
4.91
1.60
1.60
1.59
1.58
0.88
0.90
0.89
0.93
3.21
9.5 9.0 8.5 8.0 7.5 7.0 6.5 6.0 5.5 5.0 4.5 4.0 3.5 3.0 2.5 2.0 1.5 1.0 0.5
f1 (ppm)

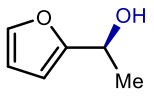
O
OH
Me

27

110.22
105.19
21.36
141.98
141.96
157.77
63.65
20 210 200 190 180 170 160 150 140 130 120 110 100 90 80 70 60 50 40 30 20 10 0 -10
f1 (ppm)

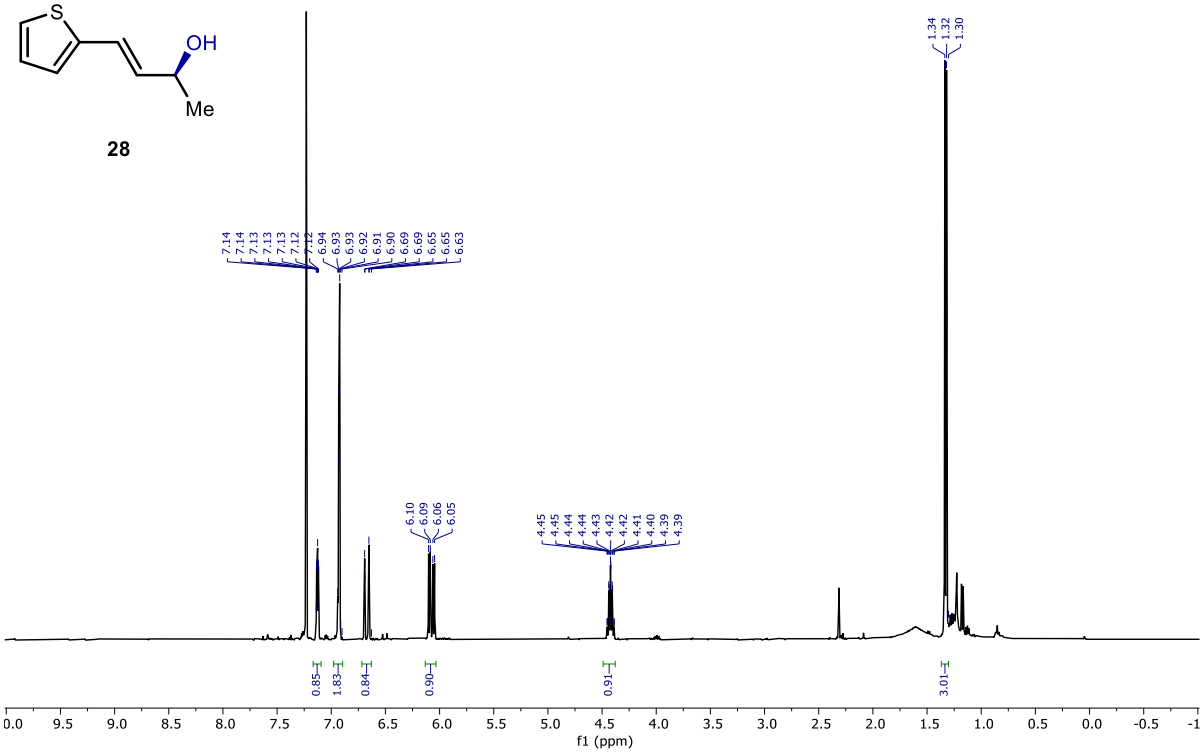
S
OH
Me
28
7.14
7.14
7.13
7.13
7.13
7.12
7.12
6.94
6.93
6.93
6.92
6.91
6.90
6.69
6.69
6.65
6.65
6.63
6.10
6.09
6.06
6.05
4.45
4.45
4.44
4.44
4.43
4.42
4.42
4.41
4.40
4.39
4.39
1.34
1.32
1.30
0.85
1.83
0.84
0.90
0.91
3.01
f1 (ppm)

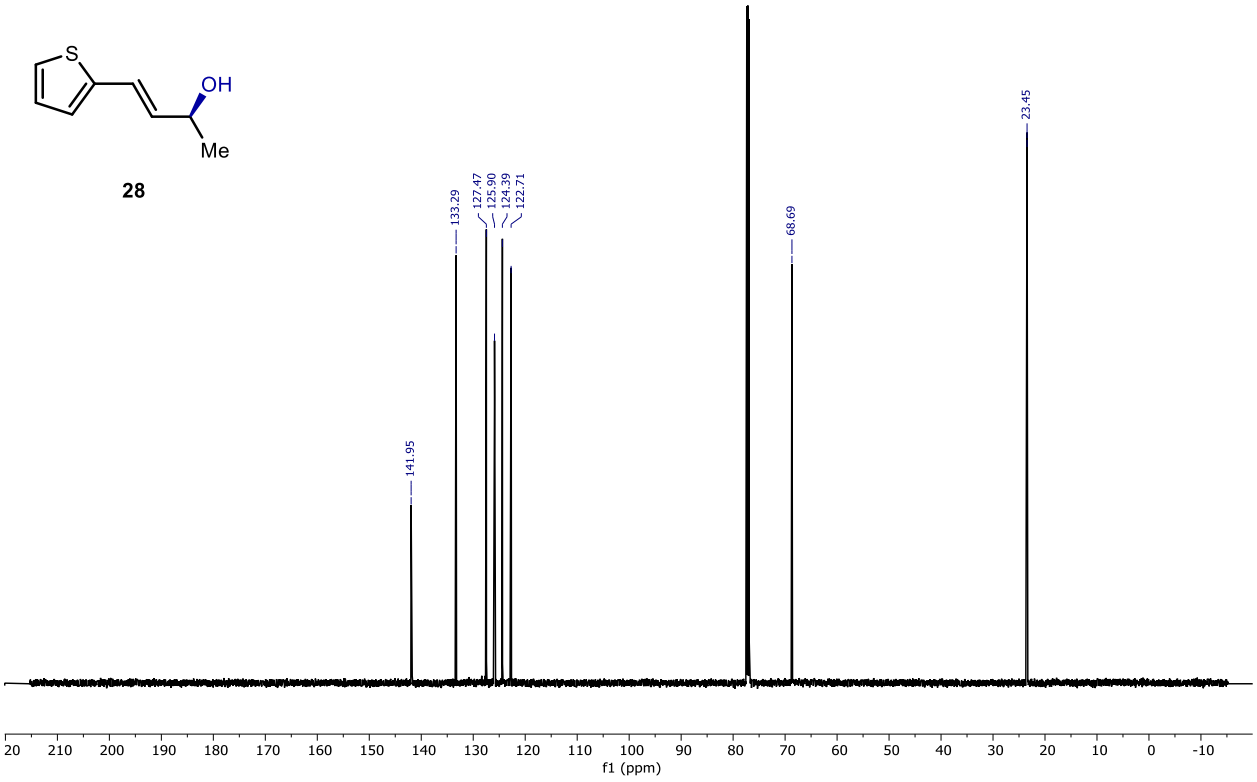
S
OH
Me
28
141.95
133.29
127.47
125.90
124.39
122.71
68.69
23.45
f1 (ppm)

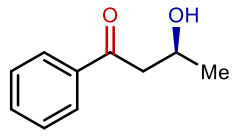
O
OH
Me

29

8.02
8.02
8.01
8.00
7.99
7.99
7.66
7.66
7.66
7.65
7.64
7.64
7.64
7.63
7.63
7.54
7.54
7.54
7.53
7.53
7.52
7.51
7.51
7.50
7.50
4.49
4.49
4.48
4.47
4.46
4.46
4.45
4.44
4.43
4.42
4.42
3.37
3.36
3.26
3.26
3.25
3.25
3.21
3.21
3.21
3.20
3.13
3.10
3.08
3.06
1.36
1.34
1.97
0.99
2.02
1.00
1.00
1.02
1.02
3.08
9.5
9.0
8.5
8.0
7.5
7.0
6.5
6.0
5.5
5.0
4.5
4.0
3.5
3.0
2.5
2.0
1.5
1.0
0.5
f1 (ppm)

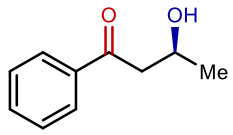
O
OH
Me

29

136.84
133.69
128.83
128.21
64.18
46.63
22.56
201.00
20
210
200
190
180
170
160
150
140
130
120
110
100
90
80
70
60
50
40
30
20
10
0
-10
f1 (ppm)

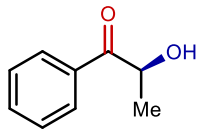
O
OH
Me

30

7.95
7.94
7.94
7.94
7.93
7.92
7.92
7.65
7.64
7.64
7.63
7.63
7.62
7.61
7.61
7.60
7.53
7.53
7.52
7.51
7.51
7.49
7.49
7.49
5.20
5.18
5.17
5.17
5.15
5.13
3.80
3.78
1.46
1.45
1.91
0.98
2.01
1.00
0.98
2.99
f1 (ppm)

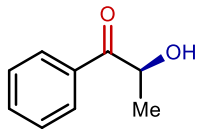
O
OH
Me

30

134.12
133.48
129.01
128.79
69.46
22.43
202.52
f1 (ppm)

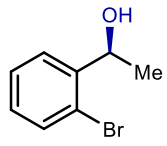
OH
Me
Br

32

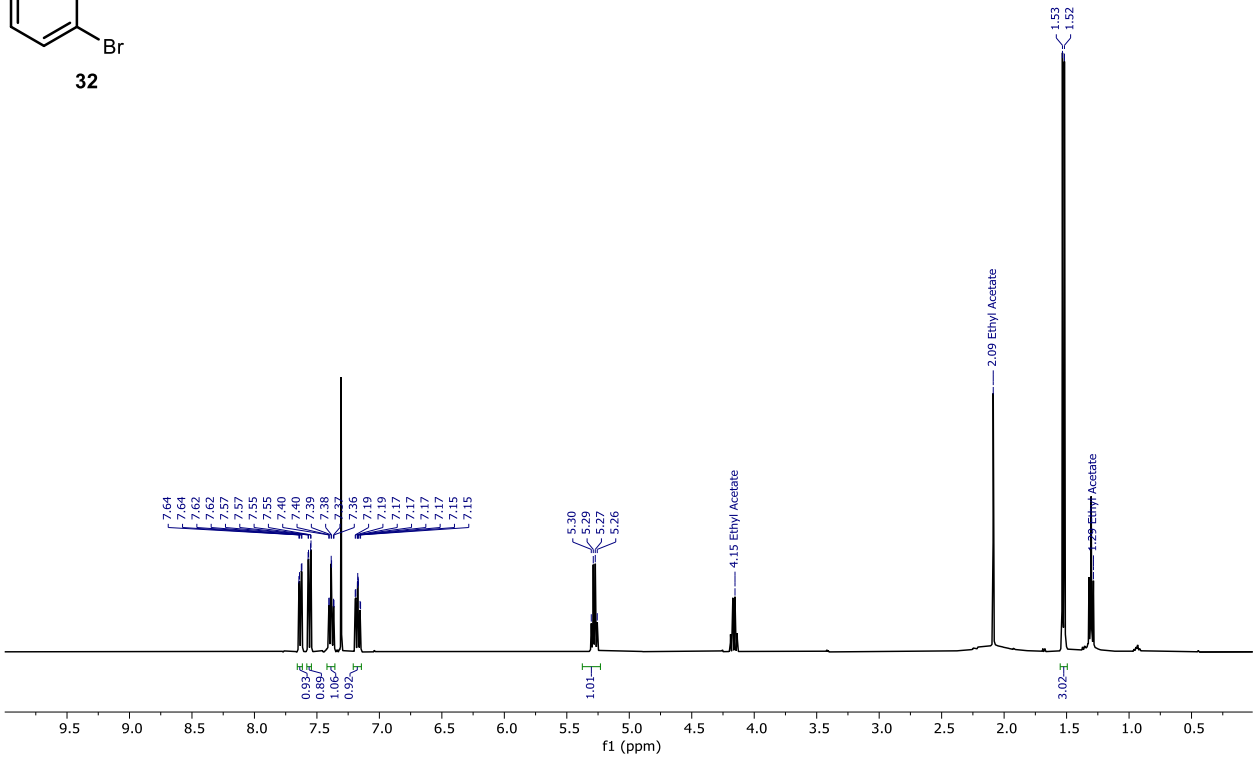
7.64
7.64
7.62
7.62
7.57
7.57
7.55
7.55
7.40
7.40
7.39
7.38
7.37
7.36
7.19
7.19
7.17
7.17
7.17
7.17
7.15
7.15
5.30
5.29
5.27
5.26
4.15 Ethyl Acetate
2.09 Ethyl Acetate
1.53
1.52
1.29 Ethyl Acetate
0.93
0.89
1.06
0.92
1.01
3.02
f1 (ppm)

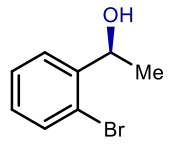
OH
Me
Br

32

144.73
132.78
128.89
127.98
126.79
121.84
69.31
23.70
f1 (ppm)

9. References

1. Key, H. M., Clark, D. S. & Hartwig, J. F. Generation, characterization, and tunable reactivity of organometallic fragments bound to a protein ligand. *J. Am. Chem. Soc.* **137**, 8261-8268 (2015).
2. Vitale, P. *et al*. Asymmetric chemoenzymatic synthesis of 1,3-diols and 2,4-disubstituted aryloxetanes by using whole cell biocatalysts. *Org. Biomol. Chem.* **14**, 11438-11445 (2016).
3. Kang, S., Han, J., Lee, E. S., Choi, E. B. & Lee, H.-K. Enantioselective synthesis of cyclic sulfamidates by using chiral rhodium-catalyzed asymmetric transfer hydrogenation. *Org. Lett.* **12**, 4184-4187 (2010).
4. Yu, J. *et al*. Iridium-catalyzed asymmetric hydrogenation of ketones with accessible and modular ferrocene-based amino-phosphine acid (f-ampha) ligands. *Org. Lett.* **19**, 690-693 (2017).
5. Kenso, S., Yuji, H. & Shuichi, S. Catalytic asymmetric synthesis of optically active secondary alcohols deuterated on the secondary carbon by the enantioselective alkylation of aldehydes. *Bull. Chem. Soc. Jpn.* **65**, 1734-1735 (1992).
6. Rowbotham, J. S., Ramirez, M. A., Lenz, O., Reeve, H. A. & Vincent, K. A. Bringing biocatalytic deuteration into the toolbox of asymmetric isotopic labelling techniques. *Nat. Commun.* **11**, 1454 (2020).
7. Chen, X. & Lu, Z. Iminophenyl oxazolinylphenylamine for enantioselective cobalt-catalyzed hydrosilylation of aryl ketones. *Org. Lett.* **18**, 4658-4661 (2016).
8. Widegren, M. B., Harkness, G. J., Slawin, A. M. Z., Cordes, D. B. & Clarke, M. L. A highly active manganese catalyst for enantioselective ketone and ester hydrogenation. *Angew. Chem. Int. Ed.* **56**, 5825-5828 (2017).
9. Sappino, C. *et al*. New chiral amino alcohol ligands for catalytic enantioselective addition of diethylzincs to aldehydes. *Org. Biomol. Chem.* **16**, 1860-1870 (2018).
10. Fuglseth, E., Sundby, E., Bruheim, P. & Hoff, B. H. Asymmetric reduction using (r)-mecbs and determination of absolute configuration of para-substituted 2-fluoroarylethanols. *Tetrahedron: Asymmetry* **19**, 1941-1946 (2008).
11. Huang, H., Zong, H., Bian, G. & Song, L. Chemo- and enantioselective addition and β-hydrogen transfer reduction of carbonyl compounds with diethylzinc reagent in one pot catalyzed by a single chiral organometallic catalyst. *J. Org. Chem.* **80**, 12614-12619 (2015).
12. Lebedev, Y. *et al*. Asymmetric hydroboration of heteroaryl ketones by aluminum catalysis. *J. Am. Chem. Soc.* **141**, 19415-19423 (2019).
13. Dong, X.-Y. *et al*. A general asymmetric copper-catalysed sonogashira c(sp3)–c(sp) coupling. *Nat. Chem.* **11**, 1158-1166 (2019).
14. Stepanenko, V. *et al*. Chiral spiroaminoborate ester as a highly enantioselective and efficient catalyst for the borane reduction of furyl, thiophene, chroman, and thiochroman-containing ketones. *Tetrahedron: Asymmetry* **20**, 2659-2665 (2009).

15. Zhu, L., Kitanosono, T., Xu, P. & Kobayashi, S. A cu(ii)-based strategy for catalytic enantioselective β-borylation of α,β-unsaturated acceptors. *Chem. Commun.* **51**, 11685-11688 (2015).
16. Li, C.-T., Liu, H., Yao, Y. & Lu, C.-D. Rearrangement of n-tert-butanesulfinyl enamines for synthesis of enantioenriched α-hydroxy ketone derivatives. *Org. Lett.* **21**, 8383-8388 (2019).
17. Schrödinger release 2020-2: Protein preparation wizard; epik, schrödinger, llc, new york, NY, 2020; impact, schrödinger, llc, new york, NY, 2020; prime, schrödinger, llc, new york, NY. (2020).
18. Madhavi Sastry, G., Adzhigirey, M., Day, T., Annabhimoju, R. & Sherman, W. Protein and ligand preparation: Parameters, protocols, and influence on virtual screening enrichments. *J. Comput. Aided Mol. Des.* **27**, 221-234 (2013).
19. Banks, J. L. *et al*. Integrated modeling program, applied chemical theory (impact). *J. Comput. Chem.* **26**, 1752-1780 (2005).
20. Schrödinger release 2020-2: Ligprep, schrödinger, llc, new york, NY. (2020).
21. Friesner, R. A. *et al*. Glide: A new approach for rapid, accurate docking and scoring. 1. Method and assessment of docking accuracy. *J. Med. Chem.* **47**, 1739-1749 (2004).
22. Schrödinger release 2020-2: Desmond molecular dynamics system, d. E. Shaw research, new york, NY, 2020. Maestro-desmond interoperability tools, schrödinger, new york, NY. (2020).
23. in *Proceedings of the 2006 ACM/IEEE conference on Supercomputing*. (Association for Computing Machinery).
24. Jorgensen, W. L., Chandrasekhar, J., Madura, J. D., Impey, R. W. & Klein, M. L. Comparison of simple potential functions for simulating liquid water. *J. Chem. Phys,* **79**, 926-935 (1983).
25. Berendsen, H. J. C., Postma, J. P. M., Gunsteren, W. F. v., DiNola, A. & Haak, J. R. Molecular dynamics with coupling to an external bath. *J. Chem. Phys,* **81**, 3684-3690 (1984).
26. Schrödinger release 2020-2: Qsite, schrödinger, llc, new york, NY. (2020).
27. Murphy, R. B., Philipp, D. M. & Friesner, R. A. A mixed quantum mechanics/molecular mechanics (qm/mm) method for large-scale modeling of chemistry in protein environments. *J. Comput. Chem.* **21**, 1442-1457 (2000).
28. Philipp, D. M. & Friesner, R. A. Mixed ab initio qm/mm modeling using frozen orbitals and tests with alanine dipeptide and tetrapeptide. *J. Comput. Chem.* **20**, 1468-1494 (1999).
29. Becke, A. D. Density-functional thermochemistry. Iii. The role of exact exchange. *J. Chem. Phys,* **98**, 5648-5652 (1993).
30. Stephens, P. J., Devlin, F. J., Chabalowski, C. F. & Frisch, M. J. Ab initio calculation of vibrational absorption and circular dichroism spectra using density functional force fields. *The Journal of Physical Chemistry* **98**, 11623-11627 (1994).
31. Wadt, W. R. & Hay, P. J. Ab initio effective core potentials for molecular calculations. Potentials for main group elements na to bi. *J. Chem. Phys,* **82**, 284-298 (1985).

32. Hay, P. J. & Wadt, W. R. Ab initio effective core potentials for molecular calculations. Potentials for the transition metal atoms sc to hg. *J. Chem. Phys,* **82**, 270-283 (1985).

33. Hariharan, P. C. & Pople, J. A. Accuracy of ah n equilibrium geometries by single determinant molecular orbital theory. *Mol. Phys.* **27**, 209-214 (1974).